

Tagged polymers as recognition agents

by



Thesis presented in partial fulfilment of the requirements for the degree of

Master of Science (Polymer Science)

at the

University of Stellenbosch

Study leader:
Prof. Ronald D. Sanderson

Stellenbosch
December 2004

Declaration

I, the undersigned, hereby declare that the work contained in this thesis is my own original work and that I have not previously in its entirety or in part submitted it an any university for a degree.

Vernon Ramiah

Signed on the 30th day of June 2004.



Abstract

Chemical and molecular tagging agents have illustrated their diversity in a number of different applications. One of the most significant applications includes the use of chemical tagging agents for product registration in industry. Industrial enterprises producing good products need to ensure product authenticity to prevent duplication through piracy and unscrupulous industrialists. Fluorescent probes are chemical compounds that satisfy most of the technical and commercial aspects that are required to be excellent tagging agents. They are generally quick to synthesize, do not affect the product integrity, display little or no impact on the uses of the product or the environment and they can be identified by relatively simple detection procedures. The aim of the present study was to synthesize fluorescent polymers as tagging agents for the paint industry.

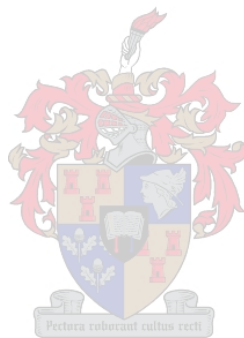
7-Hydroxy-2H-chromen-2-one (A_1) and 7-hydroxy-4-methyl-2H-chromen-2-one (B_1), commercially available fluorescent hydroxyl compounds, were selected as the starting materials. An esterification reaction resulted in the production of 2-oxo-2H-chromen-7-yl acrylate (A_2) and 4-methyl-2-oxo-2H-chromen-7-yl acrylate (B_2), which are acrylic-type monomers that were required for polymerisation. Studies showed that fluorescence was maintained during the esterification.

Copolymers poly(MMA-co- A_2), poly(MMA-co- B_2), poly(BA-co- A_2) and poly(BA-co- B_2), synthesized via homogeneous free radical initiated copolymerisation, revealed how copolymer compositions were affected by the feed compositions and the pattern of monomer incorporation over time. This was investigated by following individual monomer consumption rates by $^1\text{H-NMR}$ spectroscopy. Fluorescence studies revealed that the fluorescence behaviour of A_2 and B_2 was maintained during the copolymerisation.

Latex particles, with fluorescent behaviour, were synthesized via *in situ* miniemulsion polymerisation. High molecular weight copolymers with monodisperse particle sizes (nm range) were obtained.

A bench-top UV lamp and UV-reflectance studies confirmed the fact that fluorescent latex particles can be identified and quantified respectively, when dispersed in paints that are either free of titanium dioxide or paints that contain titanium dioxide.

Keywords: fluorescence, esterification, solubility parameter, homogeneous free radical initiated copolymerisation, miniemulsion, paint



Opsomming

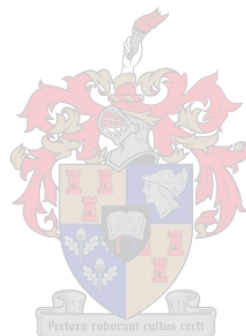
Die diversiteit van chemiese en molekulêre merkers in 'n verskeidenheid van toepassings is al telkemale geïllustreer. Een van die mees belangrike toepassings in die industrie is die gebruik van chemiese merkers vir produkregistrasie. Industrieë wat goeie produkte verskaf moet die egtheid van hul produkte kan verseker deur duplikasie via nadruk (Eng: piracy) deur ander te voorkom. Fluoreserende merkers is chemiese stowwe wat aan die meeste van die tegniese en kommersiële vereistes voldoen om as uitstekende merkers te dien. Die sintese van die merkers is gewoonlik nie tydrowend nie, beïnvloed nie die integriteit van die produk nie, het min of geen impak op die gebruike van die produk of die omgewing en kan deur relatief eenvoudige prosedures bepaal word. Die doel van hierdie studie was die sintese van fluoreserende polimere om as merkers in die verfindustrie te dien.

7-Hidroksie-2H-chromen-2-oon (A_1) en 7-hidroksie-4-metiel-2H-chromen-2-oon (B_1), fluoreserende hidroksielverbindinge wat kommersieël beskikbaar is, is gekies as uitgangstowwe vir die bereiding van die merkers in hierdie studie. 'n Esterifikasie-reaksie het gelei tot die produksie van 2-okso-2H-chromen-7-ielakrilaat (A_2) en 4-metiel-2-okso-2H-chromen-7-ielakrilaat (B_2). Hierdie produkte is tipiese akrilaat-tipe monomere wat benodig word vir polimerisasie. Ondersoeke het getoon dat fluoressensie behoue tydens esterifikasie gebly het.

Die kopolimere poli(MMA-ko- A_2), poli(MMA-ko- B_2), poli(BA-ko- A_2) en poli(BA-ko- B_2) is deur homogene vry-radikaal-geïnisieerde kopolimerisasie gesintetiseer. Daar is vasgestel hoe die kopolimeersamestelling geaffekteer is deur die samestelling van die reagentse (Eng: feed composition) en die patroon van monomeer inkorporasie met tyd. Dit was ondersoek deur die tempo van verbruik van die individuele monomere d.m.v. ^1H -KMR spektroskopie te bepaal. Daar is verder vasgestel dat die fluoressensie van A_2 en B_2 gedurende kopolimerisasie behoue gebly het. Latekspartikels, met fluoressensie gedrag, is via in-situ mini-emulsie-polimerisasie gesintetiseer. Hoë molekulêre massa kopolimere met monodisperse partikelgroottes (in die order van nanometers) is verkry.

Deur van 'n UV-lamp en UV-refleksie studies gebruik te maak is daar bepaal dat fluoresserende latekspartikels in polimere, in verf - wat of titaniumdioksied bevat of geen titaniumdioksied bevat nie -, beide geïdentifiseer and gekwantifiseer kan word.

Sleutelwoorde: fluoressensie, esterifikasie, oplosbaarheidsparameter, homogene vryeradikaal-geïnduseerdepolimerisasie, miniemulsie, verf



To Kamini



*Her blessing has anchored the production of this
work to the prominence of which it holds.*

Acknowledgements

My father once said that an education without compassion perceives the greatness of the world in tears.

It is therefore with extreme gratitude that I wish to acknowledge my parents, whom through their thoughts and loving deeds have supported, encouraged and inspired me throughout the duration of my studies. I would like to thank them for touching my imagination as well as positioning me on the path of excellence to challenge life when necessary. I have become who I am today because I am a product of their influence.

I would like to express my gratitude to the following people for all their assistance, moral support and advice, without which this thesis would not have been possible.

My supervisor, Professor Ronald D. Sanderson, for his continued guidance and his belief in me to always exert myself beyond the norm and to reach for the sky. He has broken the mould of immaturity and has sculptured a strong independent character within myself. For this I am eternally grateful.

Dr. Andre van Zyl, Dr. James B. McLeary, Jaco Vosloo and Andrew de Vries, for their inexhaustible patience and tolerance. I wish to thank them for all the help and support throughout the duration of this project.

Thalma Nieuwondt for her help, advice and whole-hearted smile during various segments of the project. I pray that her character touches each and every one of us.

Ralf Johannsen, Paul Terry and Johan Batist for their invaluable discussions on the approach required to bestow foundation into my future. Their wisdom, through experience, is inspiring.


At this point, sincere gratification must be honoured to close friends, whose enthusiasm, thoughtfulness, assistance and advice have been the prism that has reflected light into my life. I would like to thank them with my true friendship.

List of contents

Glossary	v
List of figures	ix
List of schemes	xii
List of tables	xiii

Chapter 1: Introduction

1.1	General introduction	1
1.2	Fluorescent probes	2
1.3	Miniemulsion polymerisation	3
1.4	Motivation of study	3
1.5	Objectives	4
	References	5

The image shows a watermark of a university crest, likely from the University of Cambridge, featuring a shield with various symbols, a crown on top, and a motto scroll at the bottom. The crest is semi-transparent and positioned in the center of the page, overlapping the text of the table of contents for Chapter 1.

Chapter 2: The science of tagging – an historical overview

2.1	Introduction	6
2.2	1970's - 2000	6
2.3	The turn of the century: 2000 - 2004	10
2.5	Conclusions	11
	References	13

Chapter 3: Theoretical background

3.1	Molecular fluorescence spectroscopy	14
-----	-------------------------------------	----

3.1.1	Types of luminescence	14
3.1.2	Theory of molecular fluorescence	15
3.1.3	Types of fluorescence and emission processes	17
3.1.4	Advantages of fluorescence	18
3.1.5	Factors affecting fluorescence	19
3.1.5.1	Properties of fluorescent compounds	19
3.1.5.2	Photochemical decomposition	21
3.1.5.3	Temperature	21
3.1.5.4	Concentration	21
3.1.5.5	Oxygen quenching	22
3.1.5.6	pH quenching	22
3.2	Free radical polymerisation	23
3.2.1	Kinetics	23
3.2.2	Chain growth copolymerisation	30
3.2.2.1	Solution polymerisation	36
3.2.2.2	Miniemulsion polymerisation	36
3.2.3	Determination of reactivity ratios	39
3.3	Solubility parameters	44
3.3.1	Modification of solubility parameters	46
	References	48

Chapter 4: Synthesis of monomers

4.1	Introduction	51
4.2	Experimental	52
4.2.1	Materials	52
4.2.2	Instrumentation	53
4.2.3	Esterification protocol	53
4.3	Results and discussion	54
4.3.1	Esterification of 7-hydroxy-2H-chromen-2-one (A ₁) and 7-hydroxy-4-methyl-2H-chromen-2-one (B ₁)	54

4.3.2	Nuclear magnetic resonance studies	54
4.3.2.1	2-oxo-2H-chromen-7-yl acrylate (A ₂)	54
4.3.2.2	4-methyl-2-oxo-2H-chromen-7-yl acrylate (B ₂)	56
4.3.3	Infrared spectroscopy analysis	57
4.3.4	Fluorescence studies	59
4.3.5	Conclusions	61
References		62

Chapter 5: Solubility parameters of solvents and monomers

5.1	Introduction	63
5.2	Determination of solubility parameters	63
5.3	Modification of solubility parameters	67
5.4	Experimental verification	71
5.5	Conclusions	72
References		73




Chapter 6: Solution polymerisation studies

6.1	Introduction	74
6.2	Experimental	74
6.2.1	Chemicals and their purification	74
6.2.2	Instrumentation	75
6.2.3	Determination of reactivity ratios	76
6.2.4	Molecular weight analysis	80
6.3	Results and discussion	80
6.3.1	Copolymerisation kinetics	80
6.3.2	Molecular weight determinations	86
6.3.3	Fluorescence studies	87
6.4	Conclusions	89
References		90

Chapter 7: Fluorescent – tagged paints

7.1	Introduction	91
7.2	Experimental	91
7.2.1	Materials	91
7.2.2	Synthesis of latexes by miniemulsification-ultrasonication	91
7.2.3	Analytical techniques	92
7.2.3.1	Size-exclusion chromatographic analysis	93
7.2.3.2	Transmission electron microscopy analysis	93
7.2.3.3	Particle size analysis	93
7.2.3.4	UV studies	94
7.3	Results and discussion	95
7.3.1	Size-exclusion chromatographic analysis	95
7.3.2	TEM analysis	97
7.3.3	Particle size analysis	98
7.3.4	Paint studies	98
7.4	Conclusions	101
	References	102

The image shows a watermark of a university crest. The crest features a shield with various symbols, including a cross and a crown. Above the shield is a helmet with a crest. The shield is supported by two figures. Below the shield is a motto scroll with the Latin text "Pectora roburant cultus recti".

Chapter 8: Conclusions and recommendations

8.1	Conclusions	103
8.2	Recommendations	104

Glossary

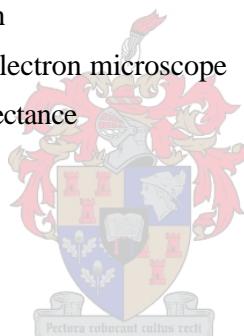
Abbreviations

ACN	acetonitrile
AIBN	2,2'-azobis(isobutyronitrile)
Avg	average
A ₁	7-hydroxy-2h-chromen-2-one
A ₂	2-oxo-2h-chromen-7-yl acrylate
a.u	arbitrary units
BA	butyl acrylate
B ₁	7-hydroxy-4-methyl-2h-chromen-2-one
B ₂	4-methyl-2-oxo-2h-chromen-7-yl acrylate
B.p	boiling point
CaCl ₂	calcium chloride
CCD	chemical composition distribution
COV	coefficient of variation
DCM	dichloromethane
DDI	distilled de-ionised
ELSD	evaporative light scattering detector
EtOH	ethanol
(Et) ₃ N	triethylamine
EA	ethyl acetate
FTIR	Fourier transform infrared spectroscopy
GPC	gel permeation chromatography
KOH	potassium hydroxide
MeOH	methanol
M ₁ , M ₂	monomer 1 and monomer 2
MM	molar mass
MMA	methyl methacrylate
MMD	molar mass distribution
Mg(SO ₄)	magnesium sulphate

NMR	nuclear magnetic resonance spectroscopy
NaOH	sodium hydroxide
PBA	poly(butyl acrylate)
PMMA	poly(methyl methacrylate)
PDI	polydispersity index, $d = m_w / m_n$
PSA	particle size analysis
PPT	precipitate
PPM	parts per million
SEC	size-exclusion chromatography
SDS	sodium dodecyl sulfate
S_p	solution polymerisation
M_{Ep}	miniemulsion polymerisation
M.p	melting point
TLC	thin layer chromatography
THF	tetrahydrofuran
TEM	transmission electron microscope
UV_R	ultraviolet reflectance
UV	ultraviolet

Notations

x	average number of dead chains produced per termination
f	quantum efficiency
\bar{x}_n	a term used to more generally express the average chain length of the growing polymer chain
r_i	rate at which initiation occurs
r_p	rate of propagation of polymerisation
r_t	rate at which termination occurs
M_r	monomer
$[M]$	the concentration of the monomer
$[M]_0$	initial monomer concentration
M	molar
M_n	number average molar mass
M_p	molar mass at the maximum of the molar mass distribution



M_w	weight average molar mass
k_d	rate constant for the first-order initiation process
k_{tc}	rate constant of termination by combination
k_{td}	rate constant of termination by disproportionation
F_1, F_2	mole fractions of monomers $(M)_1$ and $(M)_2$ in the copolymer
f_1, f_2	mole fractions of monomers $(M)_1$ and $(M)_2$ in the feed
ΔG_M	free energy of mixing
ΔH_M	enthalpy of mixing
ΔH_{vap}	molar heat of evaporation
dV	change in volume
ΔE_{coh}	change in cohesive energy density
$\Delta E_1, \Delta E_2$	change in evaporation energy
E_{coh}	cohesive energy density
E_d	dispersive term of the cohesive energy density
E_h	hydrogen bonding term of the cohesive energy density
E_{hi}	group molar contribution of the structural unit i for the 3-value solubility parameter concept
E_i	group molar contribution of structural unit i
E_p	polarity term of the cohesive energy density
E_1, E_2	energies of evaporation of compounds 1 and 2
F	group molar contribution of structural unit
F_{di}	group molar dispersion contribution of structural unit i for the 3-value solubility parameter concept
F_i	group molar contribution of structural unit i
F_{pi}	group molar polarity contribution of structural unit i for the 3-value solubility parameter concept
h	Planck's constant
g	grams
N_A	Avogadro constant
c	velocity of light
λ	wavelength
ν	frequency
t	time
V	volume
c	fractional conversion
G	ground electronic state

S	singlet electronic state
S^1	first excited singlet electronic state
T	triplet electronic state
T^1	first excited triplet state
I	incident radiant power
M_t	multiplicity, a term used to express the orbital angular momentum of a given state
e	molar absorptivity
b	path length of a cell
RT	room temperature
$[I]$	initiator concentration
V_m	total volume of the mixture
ΔU_{vap}	internal energy of evaporation
d	solubility parameter
d_d	solubility parameter dispersive term
d_p	solubility parameter polarity term
d_h	solubility parameter hydrogen bonding term
d_v	$d_v = \sqrt{(d_d^2 + d_p^2)}$
d_{THF}	solubility parameter of THF
d_{A_1}	solubility parameter of A ₁
d_{A_2}	solubility parameter of A ₂
d_{B_1}	solubility parameter of B ₁
d_{B_2}	solubility parameter of B ₂
d_t	total solubility parameter

List of figures

- Figure 3.1:** Transitions involved in the absorption process.
- Figure 3.2:** Effect of rigidity on fluorescence intensity.
- Figure 3.3:** Generation of free radicals by thermal decomposition of benzoyl peroxide.
- Figure 3.4:** Thermal decomposition of AIBN to form two radicals and nitrogen.
- Figure 3.5:** Termination by combination.
- Figure 3.6:** Termination by disproportionation.
- Figure 3.7:** Typical calorimetric curve for a miniemulsion polymerisation of styrene.
- Figure 4.1:** Chemical structures of 7-hydroxy-2H-chromen-2-one (A_1) and 7-hydroxy-4-methyl-2H-chromen-2-one (B_1).
- Figure 4.2:** $^1\text{H-NMR}$ spectrum ($\text{DMSO-}d_6$, 600 MHz) of 2-oxo-2H-chromen-7-yl acrylate (A_2).
- Figure 4.3:** (a) $^{13}\text{C-NMR}$ spectrum ($\text{DMSO-}d_6$, 150 MHz) and (b) APT NMR spectrum of 2-oxo-2H-chromen-7-yl acrylate (A_2).
- Figure 4.4:** $^1\text{H-NMR}$ spectrum ($\text{DMSO-}d_6$, 600 MHz) of 4-methyl-2-oxo-2H-chromen-7-yl acrylate (B_2).
- Figure 4.5:** (a) $^{13}\text{C-NMR}$ spectrum ($\text{DMSO-}d_6$, 150 MHz) and (b) APT NMR spectrum of 4-methyl-2-oxo-2H-chromen-7-yl acrylate (B_2).
- Figure 4.6:** Fourier transform infrared analysis of 2-oxo-2H-chromen-7-yl acrylate (A_2).
- Figure 4.7:** Fourier transform infrared analysis of 4-methyl-2-oxo-2H-chromen-7-yl acrylate (B_2).
- Figure 4.8:** (a) The effect of concentration and (b) the effect of temperature on the fluorescence intensity of 2-oxo-2H-chromen-7-yl acrylate (A_2).
- Figure 4.9:** Illustration of the absence of fluorescence in chloroform.

- Figure 4.10:** Similarity in the wavelength at which 7-hydroxy-2H-chromen-2-one (A_1) and 2-oxo-2H-chromen-7-yl acrylate (A_2) fluoresce at $26 \pm 1^\circ\text{C}$.
- Figure 4.11:** Similarity in the wavelength at which 7-hydroxy-4-methyl-2H-chromen-2-one (B_1) and 4-methyl-2-oxo-2H-chromen-7-yl acrylate (B_2) fluoresce at $26 \pm 1^\circ\text{C}$.
- Figure 5.1:** Chemical structures of (a) 7-hydroxy-2H-chromen-2-one (A_1) and (b) 7-hydroxy-4-methyl-2H-chromen-2-one (B_1).
- Figure 5.2:** Chemical structures of (a) 2-oxo-2H-chromen-7-yl acrylate (A_2) and (b) 4-methyl-2-oxo-2H-chromen-7-yl acrylate (B_2).
- Figure 5.3:** Hansen solubility parameters for A_1 , B_1 , A_2 and B_2 in selected solvents.
- Figure 6.1:** Apparatus setup for the copolymerisation reactions.
- Figure 6.2:** A typical $^1\text{H-NMR}$ spectrum of a MMA/ A_2 (6:1) copolymerisation reaction mixture (in CDCl_3) showing the region of interest. (*Reaction a*)
- Figure 6.3:** A typical $^1\text{H-NMR}$ spectrum of a BA/ B_2 (6:1) copolymerisation reaction mixture (in CDCl_3) showing the region of interest. (*Reaction d*)
- Figure 6.4:** Instantaneous copolymer composition versus feed composition for reactions (a), (b), (c) and (d) after a 30-minute reaction period.
- Figure 6.5:** $^1\text{H-NMR}$ spectroscopy results for the incorporation of respective monomers in reactions (a), (b), (c) and (d) as a function of time.
- Figure 6.6:** Calibration curves for the fluorescence analysis of A_2 and B_2 in chloroform.
- Figure 6.7:** Illustration of the absence of fluorescence in a mixture of methyl methacrylate ($1 \times 10^{-6}\text{M}$) and butyl acrylate ($1 \times 10^{-6}\text{M}$) in chloroform.
- Figure 6.8:** Fluorescence analysis of (a) 2-oxo-2H-chromen-7-yl acrylate (A_2), (b) poly(MMA-co- A_2) and (c) poly(BA-co- A_2) copolymers.
- Figure 6.9:** Fluorescence analysis of (a) 4-methyl-2-oxo-2H-chromen-7-yl acrylate (B_2), (b) poly(MMA-co- B_2) and (c) poly(BA-co- B_2) copolymers.
- Figure 7.1:** Percentage conversion of methyl methacrylate and butyl acrylate during copolymerisation of A_2 and B_2 as a function of time.
- Figure 7.2:** Molecular weight distributions of (a) poly(MMA-co- A_2), (b) poly(MMA-co- B_2), (c) poly(BA-co- A_2) and (d) poly(BA-co- B_2).

- Figure 7.3:** TEM image of a poly(MMA-co-A₂) sample at 6 300× magnification.
- Figure 7.4:** TEM image of a poly(BA-co-A₂) sample at 6 300× magnification.
- Figure 7.5:** TEM image of a poly(MMA-co-A₂) sample at 80 000× magnification, showing the contrasting effect of 2% uranyl acetate.
- Figure 7.6:** Paint without titanium dioxide: UV lamp illumination at 365 nm of (a) paint without fluorescent latex particles, (b), (c) and (d) paint containing 0.25%, 0.5% and 1.0% fluorescent latex particles respectively.
- Figure 7.8:** Paint containing 10.0% titanium dioxide: UV lamp illumination at 365 nm of (a) paint without fluorescent latex particles, (b), (c) and (d) paint containing 5.0%, 10.0% and 15.0% fluorescent latex particles respectively.
- Figure 7.9:** A typical UV-reflectance spectrum showing the regions of interest of (a) paint without titanium dioxide but containing 1.0% poly(MMA-co-A₂), (b) paint without titanium dioxide but containing 0.75% poly(BA-co-A₂) and (c) paint containing titanium dioxide homogenised with 20.0% poly(MMA-co-A₂).



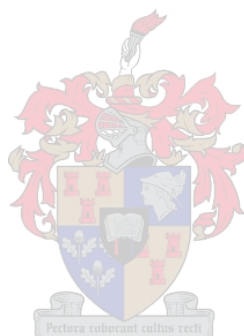
List of schemes

Scheme 3.1: a) Potential energy-level diagram of a diatomic molecule and b) the various transitions occurring within a).

Scheme 3.2: Schematic representation of the principle of miniemulsion polymerisation.

Scheme 4.1: Reaction scheme for the synthesis of the acrylate monomer.

Scheme 6.1: Reaction scheme for the copolymerisation utilising AIBN as an initiator.



List of tables

- Table 3.1:** Transitions involved in the absorption process with respect to fluorescent properties.
- Table 5.1:** Group molar attraction constants and group molar volumes according to van Krevelen, Small, Hoy and Fedors.
- Table 5.2:** Group molar attraction constants for A_1 and A_2 .
- Table 5.3:** Group molar attraction constants for B_1 and B_2 .
- Table 5.4:** Group molar attraction constants for the 3-value solubility parameter concept according to van Krevelen.
- Table 5.5:** Group molar attraction constants for A_1 and A_2 according to the 3-value solubility parameter concept.
- Table 5.6:** Group molar attraction constants for B_1 and B_2 according to the 3-value solubility parameter concept.
- Table 5.7:** Values for d_a , d_p and d_h in $J^{1/2}.cm^{-3/2}$ of A_1 , B_1 , A_2 and B_2 , calculated from group molar contributions according to Hoftyzer and van Krevelen.
- Table 5.8:** A tabulated comparison of the solubility parameters calculated by Fedors using the cohesive energy concept and the 3-value solubility concept, in $J^{1/2}.cm^{-3/2}$ proposed by Hoftyzer and van Krevelen.
- Table 5.9:** Solubility parameters for A_1 , B_1 , A_2 and B_2 evaluated by the 3-value solubility concept in $J^{1/2}.cm^{-3/2}$.
- Table 5.10:** Hansen solubility parameters for selected common solvents evaluated by the 3-value solubility concept in $J^{1/2}.cm^{-3/2}$.
- Table 5.11:** Tabulation of the percentages of A_2 and B_2 that were soluble in selected solvents at two-hour time intervals, determined experimentally.
- Table 6.1:** Amounts of comonomers, initiator, internal reference and solvent used in the copolymerisation study of *Reaction a*.
- Table 6.2:** Amounts of comonomers, initiator, internal reference and solvent used in the copolymerisation study of *Reaction b*.

- Table 6.3:** Amounts of comonomers, initiator, internal reference and solvent used in the copolymerisation study of *Reaction c*.
- Table 6.4:** Amounts of comonomers, initiator, internal reference and solvent used in the copolymerisation study of *Reaction d*.
- Table 6.5:** Amounts of monomers, initiator, internal reference and solvent used in the copolymerisation study.
- Table 6.6:** $^1\text{H-NMR}$ spectroscopy results for MMA/A₂ copolymerisation reactions.
- Table 6.7:** $^1\text{H-NMR}$ spectroscopy results for BA/A₂ copolymerisation reactions.
- Table 6.8:** $^1\text{H-NMR}$ spectroscopy results for MMA/B₂ copolymerisation reactions.
- Table 6.9:** $^1\text{H-NMR}$ spectroscopy results for BA/B₂ copolymerisation reactions.
- Table 6.10:** Reactivity ratios for the copolymer systems.
- Table 6.11:** Molecular weight data of polymers.
- Table 7.1:** Miniemulsion recipes (quantities given in grams) for the synthesis of the respective latexes.
- Table 7.2:** Molecular weight data of the synthesised copolymers.
- Table 7.3:** Particle sizes of polymers.
- Table 7.4:** UV-reflectance data at 321 nm when 1.0, 0.75, 0.5 and 0.25% of each reaction system are homogenised with a paint that contains no titanium dioxide.
- Table 7.5:** UV-reflectance data at 321 nm when 5.0, 10.0, 15.0 and 20.0% of each reaction system are homogenised with a paint that contains 10% titanium dioxide.

Chapter 1

Introduction

1.1 General introduction

Most industrial enterprises base their business survival policy on commercialising innovative as well as inexpensive products. Apart from commercialising an inexpensive process in terms of time and commodity yield, product authenticity is also important, ensuring general quality security. This encompasses the concept that companies producing good products be financially rewarded for their efforts. Their profits will enable the development of improved products and technologies. It is thus imperative that comprehensive identification mechanisms of any product be maintained. This measure might prevent duplication and unauthorised use. This ensures that intellectual property rights be reserved.

Product registration ensures general quality security and the ability to identify ones product. Product registration, implemented by the supplier, is a process whereby a so-called 'tagging agent,' which facilitates the identification of the product before, during and after use or application, 'marks' the product.

Product registration provides:

- i. Secure national and international quality.
- ii. Comprehensive national and international product/producer liability.
- iii. Protection of consumers in terms of ensuring the use of safe products.
- iv. Prevention of fake products.
- v. Proof of unintended use of a product, in the case of robbery.

Fundamentally, product registration can be differentiated between an overt (open) and covert

(hidden) registration. Overt registration systems include etiquettes, holograms and barcodes, whilst, covert registration systems (directly combined with the product) include molecular and chemical tags.¹ While both registration procedures have unique advantages and disadvantages, covert systems stand superior as a result of the inability to directly observe the 'security feature'. This illustrates the necessity for chemical and molecular tagging agents.

From a technical aspect, chemical/molecular tagging agents constructed for commercial purposes should possess the following properties:

- i. Not affect the product integrity adversely.
- ii. Maintain its chemical integrity during the lifetime of the product.
- iii. Have little or no negative impact on the users of the product and on the environment.
- iv. Have little/minimal additional cost to the users.

Commercial aspects include:

- | | | |
|------|---------------|---|
| i. | Speed | -quick to synthesize |
| ii. | Efficiency | -no wastage of commodity yield |
| iii. | Economic | -minimum usage of raw materials |
| iv. | Simplicity | -simple detection procedures |
| v. | Flexibility | -tag should function during modifications and under varying conditions of the polymer |
| vi. | Compatibility | -taking all technical properties into account |

1.2 Fluorescent probes

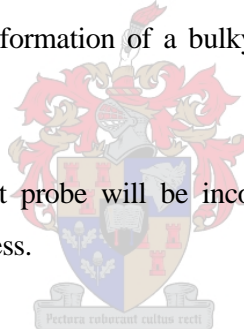
Fluorescent probes are chemical compounds that satisfy most of the technical and commercial aspects outlined above. Fluorescence detection has many advantages over analysis by other spectroscopic techniques. A major advantage is the sensitivity, as concentrations as low as an attomole ($<10^{-18}$ mole) can be detected.² Fluorescence is considered a safe technique, as samples that undergo fluorescence do so without generating hazardous by-products. Another advantage is the rapid monitoring procedures, whereby fluorescence intensity can be detected in picoseconds.³ Probably the most significant advantage of fluorescence in this application includes its simple detection mechanisms.⁴

The incorporation of a fluorescent probe into an appropriate polymer resin is essential in enforcing stability in its functioning. One of the conventional methods for attaching a monomer to a polymer involves bonding of the end of the monomer to the backbone of the polymer to form a graft copolymer via solution polymerisation.⁵ However, due to the cross-linking involved, a bulky interwoven network often results, which leads to poor processability of the material, thereby limiting its commercial viability.⁶

1.3 Miniemulsion polymerisation

Emulsion polymerisation, particularly miniemulsion polymerisation, is a process designed to overcome the problems associated with solution polymerisation. A major advantage includes the use of aqueous mediums, which has become a popular process to eliminate the use of volatile organic solvents. This inhibits the toxic effects of organic solvents in the environment and reduces health risks.^{7,8} Miniemulsion polymerisation can also be controlled to prevent the formation of a bulky polymer chain, to obtain the desired polymer structure design.⁹

In the present study a fluorescent probe will be incorporated into a polymer resin via the miniemulsion polymerisation process.



1.4 Motivation of study

At this juncture, the choice of 'polymer dependent' industry for which these particular tagging agents would be most beneficial, becomes crucial. The paint industry is a multi-billion dollar industry, with immense import and export potential.¹⁰ During exportation, certain unscrupulous industrialists may replace a high quality product with an inferior product, which may not conform with the requirements of the guarantee offered on the original product. This would result in the companies producing the original good products having to thereafter rectify guarantees for which they are not responsible. For this reason the paint industry requires protection from piracy.

Hence, this research will address the utilisation of fluorescent polymers as tagging agents for the paint industry.

1.5 Objectives

As a result of the above discussion and consequent proposal, the following mini-objectives were outlined.

- i. Select suitable monomeric fluorescent compounds, for incorporation into designated copolymers.
- ii. Synthesise acrylic-type monomers from the selected fluorescent hydroxyl compounds.
- iii. Determine whether the fluorescence behaviour is maintained after the above esterification.
- iv. Determine solubility parameters of the selected two fluorescent acrylic-type monomers.
- v. Synthesise copolymers of the above fluorescent acrylic-type monomers with methyl methacrylate and butyl acrylate via homogeneous free radical initiated copolymerisation.
- vi. To investigate basic data such as copolymer composition against feed composition, molecular weights, etc., and determine whether fluorescence will still be detected in the copolymer.
- vii. Conduct heterogeneous free radical studies, namely miniemulsification, to obtain the desired latex particles and investigate whether the fluorescent behaviour of the incorporated fluorescent monomers is maintained.
- viii. Determine whether these particles can be identified and quantified with both a bench-top UV-lamp and by UV-reflectance spectroscopy respectively, when dispersed in a paint polymer resin that is free of titanium dioxide and a paint polymer resin that contains titanium dioxide.

References

- (1) Wachkamp, K.; Rauhe, H. In *Farbe & Lack*, 2002; Vol. 107, p 97.
- (2) www.pti-nj.com/fluorescence
- (3) Skoog, D. A.; West, D. M.; Holler, F. J. *Fundamentals of analytical chemistry*, 7 Ed.; Saunders College Publishers: New York, 1997.
- (4) Guilbault, G. G. *Practical fluorescence: theory, methods, and techniques*; Marcel Dekker, Inc.: New York, 1973.
- (5) Bovey, F. A.; Winslow, F. H. *Macromolecules: an introduction to polymer science*; Academic Press: New York, 1979.
- (6) Li, H.; Ruckenstein, E. *Polymer* **1995**, *36*, 2281-2287.
- (7) Antonietti, M.; Landfester, K. *Prog. Polym. Sci.* **2002**, *27*, 689-757.
- (8) Asua, J. M. *Prog. Polym. Sci.* **2002**, *27*, 1283-1346.
- (9) Capek, I.; Chern, C. S. In *Adv. Polym. Sci.*; Springer-Verlag: Berlin Heidelberg, 2001; Vol. 155, p 101.
- (10) www.sapma.org.za (South African Paint Manufactures Assoc.)



Chapter 2

The science of tagging: an historical overview

2.1 Introduction

The relatively recent development of the science of tagging has presented numerous research opportunities and interesting challenges. The development of tagging agents for various applications is of great technological and economic significance. This thesis focuses on the synthesis and utilisation of selected tagged polymers as recognition agents. This chapter provides an historical overview of the evolution of the use of tagging agents in polymers over the past thirty years.

2.2 1970's – 2000

One of the oldest tagging agents for polymers is ^{14}C . From the early 1970's to the late 1980's it was used in numerous applications. One of the earliest applications entailed the incorporation of ^{14}C in polyethyleneimine polymers to study the flocculation of silica in water. Two ^{14}C -tagged polyethyleneimine polymers of different molecular weights were prepared in 1974 by Dixon *et al.*¹ By using the tags it was possible to determine the concentrations of the polymers required to produce flocculation, by determining the amount of polymer that was absorbed on the colloidal surface.

With specific regards to polymer chemistry, tagging agents have been employed in a number of different applications to understand various processes. These include the hierarchy of interactions in polymer coils² as well as the shape and segmental density of flexible linear macromolecules.³

From the 1970's, size-exclusion chromatography (SEM) and transmission electron microscope (TEM) analyses were used as the most conventional techniques for studying the actions of tagged polymers. The use of tagged poly(cis-isoprene) molecules in untagged poly(cis-isoprene) by Aharoni *et al.*³ in 1978, made it possible to investigate the instantaneous shape and segmental density of flexible linear macromolecules via TEM analysis. Results showed that individual molecules were neither symmetrical nor Gaussian, but became spherical or Gaussian in shape with time. In addition, the high-density regions appeared to be closer to the geometrical centre of the macromolecule. Furthermore, the use of the tag made it easier to determine polymer sizes by electron microscopy.

By the late 1970's, tagging agents such as acridine orange were used to investigate the nature of binding of fluorescent dyes to polymer compounds. Poly(methacrylic acid) and sodium polystyrene sulphonate were tagged with the fluorescent dye acridine orange and subjected to pulsed electric fields.⁴ By observing the polarised components of the fluorescent polymer system, the nature of binding of the fluorescent dye to the polymer was estimated for the first time. This work opened the door for the possibility of using fluorescent tagging agents in the science of fingerprinting. By the start of the 1980's the usefulness of fluorescent tagging agents had become much more lucrative.

In 1983 Kaplan *et al.*⁵ described the procedure for the synthesis of 500 Å diameter microspheres containing a fluorescent cross-linking tagging agent. This tag allowed for the detection of surface receptor components on erythrocytes and lymphocytes. Fluorescent analysis showed not only that the microspheres had high specific binding to monoclonal anti-thy-12, but also the presence of biotinyl groups on the cell surface of erythrocytes and lymphocytes when acetyl avidin was attached to the fluorescent microspheres.

Towards the mid 1980's fluorescent analysis was used as an analytical tool in the determination of the elements aluminium, copper, silver, etc., present in various media. This once again promoted the use of fluorescent tagging agents.

In 1985, Salgado Ordonez *et al.*⁶ used di-2-pyridyl ketone 2-furoylhydrazone as a fluorescent tagging agent to detect the concentration of aluminium (Al) in seawater. The tagging agent formed a complex with Al and, through fluorometry, Al concentrations of between 10 and 100 ng/mL were determined.

In another study, Gutierrez *et al.*⁷ used 1,1,3-tricyano-2-amino-1-propene as a fluorescent tagging agent in 1986, to determine copper concentrations in blood serum samples. Copper catalyses the oxidation of the reagent rather than complexing with it. Several kinetic methods including this particular fluorometric method is capable of detecting small concentrations of copper (1 to 35 ng/mL) with a sensitivity of about 100 times greater than spectroscopic methods.

A similar application with a similar concept, carried out in 1986 by Afonso *et al.*,⁸ involved the use of the fluorescent tagging agent pyrocatechol-1-aldehyde 2-pyridylhydrazone to detect silver in panchromatic plates. The use of this tagging agent provided information on kinetic parameters and interferences that were present.

As mentioned before, ¹⁴C is a very popular tagging agent for polymers. One of its applications, shown by Martinkenneth *et al.*⁹ in 1987, was its attachment to polyacrylate polymers to study its behaviour in a horizontal flow tank containing soil. Results showed great retention of the polymer as is expected in more conventional landfill soils. The use of the ¹⁴C tag once again proved successful for studying the behaviour of complex materials.

In 1988 Tang *et al.*¹⁰ used pyrene as a fluorescent tagging agent for polystyrene, to study the glass transition temperature (T_g). A series of pyrene end-labelled polystyrene (PS) samples, having molecular weights of between 200 and 40 000, were synthesised. This end-labelling reaction was performed by coupling the polystyryl anion with 1-bromobutylpyrene. The T_g was successfully determined and, furthermore it was found that the reaction lead to an enhancement in the thermal and hydrolytic stability of PS and the T_g of the end-labelled PS was also higher than that of the unlabelled PS, which was consistent with the Fox-Flory equation.

Assuming at this point that applications utilising fluorescent tags are exhausted, is obtuse. The 1980's merely provided a platform for the growth in the utilisation of fluorescent tags:

In 1991, Tenaka and Kirschner¹¹ used rhodamine as a fluorescent tagging agent. Microtubules of live frog embryonic neurons were tagged in an attempt to understand how microtubules were generated in the growth cone. The embryonic neurons were labelled by injecting rhodamine-labelled tubulin into the fertilised egg. Microtubule growth and the shrinkage in the growth cones could now be investigated. Results showed that the binding

of microtubules appeared to be critical in generating a new axon and, further, that the orientation of the microtubules might be an important step in neuronal path finding.

Using pyrene as a tagging agent, either covalently bonded to a polymer chain or physically dispersed in a novolac matrix, the effects of various casting parameters for films of novolacs (cresol-formaldehyde resins) were measured by Kosbur and Frank,¹² in 1992. Aggregation of the dispersed pyrene was observed by excimer fluorescence and crystallite formation of the pyrene. Results showed that phase separation was enhanced in static-cast films over spin-cast films and that pyrene aggregation is more dependent on the type of casting solvent and host polymer rather than the interaction of either with the pyrene itself.

In 1992 Capitan *et al.*¹³ used carminic acid as a fluorescent tagging agent for the simultaneous detection of trace amounts of molybdenum and tungsten. When molybdenum and tungsten are reacted with carminic acid a red fluorescence is given off, which is described by solid-phase spectrofluorometry. This method permitted for the detection of molybdenum and tungsten in synthetic mixtures in natural waters.

Anthracene is another common fluorescent tagging agent with diverse applications. An example, as described by Carlier *et al.*¹⁴ in 1993, includes its use for studying the microenvironment of supported species through non-radiative energy transfer and site accessibility. Copolymers were labelled with a carbazole chromophore (mainly in the form of a styryl derivative) and anthracene and were either crosslinked or grafted on porous silica. The carbazole chromophore was involved as an energy transfer donor, whilst the anthracene probes were generally dissolved in the solvent phase. By using the Stern-Volmer theory, whereby values are dependent on the solvent and polymer structure, information on this novel system was obtained.

Ridler and Jennings¹⁵ used fluorescent dyes in 1996 to tag the polynucleotides poly A, poly C and poly G, to observe the binding geometry and the conformation of the nucleotides when subjected to an electric field. Generally, a molecule in an electric field rotates into alignment and, in the case of polymers tagged with fluorescent dyes, such alignments are easily reflected by fluorescence. This particular application of fluorescent dyes and polynucleotides was beneficial in reflecting the base-sequence sensitivity of specific drugs for polymeric genetic material.

A copolymer consisting of sodium acrylate (NaA) and laurylmethacrylate (LM) was fluorescently tagged with fluorescein in 1998 by Blonk *et al.*¹⁶ to observe its localisation in a lamellar liquid. The continuous phase of the lamellar dispersion, a liquid detergent system, was a concentrated electrolyte solution. Fluorescent confocal scanning light microscopy was the method used to conduct and analyse the experiment. The localisation studies showed that a high concentration of the polymer was present at the interface between the lamellar droplet and the continuous electrolyte phase. Faint fluorescent signals were also observed inside the lamellar droplets and a fraction of the polymer was responsible for this fluorescence. Use of the fluorescent tagging agent and confocal scanning light microscopy demonstrated that the localisation of the NaA/LM type decoupling polymer was present in the outer regions of the lamellar droplets although the thickness of the outer region could not be measured.

The development of fluorescent sensors for the detection of organic molecules, via the procedure of template polymerisation or molecular imprinting, is of great importance in chemical, biological and pharmaceutical applications. In one particular application Liao *et al.*¹⁷ developed a fluorescent sensor in 1999, which was specific for the detection of the amino acid tryptophan. The fluorescent sensor was composed of a functional monomer with a fluorescent probe attached to it. The fluorescence could be quenched by 4-nitrobenzaldehyde. With the addition of the template tryptophan, the fluorescence intensity of the imprinted polymer/quencher increased in a concentration-dependent fashion. This was presumably because of the displacement of the quencher from the binding sites, via tryptophan. The effect of phenylalanine and alanine on the fluorescence intensity was remarkably smaller than that of tryptophan. This was due to the fact that the approach did not require the *de novo* design of the complementary binding site and also it did not depend on any specific structural features of the template molecule. Using a similar approach, the development of fluorescent sensors for the detection of other compounds could become very useful.

2.3 The turn of the century: 2000 - 2004

In April of 2000, Ladaviere *et al.*¹⁸ used a peptide sequence consisting of positively charged amino acids (lysine or arginine) as a tagging agent to study electrostatically driven immobilisation of peptides onto maleic anhydride-alt-methyl vinyl ether (MAMVE) copolymers in aqueous media. Grafting was achieved by adding the amino terminus of the

positively charged amino acids to the negatively charged copolymer, resulting in an electrostatic attractive interaction between the copolymer and the tagged peptides. Utilisation of tagged peptides showed that immobilisation was more enhanced with arginine than it was with lysine, proving that the effect was due to an electrostatic driving force.

The ability to synthesise fluorescent sensors for various analytes via template directed polymerisation or molecular imprinting holds promising for the preparation of fluorescent tags with high affinity and specific binding sites for different template molecules. Liao *et al.*¹⁷ proved this in 1999. With this in mind Gao *et al.*¹⁹ synthesised a fluorescent tag for the detection of the carbohydrate D-fructose using template directed polymerisations in 2001. The monomer that was produced was used for the preparation of imprinted polymers as sensitive fluorescent sensors for fructose. The imprinted polymers were capable of showing significant fluorescent intensity when bound to the template carbohydrate.

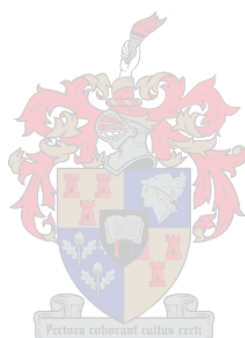
In 2002 Wang *et al.*²⁰ chemically modified poly (styrene-co-maleic anhydride) (SMA) with a fluorescent dye, 4-amino-*N*-(2,4-dimethylphenyl)-1,8-naphthalimide, to produce fluorescent poly (styrene-co-maleimide) (SMI). Fourier transform infrared (FT-IR), Ultraviolet – Visible (UV-Vis) and fluorescence studies showed that the polymer can emit strong yellow green fluorescence ($\pm 510\text{nm}$). Its thermal stability and solubility was improved, and the Tg and influences of solvent etc. could also be determined.

Southard *et al.*²¹ extended this concept in 2004 by producing polyelectrolytes (PDI<1.2) that were fluorescently tagged with single fluorophores, to study the kinetics of absorption-desorption of polyelectrolytes on solid surfaces. The incorporation of the fluorescent tag made it possible to show that poly(*t*-butylmethacrylate) polymers, absorbed onto pigments from solution, had a great influence on adhesion, pigment dispersion, rheology, foaming, wetting and gloss in coatings.

2.4 Conclusions

From this brief historical introduction it is clear that much has been achieved in the field of tagged polymers during the last 30 years. However, although tagged polymers have been synthesised and applied in numerous fields, it follows from this historical journey that certain aspects concerning chemically induced product marking remain unmentioned. This

is because detailed information about the properties and functionality of tagging agents used for product registration purposes cannot be revealed due to the protection of intellectual property. The following chapters will address the synthesis and utilisation of novel fluorescent polymers as commercial tagging agents for use in the paint industry.



References:

- (1) Dixon, J. K.; Tilton, C.; Murphy, J. *Water Research* **1974**, *8*, 659-665.
- (2) Sariban, A. A.; Birshtein, T. M.; Skvortsov, A. M. *Polymer Science U.S.S.R* **1977**, *19*, 2977-2992.
- (3) Aharoni, S. M. *Polymer* **1978**, *19*, 401-406.
- (4) Ridler, P. J.; Jennings, B. R. *Polymer* **1978**, *19*, 627-631.
- (5) Kaplan, M. R.; Calef, E.; Bercovici, T.; Gitler, C. *Biochimica et Biophysica Acta (BBA) - Biomembranes* **1983**, *728*, 112-120.
- (6) Salgado Ordonez, M.; Garcia de Torres, A.; Cano Pavon, J. M. *Talanta* **1985**, *32*, 887-891.
- (7) Gutierrez, M. C.; Gomez-Hens, A.; Valcarcel, M. *Talanta* **1986**, *33*, 567-570.
- (8) Afonso, A. M.; Santana, J. J.; Garcia Montelongo, F. *Talanta* **1986**, *33*, 779-783.
- (9) MartinKenneth, J. E.; HowardLawrence, W. F.; King, W. *Nuclear and Chemical Waste Management* **1987**, *7*, 273-280.
- (10) Tang, W. T.; Hadziioannou, G.; Smith, B. A.; Frank, C. W. *Polymer* **1988**, *29*, 1718-1723.
- (11) Tanaka, E. M.; Kirschner, M. W. *The Journal of Cell Biology* **1991**, *115*, 345-363.
- (12) Kosbar, L. L.; Frank, C. W. *Polymer* **1992**, *33*, 141-151.
- (13) Capitan, F.; Sanchez-Palencia, G.; Navalon, A.; Capitan-Vallvey, L. F.; Vilchez, J. L. *Analytica Chimica Acta* **1992**, *259*, 345-353.
- (14) Carlier, E.; Revillon, A.; Chauvet, J. P. *Eur. Polym. J.* **1993**, *29*, 825-830.
- (15) Ridler, P. J.; Jennings, B. R. *Polymer* **1996**, *37*, 4953-4960.
- (16) Blonk, J. C. G.; van de Pas, J. C.; Visser, A.; Brouwn, L. F. *Colloid and surfaces: A: physicochemical and engineering aspects* **1998**, *144*, 287-294.
- (17) Liao, Y.; Wang, W.; Wang, B. *Bioorganic Chemistry* **1999**, *27*, 463-476.
- (18) Ladaviere, C.; Lorenzo, C.; Elaissari, A.; Mandrand, B.; Delair, T. *Bioconjugate Chemistry* **2000**, *11*, 146-152.
- (19) Gao, S.; Wang, W.; Wang, B. *Bioorganic Chemistry* **2001**, *29*, 308-320.
- (20) Wang, K.; Hauang, W.; Xia, P.; Gao, C.; Yan, D. *Reactive and Functional Polymers* **2002**, *52*, 143-148.
- (21) Southard, G. E.; Woo, J. T. K.; Massingill, J. L. *Progress in Organic Coatings* **2004**, *49*, 160-164.

Chapter 3

Theoretical background

3.1 Molecular fluorescence spectroscopy

Luminescence, first observed by Monardes in 1565, is one of the oldest and most established analytical techniques. Work conducted by Sir David Brewster in 1833 on the red emission from chlorophyll also paved the pathway for Sir G. G. Stokes who later described the mechanism of the absorption as an emission process in 1852.¹

Luminescence, comprising fluorescence, chemiluminescence, phosphorescence and atomic fluorescence, renders some of the most sensitive and opportune methods for chemical analysis. This is reflected by the increasing number of papers, reviews and monographs published annually, resulting in luminescence being one of the most industrious fields of research in science today.

3.1.1 Types of luminescence

Luminescence can be differentiated into several classes according to the mechanism by which energy is supplied to excite the luminescent molecule. *Photoluminescence* can be defined as the interaction of a molecule with photons of electromagnetic radiation. If the release of electromagnetic energy is instant or from the singlet state, then the process is called *fluorescence* (this mechanism will be emphasized on later). *Phosphorescence* on the other hand is a delayed release of energy from the triplet state. If chemical energy is the source of the excitation energy then the process is referred to as *chemiluminescence*, whereas, *bioluminescence* occurs as a result of the electromagnetic radiation released by organisms. Other types of luminescence include *triboluminescence*, which occurs as a result of the energy released when certain crystals, like sugar, are broken down.

Cathodoluminescence is the release of energy by exposure to cathode rays and *thermoluminescence* is the emission of energy at a temperature below red heat by material existing in high vibrational energy levels, after being exposed to minute amounts of thermal energy.¹

3.1.2 Theory of molecular fluorescence

Light is a form of electromagnetic radiation, the propagation of which is regarded as a wave phenomenon. When light ‘impinges’ upon matter it can either be absorbed or pass through without absorption occurring. When a molecule absorbs light, energy is transferred through the absorption process. The absorption of energy occurs via integral units called quanta and the quanta-energy relationship can be expressed by the equation

$$E = h\nu = \frac{hc}{\lambda} \quad 3.1$$

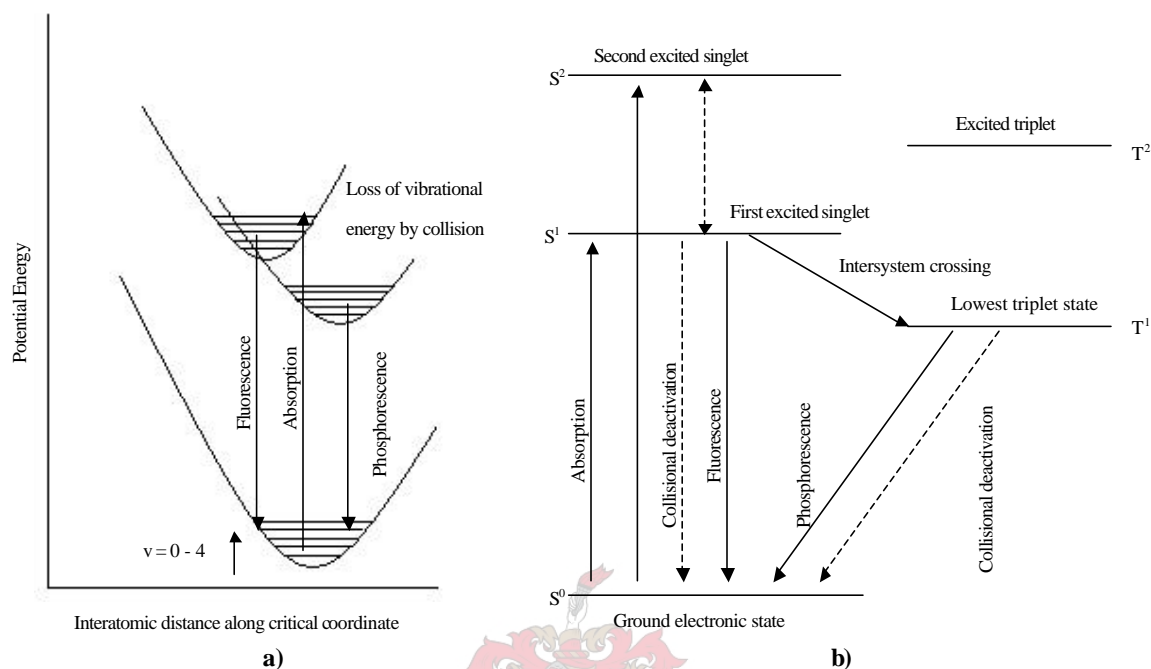
where h is Planck’s constant (6.62×10^{-27} J.Hz), ν is the frequency of light (Hz), c is the velocity of light (3×10^{10} cm/sec) and λ is the wavelength (nm).

Every molecule contains an array of closely spaced energy levels and may also exhibit various vibrational levels between each main electronic energy state. Scheme 3.1a represents the various potential energy levels of a diatomic molecule.

0 to 4 in Scheme 3.1a represents the various vibrational levels; 0, 1, 2, 3, 4. The ground state is indicated by S^0 , the first excited singlet electronic state by S^1 and the first excited triplet state by T^1 .

When a molecule is in the ground state, S^0 , it usually has an even number of electrons, with paired spins (S): one electron with $S = +\frac{1}{2}$ and another with $-\frac{1}{2}$. Multiplicity (M_s), a term used to express the orbital angular momentum of a given state, is related to spin by the equation ($M_s = 2S + 1$). Thus, when all electrons are paired, $S = 0$ ($+\frac{1}{2}, -\frac{1}{2}$) and $M_s = 1$. This is called the singlet electronic state. If the spin of any single electron is reversed, the molecule then endows two unpaired electrons and $S = 1$ ($+\frac{1}{2}, +\frac{1}{2}$). Hence, multiplicity is equal to three and this electronic state is indicative of the triplet state. The difference between

the singlet and triplet states is therefore merely the difference between the spins of electrons, S .



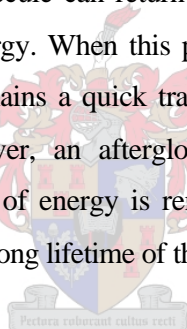
Scheme 3.1: a) Potential energy-level diagram of a diatomic molecule and b) the various transitions occurring within a).

When a quantum of light 'impinges' on a molecule, it can be absorbed in approximately 10^{-15} sec. This absorption is, however, highly specific as radiation of a 'particular' energy is absorbed only by a characteristic structure. When a molecule absorbs light of equal energy to the difference between the two energy states then a transition from a lower to a higher energy electronic state occurs. Such a transition from a lower to a higher electronic state is merely an elevation of an electron to an upper excited singlet state, S^1 , S^2 , etc. Absorption transitions usually originate in the lowest vibrational level of the ground electronic state and these ground to singlet transitions are responsible for the visible and ultraviolet absorption spectra observed for molecules.

The molecule now remains in an excited state and this occurs for approximately 10^{-4} sec.² The lifetime of an excited species is momentary, as there are a number of ways by which an excited atom or molecule can give up its excess energy and relax to its ground state. Firstly, energy that is in excess of the lowest vibrational level ($v = 0$) of the excited singlet state is attained. If the excess energy is not further 'dissipated', for example by collisions with other molecules, the electrons merely return to the electronic ground state through the emission of

energy; a phenomenon which is referred to as fluorescence. Emitted energy, which is indicative of fluorescence, is of a longer wavelength than the energy that was absorbed, as some energy is lost in the brief period before emission.

It is imperative not to confuse the difference between fluorescence and phosphorescence. With reference to Scheme 3.1b, phosphorescence is shown to involve an intersystem crossing³ or transition from the singlet to the triplet state. As mentioned previously, the triplet state is attained when one of the electrons changes its spin so as to obtain the same spin as the other electron. Hence, phosphorescence is the transition from the singlet state to the triplet state, whilst fluorescence remains as the transition from the singlet state to the ground state. A transition from the ground state to the triplet state is almost forbidden, whereas a conversion from the singlet to the triplet state is more probable due to the difference in energy between the levels. When the energy of the lowest vibrational level of T^1 is lower than that of S^1 , the molecule can return directly to S^0 . A return via S^1 would still require an external source of energy. When this phenomenon occurs, it is called delayed fluorescence. Hence, fluorescence remains a quick transition between energy levels, which is indicated by emitted energy. However, an afterglow displayed by the molecule⁴, which occurs even after the exciting source of energy is removed, characterizes phosphorescence. This occurs as a result of the relatively long lifetime of the triplet state.



3.1.3 Types of fluorescence and emission processes

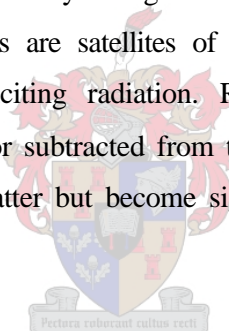
Fluorescence that commonly occurs in solution is referred to as Stokes fluorescence. This process involves the re-emission of photons that have a lower energy than that of the absorbed photons. Hence, the re-emitted photons are of a longer wavelength and lower frequency than the absorbed ones. If the emission of photons with a shorter wavelength than that which was absorbed occurs by a molecule that contains a number of highly populated vibrational levels, or one that is excited by thermal energy, then the process is referred to as anti-Stokes fluorescence. This process often occurs in dilute gases at high temperatures. A common example of this is the green emission from copper-activated cadmium sulphide excited by red light.¹

The re-emission of photons possessing the same energy as those that were absorbed undergoes a process called resonance fluorescence. This particular type of fluorescence will never occur in solution due to energy that can be emitted via the interaction with solvent

molecules. Resonance fluorescence occurs in gases and crystals. It also forms the basis for atomic fluorescence.

If a molecule absorbs a photon and re-emits within the same time frame (10^{-15} sec), the electron returns to its original state and the energy is totally conserved. During this process, the molecule is excited to a higher vibrational level with no electronic change. The emitted light is referred to as Rayleigh scattering and it has the same wavelength as the exciting light since the absorbed and emitted photons are of the same energy. Rayleigh scattering can occur at all wavelengths, however, its effect can become minimised at longer wavelengths. It may also be problematic when the absorption and fluorescence spectra of a substance are closely related and when the intensity of fluorescence is low compared to the exciting radiation.

Raman scattering, which is related to Rayleigh scattering, is another form of scattering. Raman scattering appears more commonly at higher wavelengths, although it can also occur at lower wavelengths. Raman bands are satellites of the Rayleigh-scatter, with a constant frequency difference from the exciting radiation. Raman bands occur as a result of vibrational energy either added to or subtracted from the excitation photons. Hence, Raman bands are weaker than Rayleigh scatter but become significant when high intensity sources are used.



3.1.4 Advantages of fluorescence

Fluorescence has become a useful tool in analytical techniques as fluorometric methods can detect substances with concentrations as low as one part in ten billion. This high sensitivity is due to the fact that emitted radiation is measured directly and its intensity can be altered instantaneously, with a change in the exciting light. This is one of the main reasons why fluorometric methods have a sensitivity of about 1000 times greater than spectrophotometric methods.

Other advantages that fluorometry has over spectrophotometry includes the fact that, in fluorescence, two wavelengths are used, whilst in spectrophotometry only one wavelength is used. This is extremely useful when more than one compound with similar absorption spectra are being examined. In fluorescence the compounds may have the same absorption spectra but will have different emission peaks (if emission wavelength is the same as excitation wavelength, it is known as scatter). The difference between excitation and emission peaks

range from 10 to 280 nm, hence the compounds can be differentiated. However, this may pose a problem in spectrophotometry. Another point to note is that there are fewer fluorescent compounds as compared to absorbing compounds and this increases the specificity of fluorescence. All fluorescent compounds can absorb light but not all absorbing compounds can fluoresce.

3.1.5 Factors affecting fluorescence

3.1.5.1 Properties of fluorescent compounds

Factors that influence the fluorescent behaviour of a compound include the structure, rigidity and nature of any substituents in the molecule or close to the fluorescent centre. With respect to structure, fluorescence is more enhanced in aromatic compounds when compared to heterocyclic aliphatic or saturated hydrocarbons. Heterocyclic aliphatic compounds contain nonbonding electrons, which undergo excitation to the π^* orbital. An energy difference from nonbonding electrons to the π^* orbital is much lower than a transition from the π to the π^* orbital (Fig. 3.1), hence heterocyclic aliphatic compounds exhibit a low fluorescence intensity.

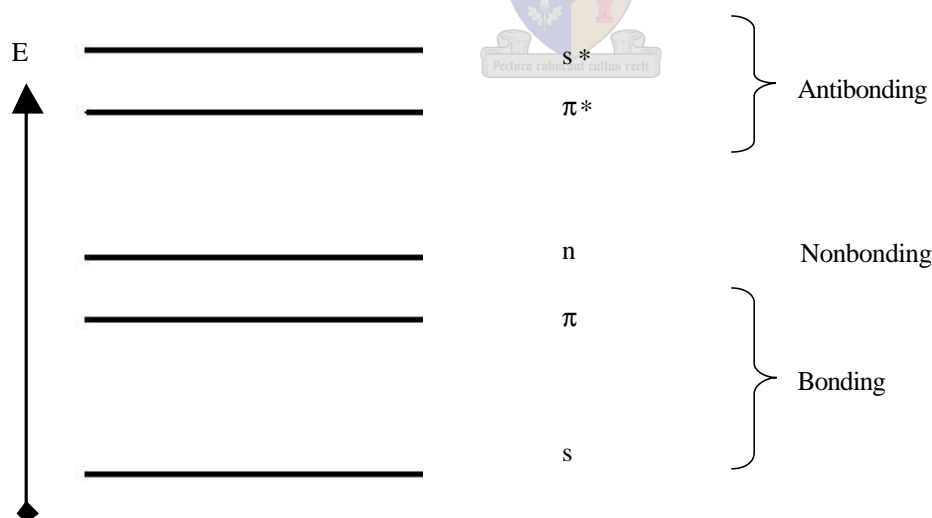


Figure 3.1 Transitions involved in the absorption process.

Saturated hydrocarbons have electronic transitions involving s-binding electrons since there are no π -bonding or non-bonding electrons. The transitions involving s-electrons show significant bond disruption in the molecule as these transitions occur at very high energy

levels. Since energy is inversely proportional to wavelength, saturated hydrocarbons show very weak fluorescence (quantum efficiency $\sim 10^{-3}$), which occurs in the 140 to 170 nm region (vacuum ultraviolet).

Aromatic compounds contain π -electrons, which can undergo excitation to π^* antibonding orbitals by the absorption of fairly low energy. Energy transitions from π to π^* result in a very high fluorescent intensity. In addition to this, aromatic hydrocarbons are not as strongly bonded as s-electrons and therefore excitation does not involve extensive bond disruption. Thus, aromatic hydrocarbons display ideal fluorescence.¹ Table 3.1 provides a summary of the above-mentioned orbital transitions that occur in the different types of structural compounds, with respect to fluorescence intensity.

Table 3.1: Transitions involved in the absorption process with respect to fluorescent properties.

Transition	Compound type	Fluorescence intensity	Comments
n to π^*	Heterocyclics	Medium	Observed in fluorometry
π to π^*	Aromatic hydrocarbons	Strong	Observed in fluorometry
s to π^*	Saturated hydrocarbons	Weak	Not observed (high energy – low I)

It has been shown experimentally that fluorescence is enhanced in more rigid molecules, e.g. the quantum efficiency (f) of fluorene is 1.0 whereas that of biphenyl is 0.2.² (Fig. 3.2) The difference can be attributed to the increased rigidity of fluorene due to the bridging methylene group. Increased rigidity lowers the rate of nonradiative relaxation to a point where relaxation by fluorescence has more time to occur.



Figure 3.2: Effect of rigidity on fluorescence intensity.

Changes in fluorescence efficiency can also be attributed to substitution on an aromatic ring, whereby the substituent can alter the wavelength of absorption as well as the chemical and physical properties of the compound, and thereby affect fluorescence efficiency.¹ For example, the relative fluorescence intensity of benzene is 10, toluene 17 and chlorobenzene 5.² Generally, ortho-para-directing substituents (e.g. -OH, -OCH₃) often enhance fluorescence, whilst meta-directing substituents (e.g. carbonyl substituents and -NO₂ groups) suppress it. This is because meta-directing substituents exhibit n to π^* transitions.

3.1.5.2 Photochemical decomposition

The use of certain excitation sources such as ultraviolet light may result in photochemical decomposition of the fluorescent compound, eventually resulting in a decrease of the reading. Measures that can be taken to prevent decomposition include measuring fluorescence instantly and not allowing the exciting light to interact with the sample for long periods of time.⁵ Other measures include using exciting radiation with longer wavelengths and photochemically protecting unstable compounds from sunlight or other laboratory light sources.

3.1.5.3 Temperature

An increase in temperature increases the molecular motion and collisions of a compound, which can result in a loss of energy and therefore decrease fluorescence.^{6,7} The change in fluorescence is normally 1% per 1°C, but it can vary between different compounds. For example, in compounds such as tryptophan and rhodamine B the change can be up to 5% per 1°C. Increases in temperature can also produce more band maxima due to the increase in the number of higher vibrational levels.^{8,9} For this reason it is best to maintain all samples and standards at the same temperature whilst measuring fluorescence.¹⁰

3.1.5.4 Concentration



$$F = fI_0(1 - e^{-abc}) \quad 3.2$$

With references to the above equation, where f is the quantum efficiency, I_0 is the incident radiant power, e is the molar absorptivity, b is the path length of the cell and c is

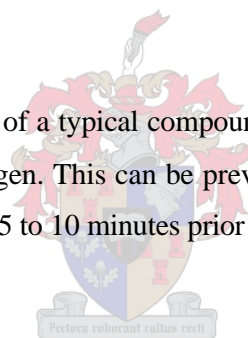
the molar concentration, fluorescence intensity is proportional to low concentrations and reaches a maximum at higher concentrations.²

In addition, Eqn. 3.2 indicates that there are three major factors that affect fluorescence intensity.^{1,3}

- The greater the quantum efficiency f , the greater will be the fluorescence.
- The more intense the incident radiation I_0 from the source is, the greater the fluorescence intensity. However, a very intense source can cause photodecomposition of the sample. Mercury or Xenon lamps have been used to circumvent this problem.
- The higher the molar absorptivity ϵ , the better will be the fluorescence intensity of the compound will be. It is for this reason that saturated nonaromatic compounds are nonfluorescent.

3.1.5.5 Oxygen quenching

The fluorescence intensity of a typical compound is reduced by ~20% if it is present in a solution containing 10^{-3} M oxygen. This can be prevented by bubbling an inert gas, such as nitrogen, through the solution for 5 to 10 minutes prior to analysis.



3.1.5.6 pH quenching

The fluorescence spectra of most aromatic compounds containing acidic or basic functional groups are extremely sensitive to the pH of the solution. An excellent example is 2-naphthol, which exhibits a single broad fluorescence peak in aqueous solution at 395 nm, whilst the 2-naphtholate anion exhibits a fluorescence peak at 429 nm. Thus, pH can be used as a parameter in fluorometric analysis to obtain the most strongly fluorescent species for analysis.

3.2 Free radical polymerisation

3.2.1 Kinetics

Essential for copolymer synthesis, is an understanding of chemical kinetics during homo- and copolymerisation. This section will review the kinetics of free radical initiated polymerisations and copolymerisations.

(1) Initiation, (2) propagation, and (3) termination are the three main kinetic steps that occur during polymerisation. Methods that can be used to initiate free radical polymerisations are thermal initiation or high-energy radiation of the monomers. However, the addition of initiators, when heated or irradiated, allow for the formation of free radicals. Benzoyl peroxide (BPO) and azobisisobutyronitrile (AIBN) are two common examples of such compounds, which facilitate the formation of free radicals.

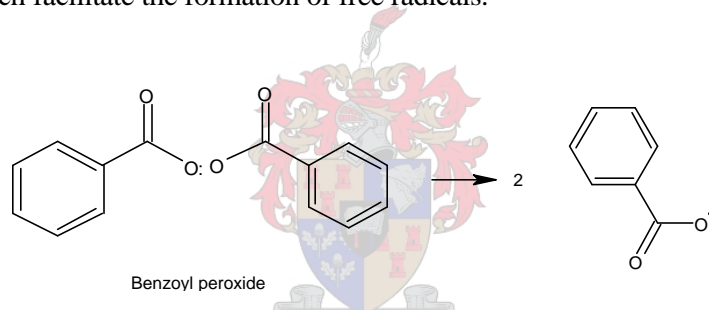


Figure 3.3: Generation of free radicals by thermal decomposition of benzoyl peroxide.

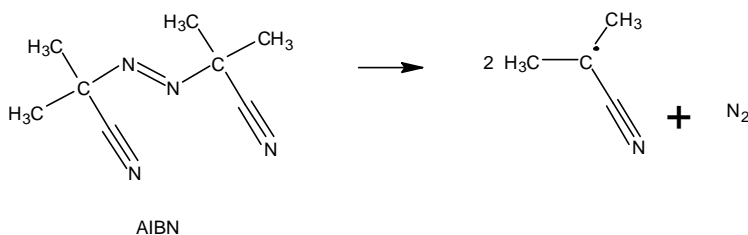
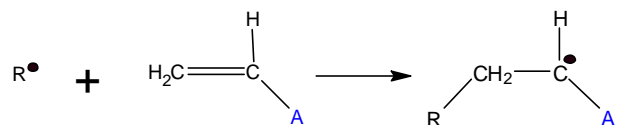


Figure 3.4: Thermal decomposition of AIBN to form two radicals and nitrogen.

Depicted in Fig. 3.3 is the thermal decomposition of BPO to form two oxy-radicals. Fig. 3.4 illustrates the decomposition of AIBN to form two nitrile stabilized carbon based radicals (reaction 3.a).



where K_d is the rate constant which describes the first order decomposition process. The radical that is formed can now add to the double bond of the monomer and initiate polymerisation:



(M) will represent the monomer and the rate constant for this process will be k_i , as described in reaction 3.b.



These two reactions, the radical generation and the addition to the monomer, forms the process of initiation. Usually, the assumption that is taken into consideration is that the first step is the rate-determining step. The rate of radical formation, r_i is illustrated by the following equation:

$$r_i = \frac{d[M_1^\bullet]}{dt} = 2k_d[I] \quad 3.3$$

The numerical 2 is obtained from the fact that a maximum of two radicals can be generated for the initiation:

$$\frac{-d[I]}{dt} = \frac{1}{2} \frac{d[M_1^\bullet]}{dt} = k_d[I] \quad 3.4$$

However, not all of the primary radicals that are produced by the decomposition of the initiator will inevitably react with the monomer, meaning that several other competing reactions may occur.¹¹ Therefore, to permit for the determination of the rate of initiation, the fraction of initially formed radicals that actually starts chain augmentation will be denoted by f , and the rate of the initiation becomes:

$$r_i = \frac{d[M^\bullet]_i}{dt} = 2fk_d[I] \quad 3.5$$

The propagation of the reaction will now proceed via the consecutive addition of monomer. An expression to best explain this is the form:



Flory^{12,13} postulated the assumption that the reactivity of the addition of each monomer is independent of the chain length, which is evident in the above two equations. The propagation rate constant, k_p , used for both these equations implies that the rate constant is independent of chain length. The rate of the propagation, r_p , of this polymerisation, or the rate of monomer depletion, is thus given by:

$$r_p = \frac{-d[M]}{dt} = k_p [M \bullet] [M] \quad 3.6$$

Termination of growing radical chains occurs in two ways: the formation of a new bond in-between the two radicals, which is called combination and termination by a process where a hydrogen atom from one of the chains is transferred to the other, which is called disproportionation. The chain that the proton was removed from forms a double bond. The mechanisms can be seen in Figs. 3.5 and 3.6.

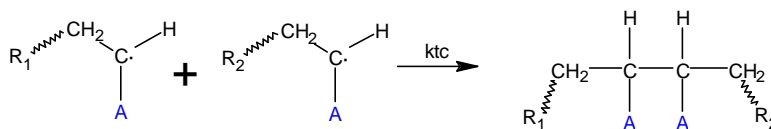


Figure 3.5: Termination by combination.

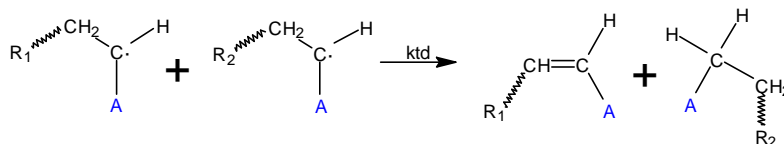


Figure 3.6: Termination by disproportionation.

Schematically, the reactions can be represented as follows:



where k_{ic} denotes the rate constant of termination by combination, and k_{id} the rate constant of termination by disproportionation. As both of these reactions use two radical species and have similar kinetics, the overall equation for the rate of termination is:

$$r_t = \frac{-d[M\bullet]}{dt} = 2k_t[M\bullet]^2 \quad 3.7$$

where $k_t = k_{ic} + k_{id}$ and the numerical 2 implies that there are two radicals that are terminated in each termination reaction. Both the temperature and the monomer structure determine the type of termination that is most dominant in any given reaction. For most systems, the amount of one termination type far exceeds the other.

At this point, the rate of polymerisation, R_p , and the degree of conversion as a function of time can be established. The assumption of the steady state concentration of transient species must be used here, where the transient species is radical $M\bullet$. For the steady state approximation to hold true, the rate at which initiation occurs, r_i , must be equal to the rate at which termination occurs, r_t . Basically, radicals must be generated at the same rate at which they are terminated. This assumption leads to the following equation:



$$fk_d[I] = 2k_t[M\bullet]^2 \quad 3.8$$

which gives an expression for the radical species:

$$[M\bullet] = \left(\frac{fk_d[I]}{k_t} \right)^{\frac{1}{2}} \quad 3.9$$

To make use of this equation experimentally would be difficult. However, by substituting Eqn. 3.9 in Eqn. 3.10 the rate of polymerisation, R_p , can be obtained:

$$R_p = \frac{-d[M]}{dt} = k_p \left(\frac{fk_d[I]}{k_t} \right)^{\frac{1}{2}} [M] \quad 3.10$$

It can now be deduced that the rate of polymerisation is directly proportional to the monomer concentration and to the initiator concentration to the one half power. R_p is first order with regards to the monomer concentration.

Assuming that the initiator concentration is an exponential decay, the consumption of the initiator can be added into the calculations. Hence, initiator consumption can be formulated as follows:

$$\frac{d[I]}{dt} = k_d[I] \quad 3.11$$

Then, by the process of mathematical integration:

$$[I] = [I]_0 e^{-k_d t} \quad 3.12$$

Thus, the rate of polymerisation becomes:

$$R_p = \left[k_p \left(\frac{fk_d}{k_t} \right)^{\frac{1}{2}} \right] \left[[I]_0^{\frac{1}{2}} [M] \right] e^{-k_d \frac{t}{2}} \quad 3.13$$

This equation can be broken down into three different parts.

The first term suggests that the rate of polymerisation is proportional to $\frac{k_p}{k_t^{1/2}}$. When experiments are performed to probe kinetics of reactions in solution, the expected first order dependence on monomer concentration is observed. However, when experiments are performed in concentrated solvents or even in bulk, the polymerisation kinetics accelerate. The reason for this is that the viscosity increases as the polymerisation proceeds because the polymer has a higher viscosity than the monomers. k_p is not affected, but k_t is.

The second term indicates that the rate of polymerisation is still proportional to the monomer concentration to the first power and the initiator concentration to the one half power, however, the initiator concentration is now the initial concentration. Hence, in solution

polymerisation, by increasing the initial concentration of an initiator, the rate of the reaction should proportionally increase to the square root of the amount of initiator added.

The third term indicates that as the initiator is consumed, the polymerisation slows down exponentially with time. It also slows as the monomer is depleted.

By knowing that:

$$R_p = \frac{-d[M]}{dt} \quad 3.14$$

the degree of conversion can now be expressed as a function of time. Substituting the earlier equation for R_p (Eqn. 3.13) and integrating it one obtains the following:

$$\ln \frac{[M]_0}{[M]} = 2k_p \left(\frac{fk_d}{k_t} \right)^{\frac{1}{2}} [I]_0^{\frac{1}{2}} \left(1 - e^{-k_d \frac{t}{2}} \right) \quad 3.15$$

In addition, $\left(\frac{[M]_0 - [M]}{[M]_0} \right)$ equals the degree of conversion and is the fraction of the monomer that has been reacted, where $[M]$ is the concentration of the monomer that is left after the reaction and $[M]_0$ is the initial monomer concentration. Thus, $[M]_0 - [M]$ is the concentration of the monomer that has reacted. The conversion can be expressed as:

$$\text{Fractional conversion} = \frac{[M]_0 - [M]}{[M]_0} = 1 - \frac{[M]}{[M]_0} \quad 3.16$$

which can also be expressed as:

$$\text{Conversion} = 1 - \exp \left[- 2k_p \left(\frac{fk_d}{k_t} \right)^{\frac{1}{2}} [I]_0^{\frac{1}{2}} \left(1 - e^{-k_d \frac{t}{2}} \right) \right] \quad 3.17$$

As is always expected, the conversion never reaches 100% or a factor of 1 given by the exponential term. Therefore, at infinite time, the expression that is obtained for maximum

conversion that is less than 1, by an amount that is dependent on the initial initiator concentration, is:

$$\text{Maximum conversion} = 1 - \exp\left[-2k_p\left(\frac{fk_d}{k_t}\right)^{\frac{1}{2}}[I]_0^{\frac{1}{2}}\right] \quad 3.18$$

The conversion theoretically approaches a value of 1 after prolonged periods of time if the steady state approximation for the initiator concentration had been carried through these calculations and equations.

In free radical polymerisations, distributions of the average chain lengths during and after a polymerisation are evident, due to the random termination reactions that occur in the solutions. The kinetic chain length, ν , is the rate of monomer addition to growing chains over the rate at which chains are initiated by radicals. This is the expression for the number average chain length, which is the average number of monomer units per growing chain radical at a certain instant.¹⁴ Hence, the initiator radical efficiency in polymerising the monomers is:

$$\nu = \frac{r_p}{r_i} = \left[\frac{k_p[M]}{2(fk_d k_t)^{\frac{1}{2}}[I]^{\frac{1}{2}}} \right] \quad 3.19$$

Termination occurring mainly by combination results in the chain length of the polymer chains doubling in size (on average), assuming nearly equal length chains combine. But, if the growing chains do not undergo any change in chain length during the process, disproportionation primarily occurs. The expressions are thus:

$$\bar{x}_n = 2\nu \quad (\text{termination by combination}) \quad 3.20$$

$$\bar{x}_n = \nu \quad (\text{termination by disproportionation}) \quad 3.21$$

\bar{x}_n , a term used to more generally express the average chain length of the growing polymer chain, is the average number of dead chains produced per termination, \mathbf{x} . This value is equal to the rate of dead chain formation over the rate of termination reactions. Taking into account

that in combination only one dead chain is produced, and in disproportionation reactions two dead chains are produced, the equations can therefore be written as:

$$\text{Rate of dead chain formation} = (2k_{td} + k_{tc})[M\bullet]^2 \quad 3.22$$

$$\text{Rate of termination reactions} = (k_{tc} + k_{td})[M\bullet]^2 \quad 3.23$$

$$\mathbf{x} = \frac{k_{tc} + 2k_{td}}{k_{tc} + k_{td}} = \frac{k_{tc} + 2k_{td}}{k_t} \quad 3.24$$

In addition, the instantaneous number average chain length can be expressed in terms of the rate of addition of the monomer units divided by the rate of dead polymers forming. This is illustrated as:

$$\bar{x}_n = \left[\frac{k_p [M\bullet][M]}{(2k_{td} + k_{tc})[M\bullet]^2} \right] = \left[\frac{k_p [M]}{\mathbf{x}(fk_d k_t)^{\frac{1}{2}} [I]^{\frac{1}{2}}} \right] \quad 3.25$$

From this equation,¹⁴ it is evident that the rate of polymerisation is proportional to the initiator concentration to the half power, $[I]^{1/2}$, and that the instantaneous number average chain length, \bar{x}_n , is proportional to the inverse of the initiator concentration to the one half power, $1/[I]^{1/2}$. Hence, if using more initiator accelerates the polymerisation, the resultant chains will be shorter, which may not be desirable.¹¹

3.2.2 Chain growth copolymerisation

For many free radical polymerisations, two monomers are used in the process. For example, methyl methacrylate and 2-oxo-2H-chromen-7-yl acrylate or butyl acrylate and 4-methyl-2-oxo-2H-chromen-7-yl acrylate, and the subsequent copolymers are expected to contain both structures in the chain. The reactivities and the relative concentrations of the two monomers should determine the concentration of each comonomer that is incorporated into the copolymer.

Most of the knowledge of the reactivity of monomers via carbocations, free radicals, and carboanions in chain polymerisations has been derived from chain copolymerisation studies. The chemical structure of these monomers strongly influences reactivity during copolymerisation. In addition, from a technological perspective, copolymerisation has been

critical to the design of copolymer products with a variety of specifically desired properties. As compared to homopolymers, an unlimited number of different sequential arrangements can be produced from the synthesis of copolymers, where the changes in relative amounts and chemical structures of the monomers produce materials of varying chemical and physical properties.

Several different types of copolymers are known and the process of copolymerisation can often be altered in order to obtain these structures. Some type of statistical law may be obeyed by a statistical or random copolymer, which relates to the distribution of each type of comonomer that has been incorporated into the copolymer. Thus, it may follow zero- or first- or second-order Markov statistics,¹⁵ for example. Copolymers that are formed via a zero-order Markov process, or Bernoullian, contain two monomer structures that are randomly distributed, and could be termed random copolymers:

-AABBBABABAABA-

The other three types of copolymer structures are alternating, block and graft copolymers. Alternating copolymers have equimolar compositions with a regularly alternating distribution of monomer units:

-ABABABABABABAB-

Block copolymers are linear copolymers that contain one or more long, uninterrupted sequences of each of the comonomer species:

-AAAAAA-BBBBBBBB-

A graft copolymer is a linear chain of one type of monomer structure and one or more side chains that consist of linear chains of another monomer structure.

-AAAAAAAAAAAAAAAAA-
 B B
 B B
 B B
 B B

This discussion that follows will focus on randomly distributed or statistical copolymers.

The composition of the starting materials charged into the system is usually different from the copolymer composition. Therefore, monomers have varying tendencies to be incorporated into the copolymer, which also means that each type of comonomer reacts at varying rates with the two free radical species present. In work conducted by Staudinger,¹⁶ it was noted that the copolymer formed had almost no similar characteristics to those of the homopolymers derived from each of the monomers. In addition, the relative reactivities of the monomers in a copolymerisation were also quite different from their reactivities in the homopolymerisations. Hence, some monomers were more reactive while some were less reactive during copolymerisation than during their homopolymerisations. This is because the rate of polymerization is determined by the affinity of a radical centre for the olefinic moiety. This means that a specific radical centre from a certain monomer may be able to cross-propagate faster than homo-propagate (i.e. the second monomer in the system is more susceptible to the attack of the first monomers radical). This then provides an increase in reaction rate. Certain monomers, for example maleic anhydride, are too sterically constricted to homopropagate and for that reason are commonly polymerized in the presence of a comonomer which then acts as a spacer. An even more interesting fact is that some monomers that do not polymerise at all during homopolymerisation copolymerise relatively well in the presence of a second monomer, to form copolymers.

Alfrey (1944), Mayo and Lewis (1944), and Walling (1957),¹⁷⁻¹⁹ demonstrated that the copolymerisation composition could be determined by the chemical reactivity of the free radicals propagating chain terminal unit during copolymerisation. The terminal model of copolymerisation was proposed once the application of the first-order Markov statistics was used. The use of two monomers, M_1 and M_2 , during copolymerisation leads to two types of propagating species. The first of these species is a propagating chain that ends with a monomer structure M_1 and the second species is a propagating chain that ends with a monomer structure M_2 . The two structures can be represented by $\text{www} - M_1 \bullet$ and $\text{www} - M_2 \bullet$, where the www represents the chain and $M \bullet$ represents the radical at the growing end of the chain. The terminal unit model¹² is based in the assumption that the reactivity of these propagating species only depends on the monomer unit at the end of the chain. This being the case, only four propagating reactions are possible for a two-monomer system. The propagating chain that ends in $M_1 \bullet$ can either add a monomer of type M_1 or of

type M_2 . In addition, the propagating chain that ends in $M_2 \bullet$ can add a monomer unit of type M_2 or of type $M_1 \bullet$. Hence, these equations can be written with the rate constants of reactions²⁰:



where k_{11} is the rate constant for the reaction of the propagating chains that ends in M_1 and adds another M_1 to the end of the chain, and k_{21} is the rate constant for the propagation reaction that adds M_1 to the M_2 end of the chain, and so on. This is referred to as cross-propagation. The addition of a monomer unit to the chain that ends with the same monomer unit is termed self-propagation.

Reactions 3.f and 3.h indicate that monomer M_1 is consumed, whilst reactions 3.g and 3.i indicate that monomer M_2 is consumed. The rates of addition of monomer into the copolymer and the rates of disappearance of the two monomers are given by:

$$\frac{-d[M_1]}{dt} = k_{11}[\text{www-} M_1 \bullet][M_1] + k_{21}[\text{www-} M_2 \bullet][M_1] \quad 3.26$$

$$\frac{-d[M_2]}{dt} = k_{12}[\text{www-} M_1 \bullet][M_2] + k_{22}[\text{www-} M_2 \bullet][M_2] \quad 3.27$$

Eqn. 3.26 is divided by Eqn. 3.27 in order to determine the rate at which the two monomers are added to the copolymer, to give the copolymer composition equation:

$$\frac{d[M_1]}{d[M_2]} = \frac{k_{11}[\text{www-} M_1 \bullet][M_1] + k_{21}[\text{www-} M_2 \bullet][M_1]}{k_{12}[\text{www-} M_1 \bullet][M_2] + k_{22}[\text{www-} M_2 \bullet][M_2]} \quad 3.28$$

The low concentrations (e.g. 10^{-8} moles/litre) of the radical chains in the system are very difficult to determine experimentally; hence it can be removed from this equation by

employing steady state approximations. A steady state concentration is therefore assumed for both of the species $www - M_1 \bullet$ and $www - M_2 \bullet$. In order for the concentrations of each species to remain constant, the interconversion between the two species must be equal, hence, the rates of reactions 3.g and 3.h must be equal:

$$k_{21}[www - M_2 \bullet][M_1] = k_{12}[www - M_1 \bullet][M_2] \quad 3.29$$

Rearranging Eqn. 3.29 and combination with Eqn. 3.28 gives:

$$\frac{d[M_1]}{d[M_2]} = \frac{\left(\frac{k_{11}k_{21}[www - M_2 \bullet][M_1]^2}{k_{12}[M_2]} \right) + k_{21}[www - M_2 \bullet][M_1]}{k_{22}[www - M_2 \bullet][M_2] + k_{21}[www - M_2 \bullet][M_1]} \quad 3.30$$

By simplifying Eqn. 3.30 and combining the results with parameters r_1 and r_2 , which are defined to be the reactivity ratios,

$$r_1 = \frac{k_{11}}{k_{12}} \quad \text{and} \quad r_2 = \frac{k_{22}}{k_{21}} \quad 3.31$$

the most familiar form of the copolymerisation composition equation is then obtained as:

$$\frac{d[M_1]}{d[M_2]} = \frac{[M_1](r_1[M_1] + [M_2])}{[M_2] + ([M_1] + r_2[M_2])} \quad 3.32$$

The ratio of the rates of addition of each monomer can be considered to be the ratio of the molar concentrations of the two monomers incorporated in the copolymer, which is denoted by (m_1 / m_2) . The copolymer composition equation can then be written as:

$$\frac{m_1}{m_2} = \frac{[M_1](r_1[M_1] + [M_2])}{[M_2] + ([M_1] + r_2[M_2])} \quad 3.33$$

The molar ratios of the two monomers that are incorporated into the copolymer, $\frac{d[M_1]}{d[M_2]}$, are defined by the copolymer composition equation. The monomer reactivity ratio for each

monomer in the system is defined as the ratio of the rate constant for addition of its own type of monomer to the rate constant for the addition of the other type of monomer. The r_1 value is greater than one when $\text{www-}M_1\bullet$ prefers to add the monomer M_1 instead of monomer M_2 . When the monomer M_1 is not capable of adding to itself, the r_1 value is equal to zero, which means that homopolymerisation is not possible.

Instead of concentrations, mole fractions can also be used to express the copolymer composition equation, making the equation more useful for experimental studies. In order to put the equation into these terms, F_1 and F_2 are the mole fractions of M_1 and M_2 in the copolymer, and f_1 and f_2 are the mole fractions of monomers M_1 and M_2 in the feed. Hence:

$$f_1 = 1 - f_2 = \frac{[M_1]}{[M_1] + [M_2]} \quad 3.34$$

and

$$F_1 = 1 - F_2 = \frac{d[M_1]}{d[M_1] + d[M_2]} \quad 3.35$$

Combining Eqns. 3.34, 3.35 and 3.32 gives:

$$F_1 = \frac{r_1 f_1^2 + f_1 f_2}{r_1 f_1^2 + 2f_1 f_2 + r_2 f_2^2} \quad 3.36$$

This form of the copolymer equation gives the mole fraction of monomer M_1 introduced into the copolymer.¹²

Different types of monomers follow different types of copolymerisation behaviour. The copolymers, depending on the reactivity ratios of the monomers, can incorporate the comonomers in different ways. The three main types of behaviour that copolymerisations tend to follow correspond to the conditions where r_1 and r_2 are both equal to one, where $r_1 r_2 < 1$ and where $r_1 r_2 > 1$.

When both the r_1 and r_2 values are equal to one, a perfectly random copolymerisation is achieved. This type of copolymerisation will occur when the two different types of propagating species, $\text{www-}M_1\bullet$ and $\text{www-}M_2\bullet$, show the exact same preference for

the addition of each type of monomer. Basically, the growing radical chains do not prefer to add one of the monomers more than the other monomer, which results in perfectly random incorporation into the copolymer.

When $r_1 = r_2 = 0$, an alternating copolymer is obtained. The polymer product in this type of copolymerisation shows a non-random equimolar amount of each comonomer that is incorporated into the copolymer, because the growing radical chains will not add to its own monomer. Thus, the second monomer will have to be added to produce a growing chain and a perfectly alternating chain results.

Block copolymers are produced, theoretically, when both of the monomers want to add to themselves and when $r_1 > 1$ and $r_2 > 1$. Such copolymerisations may produce either very undesirable or very desirable heterogeneous products, which include homopolymers, due to the short lifetime of the propagating radicals. Hence, physical properties such as transparency would not be achieved and macroscopic phase separation could occur.

3.2.2.1 Solution polymerisation

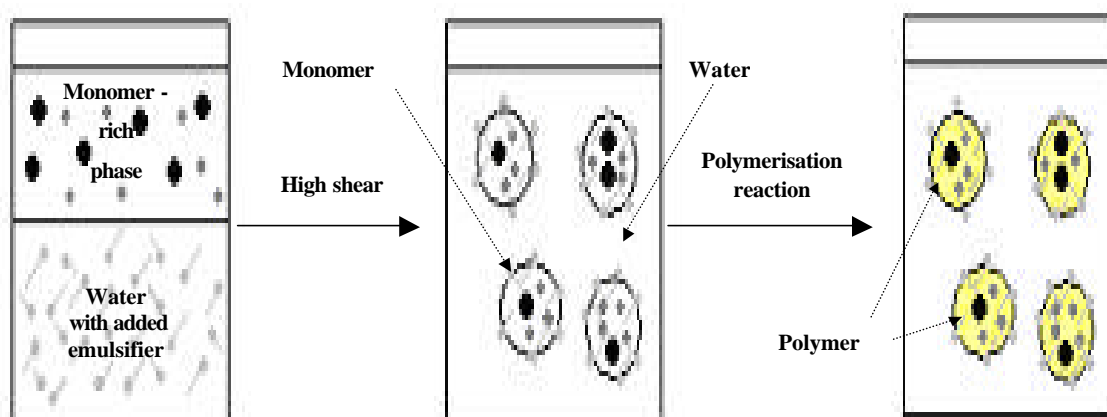
The solution polymerisation process is a slight modification of the bulk polymerisation process. During bulk polymerisation (the simplest polymerisation process), an initiator is added to neat monomer and the reaction is heated to a temperature where the initiator fragments to produce free radicals. Energy transfer in this reaction is very poor, hence a major disadvantage of this process includes the high exothermicity. Solution polymerisation employs the use of a solvent, which can serve to overcome this limitation. Heat transfer occurs more rapidly in this process and therefore there is greater thermal control. The heat of polymerisation can be removed if the reaction is carried out at the reflux temperature of the solvent, as the heat would be removed as the latent heat of vaporisation. Solution free radical polymerisation studies reveal information about how the feed composition affects the copolymer composition, reactivity ratios, etc.

3.2.2.2 Miniemulsion polymerisation

Emulsion polymerisation is a heterogeneous process whereby monomer droplets are dispersed in a continuous aqueous phase by means of a surfactant and a stable emulsion is produced. During emulsion polymerisation, the monomer required for polymerisation has to

be transported to the micelles by diffusion through the aqueous phase. This could pose as a problem since the transfer of the monomer is diffusionally dependent and may therefore not be readily incorporated into the polymer chain. Nucleation of the monomer particles would facilitate a lower demand for the transport of the monomer through the aqueous phase. However, droplet nucleation can only occur if the monomer surface area is larger than that of the micelles, which would require submicron droplet sizes.²¹ In 1973, limitations in the conventional emulsion polymerisation process led to the establishment of the miniemulsion polymerisation process. Ugelstad *et al.*,²² were the first to report that under conditions where the droplet size was minute enough, nucleation of monomer droplets would result in an integral part of the particles formed.

Miniemulsions are dispersions of critically stabilized oil droplets, with a size between 50 and 500 nm, prepared by shearing a system containing monomers, water, a surfactant and a hydrophobe. This results in latex particles that have about the same size as the initial droplets, as shown by a combination of Small-angle neutron scattering (SANS), surface tension and conductivity measurements.^{23,24} This means that the appropriate formulation of a miniemulsion suppresses coalescence of droplets or Ostwald ripening. The polymerisation of miniemulsions extends the possibilities of the widely applied emulsion polymerisation and provides advantages with respect to copolymerisation reactions of monomers with different polarities, incorporation of hydrophobic materials, or with respect to the stability of the formed latexes.²⁵ The principle of miniemulsion polymerisation is schematically shown in Scheme 3.2.



Scheme 3.2: Schematic representation of the principle of miniemulsion polymerisation.

The kinetic behaviour of miniemulsion polymerisation, in which water-soluble initiators were used, was examined by calorimetry. The objective was to further enlighten the miniemulsion polymerisation process by selectively changing parameters such as the amount of initiator and surfactant.²⁶ Three distinct intervals can be categorized for miniemulsion polymerisation kinetics (Fig. 3.7). Contrary to emulsion polymerisation, only intervals I and III are found in the miniemulsion process. Additionally, interval IV describes the gel peak. Intervals I and III can be defined by the average number of radicals per particle. During interval I, the average number of radicals per particle increases until a plateau value of 0.5 is reached at the onset of interval III. A sharp increase of the average number of radicals per particle indicates the beginning of interval IV. Interval III reveals similarity towards a suspension polymerisation. The droplet nucleation interval (interval I) is unexpectedly short as after only 10 min (15% conversion) every droplet is nucleated and the average number of radicals per particle = 0.5 is reached.

The slow increase in the average number of radicals per particle is due to a slow radical flux through the droplet interface. Therefore, the start of the polymerisation in each miniemulsion droplet is not simultaneous. Hence the evolution of conversion in each droplet is different, as shown by TEM. Each miniemulsion droplet can be perceived as a separate nanoreactor, which does not interact with others. It could be shown that the value of the average number of radicals per particle = 0.5 during interval III is independent of the amount of initiator, and therefore during this interval an increase in the initiator concentration does not result in an acceleration of the polymerisation process. The value of the average number of radicals per particle during stage III remains 0.5 and is independent of the particle size. Therefore, only the number of active sites defines the net polymerisation time: the smaller the particles, the shorter the net polymerisation time.

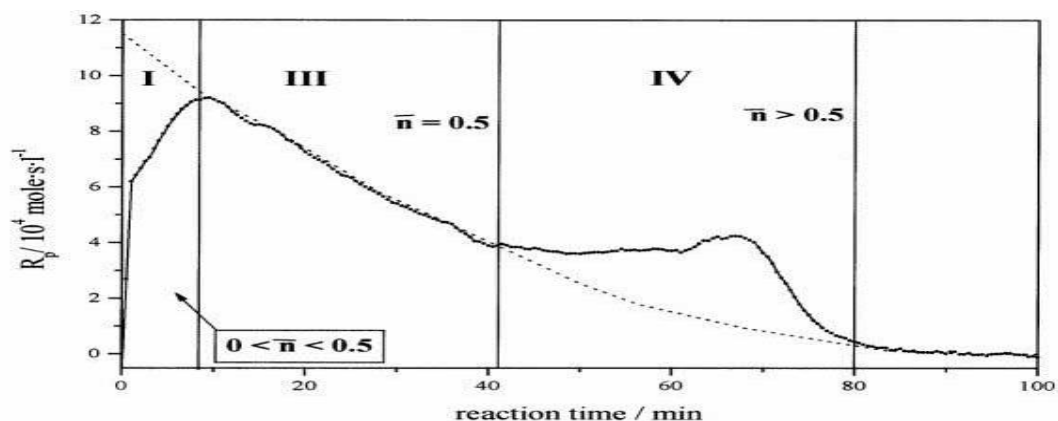


Figure 3.7: Typical calorimetric curve for a miniemulsion polymerisation of styrene.²⁶

3.2.3 Determination of reactivity ratios

Many methods have been used to estimate the reactivity ratios of a large number of comonomers during copolymerisation.²⁷ Conversion may not be independent of copolymer composition. The disappearance of one monomer may be faster than that of the second monomer, if one monomer is being incorporated into the copolymer at a faster rate. Hence, it has a greater reactivity ratio than the other monomer.

The simplest method that has been used to calculate the reactivity ratios of copolymer systems is the approximation method.²⁸ This method is based on the fact that r_1 , the reactivity ratio of component one, is mainly dependent on the composition of monomer two, m_2 , that has been incorporated into the copolymer, at low concentrations of monomer two in the feed, M_2 . Thus, the expression follows:

$$r_1 = \left(\frac{M_2}{m_2} \right) \quad 3.37$$

Only one experiment is necessary to determine the value of the reactivity ratio for component one, but the value is only an approximation and does not provide any validity of the estimated r_1 . The approximation method is limited when the reactivity ratio of one of the components in the system has a value of less than 0.1 or greater than a value of 10. However, good insight into the reactivity ratio values for many copolymer systems is seen by this method. The approximation of reactivity ratios can be easy and quick when using this method of evaluation.

The Mayo-Lewis intersection method^{18,29} uses a linear form of the copolymerisation equation where r_1 and r_2 are linearly related:

$$r_1 = r_2 \left(\frac{m_1 M_2^2}{m_2 M_1^2} \right) + \left(\frac{M_2}{M_1} \right) \left(\frac{m_1}{m_2} - 1 \right) \quad 3.38$$

Eqn. 3.38 shows a linear relationship; using $\left(\frac{m_1 M_2^2}{m_2 M_1^2} \right)$ represented by the slope and $\left(\frac{M_2}{M_1} \right) \left[\left(\frac{m_1}{m_2} \right) - 1 \right]$ as the abscissa intercept, a plot can be produced for a set of

experiments, after the copolymer composition has been determined. The straight lines that are produced on the plot for each experiment, where r_1 represents the ordinate and r_2 represents the abscissa, intersect at a point on the r_1 vs. r_2 plot. r_1 and r_2 for the system under study is taken at the point where these lines meet. A qualitative observation of the validity of the intersection area is the major advantage of this method. Good definition of data is achieved by allowing for more compact intersections. However, the method requires a visual check of the data and a quantitative estimation of the error is impossible. Hence, weighting of the data is needed to determine the most precise values of r_1 and r_2 .

Another form of the copolymer equation is used by the Fineman-Ross linearization method,³⁰ which is expressed as follows:

$$G = r_1 H - r_2 \quad 3.39$$

where

$$G = \left(\frac{m_1}{m_2} \right)^2 \left[1 - \left(\frac{M_2}{M_1} \right) \right] \quad 3.40$$

and

$$H = \left(\frac{m_1}{m_2} \right)^2 \left(\frac{M_2}{M_1} \right) \quad 3.41$$

In this method, by plotting G vs. H for all the experiments, a straight line will be obtained, where the slope is the value of r_1 and the value of r_2 is represented by the intercept of the line. This method of reactivity ratio determination has similar advantages and disadvantages of the method described above, but this treatment is a linear least squares analysis instead of a graphical analysis. By weighting the data the estimates of r_1 and r_2 can change with each experimenter, thus this method's validity is only qualitative. In addition, large effects on the calculated values of r_1 and r_2 are witnessed when high and low experimental composition data are unequally weighted. Therefore, different values of r_1 and r_2 can be produced depending on which monomer is chosen as M_1 .

Kelen and Tudos³¹⁻³³ introduced a refinement of the linearization method by adding an arbitrary positive constant a into the Fineman-Ross Eqn. 3.39. This technique spreads the data more evenly over the entire composition range to produce equal weighting to all the data.¹² The refined equation is as follows:

$$\mathbf{h} = \left[r + \frac{r_2}{\mathbf{a}} \right] \mathbf{x} - \frac{r_2}{\mathbf{a}} \quad 3.42$$

where

$$\mathbf{h} = \frac{G}{(\mathbf{a} + H)} \quad 3.43$$

and

$$\mathbf{x} = \frac{H}{(\mathbf{a} + H)} \quad 3.44$$

Plotting a straight line (\mathbf{h} vs. \mathbf{x}), with $-r_2/\mathbf{a}$ and r_1 as the intercepts on extrapolation to $\mathbf{x} = 0$ and $\mathbf{x} = 1$, respectively. By choosing the \mathbf{a} value to be $(H_m H_M)^{1/2}$, where H_m and H_M are the lowest and highest H values, respectively, symmetrical distribution of the experimental data is achieved. Even with this more complicated monomer reactivity ratio technique, statistical limitations are inherent in these linearization methods.^{34,35} O'Driscoll *et al.*³⁷ and Reilly³⁶ determined that the dependent variable does not truly have a constant variance and the independent variable in any form of the linear copolymer equation is not truly independent. Hence, using a non-linear method for composition data analysis has come to be the most statistically sound technique.

A non-linear or curve-fitting method¹⁷ is based on the copolymer composition equation in the form:

$$\frac{m_1}{m_2} = \frac{(r_1 M_1^2 + M_1 M_2)}{(r_2 M_2^2 + M_1 M_2)} \quad 3.45$$

This equation is based on the assumptions that the monomer concentrations do not change much throughout the reaction and that the molecular weight of the resulting polymer is relatively high. In order to determine reactivity ratios from experimental data, a graph must be generated for the observed comonomer amount that was incorporated into the copolymer, m_1 , versus the feed comonomer amount, M_1 , for the entire range of comonomer concentrations. A curve can subsequently be drawn through the points for selected r_1 and r_2 values and validity of the chosen reactivity ratio values can be verified by changing the r_1 and r_2 values until the experimenter can demonstrate that the curve best fits the data points.

The main advantage of using the reactivity ratio determination methods deliberated on thus far is the fact that the results can be visually and qualitatively checked. Disadvantages

include a direct dependence of the composition on conversion for most polymer systems, thus, low conversion is needed to determine the reactivity ratios. In addition, the method requires extensive calculations, but only qualitative measurements of precision can be obtained. Finally, weighting of the experimental data for the methods to determine precise reactivity ratios is difficult to reproduce from one experimenter to another.

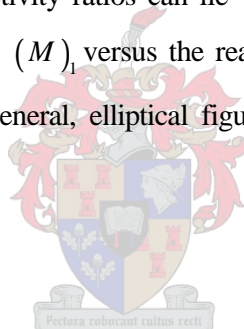
Mortimer and Tidwell proposed a technique that allows for rigorous application of statistical analysis for r_1 and r_2 , which they called the non-linear least squares method.^{28,38-41} This method can be considered to be a modification of the curve fitting method. The sum of the squares of the difference between the observed and the computed polymer compositions is minimized for selected values of r_1 and r_2 . By making use of this criterion for the non-linear least squares method of analysis, the values for the reactivity ratios are unique for a given set of data. By following the calculations, all investigators will arrive at the same values for r_1 and r_2 . Van Herk^{42,43} recently published a computer program which allows rapid data analysis of the non-linear calculations and permits the calculations of the validity of the reactivity ratios in a quantitative fashion.⁴⁴ The computer program produces reactivity ratios for the monomers in a system with a 95% joint confidence limit determination. The joint confidence limit is a quantitative estimation of the validity of the results of the experiments and the calculations performed. This method of data analysis consists of obtaining initial estimates of the reactivity ratios for the system and experimental data of comonomer charge amounts and comonomer amounts that have been incorporated into the copolymer, both in mole fractions. Many repeated sets of calculations are performed by the computer, which rapidly determines a pair of reactivity ratios that fit the criterion, wherein the value of the sum of the squares of the differences between the observed polymer composition and the computed polymer composition is minimized.^{45,46} This method uses a form of the copolymer composition equation with mole fractions of the feed. It amounts to determining the mole fraction of the comonomer that should be incorporated into the copolymer during a differential time interval.

$$F_1 = \frac{r_1 f_1^2 + f_1 f_2}{r_1 f_1^2 + 2f_1 f_2 + r_2 f_2^2} \quad 3.46$$

In this equation, F_1 represents the mole fraction of M_1 that was calculated to be incorporated into the copolymer and f_1 and $f_2 = 1 - f_1$ represent the mole fractions of each comonomer

that were fed into the reaction mixture. The use of the Gauss-Newton non-linear least squares procedure predicts the reactivity ratios for a given set of data after repeating the calculations so that the difference between the experimental data points and the calculated data points on a plot of mole fraction of comonomer incorporated versus comonomer in the feed is reduced to the minimum value.^{46,47} Hence, the last iteration of the calculations produces a convergence on the least squares estimate of r_1 and r_2 .⁴⁸

Estimation of errors for this type of calculation depends on the assumption that the random errors inherent in the experimentally determined values for the comonomer fraction incorporated into the copolymer are evenly distributed throughout the experimental data. Hence, it would follow that the differences in the values for the comonomer fractions in the copolymer during the time intervals are evenly distributed with constant variances and will produce a method for determining joint confidence limits. The 95% joint confidence limits determine the values where the reactivity ratios can lie with a 95% probability. On a plot of the reactivity ratio of monomer one (M_1) versus the reactivity ratio of monomer two (M_2), the joint confidence limits are, in general, elliptical figures due to the non-linear calculations that were performed.²⁸



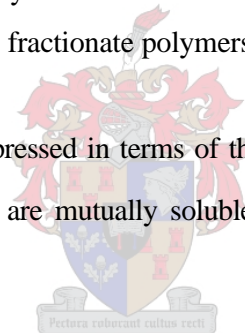
3.3 Solubility parameters

A *solubility parameter* is used for correlating and understanding substance-solvent interactions and is defined as the square root of the cohesive energy density, which is the cohesive energy per unit volume.⁴⁹

In the following sections, the principle of solubility parameters and its application to the current study will be detailed.

The solubility of a compound in a given solvent is governed by its chemical structure: structural and polar similarity favour solubility. This means that the solubility of a given substance in a given solvent is favoured if the solubility parameters of the substance and the solvent are similar.⁴⁹ Hence, it is imperative to link the solubility parameter of any compound with its chemical structure. Solubility also decreases with an increase in molecular mass,^{50,51} and this phenomenon can be used to fractionate polymers according to molecular mass.⁵²

The solubility of a compound is expressed in terms of the free energy of mixing ΔG_m , where ΔG_m is negative if two substances are mutually soluble. The free energy of mixing can be defined as:



$$\Delta G_m = \Delta H_m + T\Delta S_m \quad 3.47$$

where ΔH_m is the enthalpy of mixing, ΔS_m is the entropy of mixing and T is the absolute temperature.

Due to the fact that ΔS_m has a positive value, arising from increased conformational mobility of the compound in solution, the magnitude of ΔH_m determines the sign of ΔG_m .

In 1949 Hildebrand⁵³ proposed that the heat of mixing, ΔH_m , for a binary system is related to concentration and energy parameters by the expression

$$\Delta H_m = V_m \left[\left(\frac{\Delta E_1}{V_1} \right)^{\frac{1}{2}} - \left(\frac{\Delta E_2}{V_2} \right)^{\frac{1}{2}} \right]^2 f_1 f_2 \quad 3.48$$

where V_m is the total volume of the mixture, V_1 and V_2 are molar volumes (molecular mass/density) of the two components, f_1 and f_2 are their volume fractions and E_1 and E_2 are the energies of evaporation (cohesive energies). The terms $\Delta E_1/V_1$ and $\Delta E_2/V_2$ are called the cohesive energy densities.

The cohesive energy, E_{coh} , is closely related to the molar heat of evaporation (ΔH_{vap}) through the equation:

$$E_{coh} = \Delta U_{vap} = \Delta H_{vap} - p\Delta V \approx \Delta H_{vap} - RT \quad 3.49$$

where ΔU_{vap} is the internal energy of evaporation.

The solubility parameter is written as the square root of the cohesive energy density, E_{coh} at 298 K,

$$d = \left(\frac{E_{coh}}{V} \right)^{\frac{1}{2}} \quad 3.50$$

where V is the total volume of the mixture.

Solubility parameters for solvents can be determined by using the latent heat of vaporization (ΔH_{vap}) and the equation

$$\Delta E = \Delta H_{vap} - RT \quad 3.51$$

Eqn. 3.51 is not applicable to polymers as degradation will occur rather than vaporization at high temperatures.⁵⁴ Therefore d has to be calculated by using group molar attraction constants as proposed by Small, van Krevelen, Hoy and Fedors.^{49,55}

With the use of the Fedors method, the E_{coh} value can be substituted into Eqn. 3.50 and the solubility parameter can be calculated. With the Small, van Krevelen and Hoy method, the E_{coh} value is calculated (Eqn. 3.52, where F_i is the group molar attraction constant) and then substituted into Eqn. 3.60 for the solubility parameter to be calculated.

$$E_{coh} = \frac{\left[\left(\sum_i F_i \right)^2 \right]}{\left[\left(\sum_i V_i \right) \right]} \quad 3.52$$

3.3.1 Modification of solubility parameters

Hildebrand only used dispersion forces between structural units in calculating solubility parameters. Due to the fact that in many substances the cohesive energy is also dependent on interaction between the polar groups and hydrogen bonds,⁴⁹ Hildebrand's definition for the solubility parameter was refined to incorporate these interactions in the following expression:

$$E_{coh} = E_d + E_p + E_h \quad 3.53$$

where E_d is the dispersive term, E_p is the polar term and E_h is the hydrogen bonding term.

The solubility parameter can therefore be written as

$$d_t = \left(d_d^2 + d_p^2 + d_h^2 \right)^{\frac{1}{2}} \quad 3.54$$

where d_d , d_p and d_h are the contributions of dispersion forces, polar forces and hydrogen bonding, respectively. Values for d_d , d_p and d_h can be calculated from group molar contributions according to Hoftyzer and van Krevelen,⁴⁹ who made use of the following equations:

$$\mathbf{d}_d = \left(\frac{\sum (F_d)_i}{V} \right) \quad 3.55$$

$$\mathbf{d}_p = \frac{\sqrt{\sum (F_p)_i^2}}{V} \quad 3.56$$

$$\mathbf{d}_h = \sqrt{\frac{\sum (E_h)_i}{V}} \quad 3.57$$

where F is the group contribution of dispersion and polarity components (shown in Eqns. 3.55 and 3.56, respectively) and E_h is the hydrogen bonding energy, per structural group.

By plotting a graph of \mathbf{d}_v (contribution of dispersion and polar forces to the solubility parameter) against \mathbf{d}_h , where

$$\mathbf{d}_v = \sqrt{(\mathbf{d}_d^2 + \mathbf{d}_p^2)} \quad 3.58$$

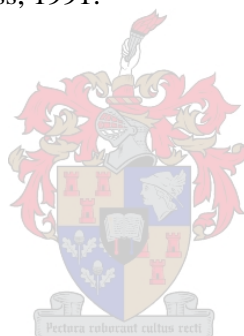
for a specific compound and different solvents, the preferred solvents for dissolving a particular compound can be determined thereof.

References:

- (1) Guilbault, G. G. *Practical fluorescence: theory, methods, and techniques*; Marcel Dekker, Inc.: New York, 1973.
- (2) Skoog, D. A.; West, D. M.; Holler, F. J. *Fundamentals of analytical chemistry*, 7 Ed.; Saunders College Publishers: New York, 1997.
- (3) Miller, J. N. *Standards in fluorescence spectroscopy: ultraviolet spectrometry group*; Chapman and Hall: London, 1981; Vol. 2.
- (4) Pringsheim, P. *Fluorescence and phosphorescence*; Interscience Publishers: New York, 1949.
- (5) Lukasiewicz, R. J.; Fitzgerald, J. M. *Anal. Chem* **1973**, *45*, 511.
- (6) Parker, C. A. *Photoluminescence of solutions*; Elsevier: Amsterdam, 1986.
- (7) Olmsted, J. *Chem. Phys. Letters* **1976**, *38*, 287.
- (8) Bowen, E. J.; Sahu, J. *J. Phys. Chem.* **1959**, *63*, 4.
- (9) Suzuki, S.; Fujii, T.; Imai, A.; Akahori, H. *J. Phys. Chem.* **1977**, *81*, 1592.
- (10) Chehelnik, E. D.; Cundall, R. B.; Lockwood, J. R.; Palmer, T. F. *J. Phys. Chem.* **1975**, *79*, 1369.
- (11) Painter, P. C.; Coleman, M. M. *Fundamentals of polymer science*; Technomic Publishing Inc.: Lancaster, 1997.
- (12) Odian, G. *Principles of polymerisation*, 3 Ed.; John Wiley and Sons Inc.: New York, 1991.
- (13) Moad, G.; Solomon, D. H. *The chemistry of free radical polymerisation*; Pergamon Press: New York, 1995.
- (14) Rosen, S. L. *Fundamental principles of polymeric materials*; John Wiley and Sons Inc.: New York, 1993.
- (15) Tirrell, D. A. *Encyclopedia of polymer science and engineering*; Wiley Interscience: New York, 1986; Vol. 4, pp 192-233.
- (16) Staudinger, H.; Schneiders, J. *Ann. Chim.* **1939**, *541*, 151.
- (17) Alfrey, T.; Bohrer, J. J.; Mark, H. *Copolymerisation*; Interscience: New York, 1952.
- (18) Mayo, F. R.; Lewis, F. M. *J. Am. Chem. Soc.* **1944**, *66*, 1594.
- (19) Walling, C. *Free radicals in solutions*; Wiley: New York, 1957.
- (20) Flory, P. J. *Principles of polymer chemistry*; Cornell University Press: Ithaca, 1953.
- (21) Asua, J. M. *Prog. Polym. Sci.* **2002**, *27*, 1283-1346.
- (22) Ugelstad, J.; El-Aasser, M. S.; Vanderhoff, J. W. *J. Polym. Sci. Lett. Ed.* **1973**, *11*, 503-513.

- (23) Landfester, K. *Macromol. Rapid Comm.* **2001**, 896-939.
- (24) Landfester, K.; Bechtold, N.; Tiarks, F.; Antonietti, M. *Macromolecules* **1999**, *32*, 5222.
- (25) Landfester, K. *Macromol. Symp.* **2000**, *150*, 171.
- (26) Bechtold, N.; Landfester, K. *Macromolecules* **2000**, *33*, 4682-4689.
- (27) Polic, A. L.; Duever, T. A.; Penlidis, A. *J. Polym. Sci. Part A* **1998**, *36*, 813.
- (28) Tidwell, P. W.; Mortimer, G. A. *J. Polym. Sci. Part A* **1965**, *3*, 369.
- (29) Davis, T. P. *J. Polym. Sci. Part A* **2001**, *39*, 597.
- (30) Fineman, M.; Ross, S. D. *J. Polym. Sci.* **1950**, *5*, 259.
- (31) Kelen, T.; Tudos, F.; Turcsanyi, B. *Polymer Bull.* **1980**, *2*, 71-76.
- (32) Tudos, F.; Kelen, T.; Foldes-Berezsnich, T.; Turcsanyi, B. *J. Macromol. Sci. Part A* **1976**, *10*, 1513-1540.
- (33) Tudos, F.; Kelen, T. *J. Macromol. Sci. Part A* **1981**, *16*, 1283.
- (34) Greenley, R. Z. *Polymer handbook*, 4 Ed.; John Wiley: New York, 1999.
- (35) Greenley, R. Z. *Polymer handbook : Part II*, 3 Ed.; John Wiley: New York, 1989.
- (36) O'Driscoll, K. F.; Reilly, P. M. *Makromol. Chem., Makromol. Symp.* **1987**, *10/11*, 355.
- (37) O'Driscoll, K. F.; Kale, L. T.; Garcia-Rubio, L. H.; Reilly, P. M. *J. Polym. Sci.: Polym. Chem. Ed.* **1984**, *22*, 2777.
- (38) Hill, D. J. T.; O'Donnell, J. H. *Makromol. Chem., Makromol. Symp.* **1987**, *10/11*, 375.
- (39) Hill, D. J. T.; Lang, A. P.; O'Donnell, J. H.; O'Sullivan, P. W. *Eur. Polym. J.* **1989**, *25*, 911.
- (40) Hill, D. J. T.; Lang, A. P.; O'Donnell, J. H. *Eur. Polym. J.* **1991**, *27*, 765.
- (41) Hill, D. J. T.; Lang, A. P.; O'Donnell, J. H. *Eur. Polym. J.* **1991**, *27*, 765-772.
- (42) van Herk, A. M. *J. Chem. Ed.* **1995**, *72*, 138.
- (43) van Herk, A. M.; Manders, B. G.; Smulders, W.; Aerdts, A. *Macromolecules* **1997**, *30*, 322-323.
- (44) Mott, G.; Brendlein, W.; Braun, D. *Eur. Polym. J.* **1973**, *9*, 1007-1012.
- (45) Davis, T. P.; O'Driscoll, K. F.; Piton, M. C.; Winnik, M. A. *J. Polym. Sci.: Part C: Polym. Lett.* **1989**, *27*, 181.
- (46) Davis, T. P.; O'Driscoll, K. F.; Piton, M. C.; Winnik, M. A. *Polym. Int.* **1991**, *24*, 65.
- (47) Ghi, P. Y.; Hill, D. J. T.; O'Donnell, J. H.; Pomeroy, P. J.; Whittaker, A. K. *Polymer Gels and Networks* **1996**, *4*, 253.
- (48) Hagiopol, C. *Copolymerisation: Toward a systematic approach*; Kluwer Academic: New York, 1999.

- (49) van Krevelen, D. W. *Properties of polymers: their correlation with chemical structure; their numerical estimation and prediction from additive group contributions*, 3 Ed.; Elsevier Science Publishers, 1997.
- (50) Shalliker, R. A.; Kavanagh, P. E.; Russel, I. M. *Jnl. of Chromatography* **1991**, 543, 157-169.
- (51) Glöckner, G. *Gradient HPLC of copolymers and chromatographic cross fractionation*; Springer-Verlag: Heidelberg Berlin, 1991.
- (52) Van Zyl, A. J. P. M.Sc. thesis; University of Stellenbosch: Stellenbosch, 1999; p 221.
- (53) Billmeyer, F. W. *Textbook of polymer science*, 2 Ed.; Wiley-Interscience, a Division of John Wiley and Sons, Inc, 1962.
- (54) Brandrup, J.; Immergut, E. H. *Polymer handbook*, 2 Ed.; Wiley-Interscience Publication, 1975.
- (55) Barton, A. F. M. *CRC Handbook of solubility parameters and other cohesion parameters*, 2 Ed.; CRC Press, 1991.



Chapter 4

Synthesis of monomers

4.1 Introduction

Two commercially available fluorescent compounds were utilised in this study: 7-hydroxy-2H-chromen-2-one (A_1) and 7-hydroxy-4-methyl-2H-chromen-2-one (B_1) (Fig. 4.1). These compounds contain hydroxy groups that are capable of undergoing esterification reactions. This is especially useful when it is desired to convert the fluorescent compounds to e.g. acrylic-type monomers that can be used in polymerisation reactions. The aim of this part of the study was to establish whether the fluorescence behaviour of A_1 and B_1 would be maintained after esterification of the hydroxy groups.



7-hydroxy-2H-chromen-2-one (A_1)

7-hydroxy-4-methyl-2H-chromen-2-one (B_1)

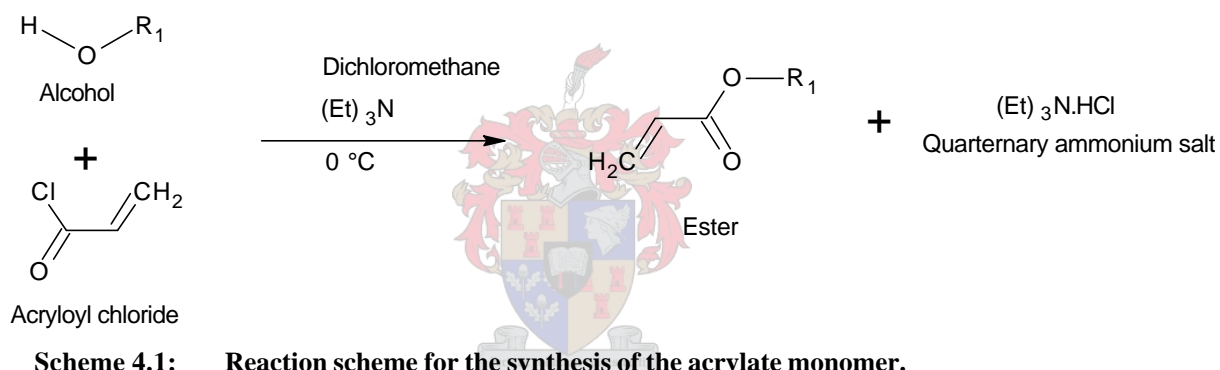
Figure 4.1: Chemical structures of 7-hydroxy-2H-chromen-2-one (A_1) and 7-hydroxy-4-methyl-2H-chromen-2-one (B_1).

7-Hydroxy-2H-chromen-2-one (A_1) and 7-hydroxy-4-methyl-2H-chromen-2-one (B_1) were selected as the most suitable starting materials since they are rigid molecules, have aromatic electron structures, exhibit fluorescent behaviour and contain hydroxy groups that are capable of being converted to other functional groups.

Esterification by alcoholysis (reaction between an alcohol and an acid halide) was chosen as a more suitable process compared to the Fischer process (reaction between an acid and an

alcohol).^{1,2} Fischer esterification is an equilibrium reaction, which requires one of the reagents to be in excess in order to obtain high yields. This leads to the Fischer process being more expensive than alcoholysis. The Fischer process also requires significantly more aggressive reaction conditions, such as reflux at high temperatures for extended periods of time.

Alcohols react with acid chlorides to yield esters. (Scheme 4.1) The reaction is relatively fast and requires no catalyst. This is because the leaving group in this substitution reaction is a chloride ion, which is an excellent leaving group.³ Alcoholysis reactions are substitution reactions, which in this case are usually carried out in the presence of a base like triethylamine (Et_3N) to neutralize the HCl formed (formation of a quaternary ammonium salt), thus preventing hydrolysis of the prepared ester to a carboxylic acid and an alcohol.⁴



4.2 Experimental

4.2.1 Materials

7-Hydroxy-2H-chromen-2-one (A_1), 7-hydroxy-4-methyl-2H-chromen-2-one (B_1), umbelliferone, 4-methyl umbelliferone (all Fluka, 98%), acryloyl chloride (Aldrich, 96%), triethylamine (Et_3N , Aldrich, 99.5%), sodium hydroxide pellets (Associated Chemicals Enterprises), dichloromethane (Aldrich, 97%), ethyl acetate (Aldrich, 99.8%), n-pentane (Aldrich, 98%) and anhydrous magnesium sulphate (Merck) were used as received. Water was distilled and deionised (DDI).

TLC aluminium sheets (Merck) with a pre-coated silica gel (60 F₂₅₄) (0.2 mm layer thickness) were used for TLC analyses.

4.2.2 Instrumentation

NMR spectra were recorded on a 300 MHz Varian VXR spectrometer equipped with a Varian magnet (7.0 T), and a 600 MHz Varian Unity Inova spectrometer equipped with an Oxford magnet (14.09 T). Standard pulse sequences were used for obtaining ^1H , ^{13}C , and APT spectra.

Fourier transform infrared spectra were recorded on a Nexus FT-IR spectrometer using a DTGS-KBr detector.

Fluorescence analysis was conducted on a Perkin Elmer Luminescence Spectrometer LS 50B and 10 mm Quartz cuvettes (PECSA Analytical) were used for all analyses.

4.2.3 Esterification protocol

Synthesis procedures outlined by Reddy and Balasubramian⁵ and D'Agosto *et al.*⁶ were used. 7-Hydroxy-2H-chromen-2-one (A_1) and 7-hydroxy-4-methyl-2H-chromen-2-one (B_1) (both 30 mmol respectively) were dissolved separately in dichloromethane (150 mL) and placed in two separate 500 mL three-necked round bottom flasks together with triethylamine (33 mmol). The reaction mixtures were stirred at 0°C. Acryloyl chloride (33 mmol), dissolved in dichloromethane (25 mL), was added dropwise from a dropping funnel to each reaction vessel. The reactions were allowed to run for 1 hour at 0°C and thereafter 4 hours at room temperature to ensure completion.

The organic layers were washed with water (5 times) and a 5% NaOH solution to remove quaternary ammonium salts and unreacted starting materials. The organic layers were subsequently dried on anhydrous MgSO_4 , filtered and the solvent removed by rotary evaporation (45°C, 990 mbar).

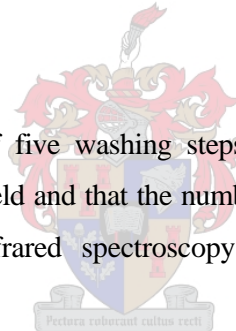
An ethyl acetate: n-pentane (1:15 v/v) mixture was added to the isolated products and the respective compounds 2-oxo-2H-chromen-7-yl acrylate (A_2) (creamish-white powder) and 4-methyl-2-oxo-2H-chromen-7-yl acrylate (B_2) (white flakes) precipitated immediately. These products were redissolved in dichloromethane and recrystallised in an ethyl acetate: n-pentane (1:15 v/v) mixture.

4.3. Results and discussion

4.3.1 Esterification of 7-hydroxy-2H-chromen-2-one (A₁) and 7-hydroxy-4-methyl-2H-chromen-2-one (B₁)

Thin layer chromatography (TLC) was used as a quick lab test to analyse product purity and to determine R_f -values for the respective compounds (A₂ and B₂) in an ethyl acetate: pentane (1:1 v/v) solvent system. An ultraviolet visualization box was used to visualize compounds on the TLC plates. At a wavelength of 254 nm, compounds A₂ and B₂ (product of the esterification of 7-hydroxy-2H-chromen-2-one (A₁) and 7-hydroxy-4-methyl-2H-chromen-2-one (B₁)), appeared black, with R_f -values of 0.71 and 0.74, respectively. Compounds A₁ and B₁ appeared neon blue and had similar R_f -values at 0.59 and 0.60, respectively. At 365 nm, the presence of compounds A₂ and B₂ were not evident, whilst A₁ and B₁ appeared neon purple in colour and had similar R_f -values, 0.59 and 0.60, respectively.

It was found that a minimum of five washing steps was required to achieve both a pure product and a high percentage yield and that the number of washing steps played a role in the percentage yield. NMR and infrared spectroscopy were used to characterize the pure products.



Final yields and melting points of A₂ and B₂ were as follows:

A₂: 92.3%; 140 – 143°C

B₂: 89.9%; 141 – 145°C

4.3.2 Nuclear magnetic resonance studies

4.3.2.1 2-oxo-2H-chromen-7-yl acrylate (A₂)

Fig. 4.2 shows the vinylic protons are in the region of $\delta = 6.1$ to 6.6. H-16a (6.13, d) is in the cis and H-16b (6.61, d) in the trans position relative to hydrogen 15a (6.41, t). Signals due to 3a, 7a, 9a, 10a and 4a appear with chemical shifts (δ) and multiplicities of 6.33 (d), 7.76 (s), 7.15 (d), 7.56 (d) and 7.76 (d), respectively.

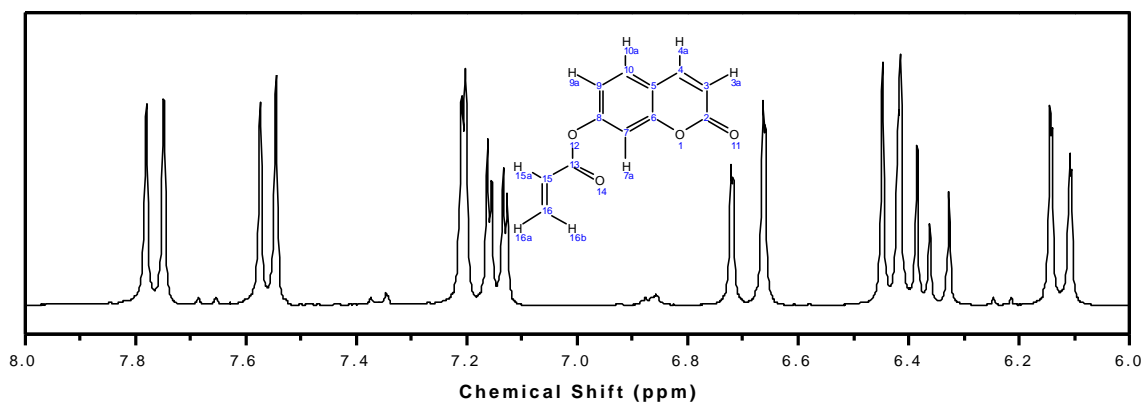


Figure 4.2: ^1H -NMR spectrum (DMSO- d_6 , 600 MHz) of 2-oxo-2H-chromen-7-yl acrylate (A_2).

In the ^{13}C -NMR and APT-NMR spectra (Fig. 4.3), the appearance of C-13, 15 and 16 with chemical shifts (δ) of 160.45, 127.32 and 133.71 is indicative of ester formation. C-2 appears at $\delta = 163.86$. Signals due to C-3, 4, 7, 9 and 10 appear at $\delta = 143.05$, 115.97, 128.69, 118.35 and 110.31, respectively. C-8, which attaches the ester functional group to the aromatic ring, appears at $\delta = 153.16$.

In Fig. 4.3b, the use of APT-NMR spectroscopy allowed all $-\text{CH}_2$ and $-\text{C}$ atoms to be represented by positive peaks and all $-\text{CH}_3$ and $-\text{CH}$ atoms to be represented by negative peaks.

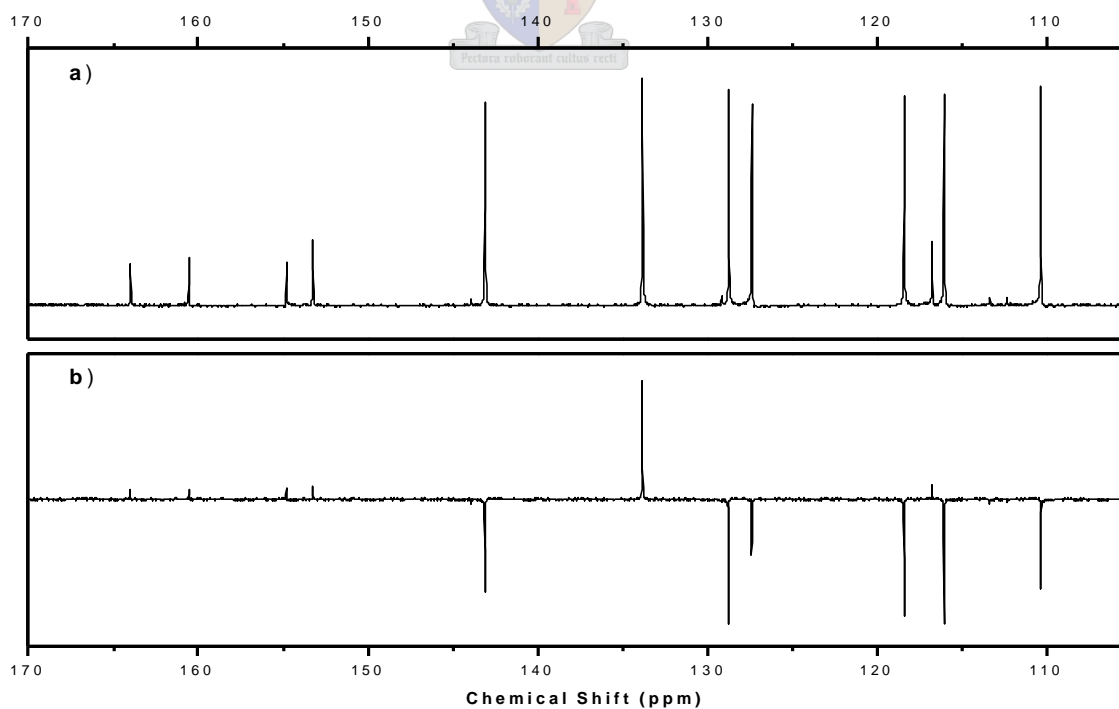


Figure 4.3: (a) ^{13}C -NMR spectrum (DMSO- d_6 , 150 MHz) and (b) APT-NMR spectrum of 2-oxo-2H-chromen-7-yl acrylate (A_2).

4.3.2.2 4-methyl-2-oxo-2H-chromen-7-yl acrylate (B₂)

Fig. 4.4 shows the vinylic protons are in the region of $\delta = 6.1$ to 6.6. H-17a (6.69, d) is in the cis and H-17b (6.11, d) in the trans position relative to hydrogen 16a (6.39, t). The signals due to protons 3a, 7a, 9a and 10a appear with chemical shifts (δ) and multiplicities of 6.29 (d), 7.21 (s), 7.15 (t) and 7.68 (d). Methyl protons on C-12 appear at $\delta = 2.43$ as a singlet.

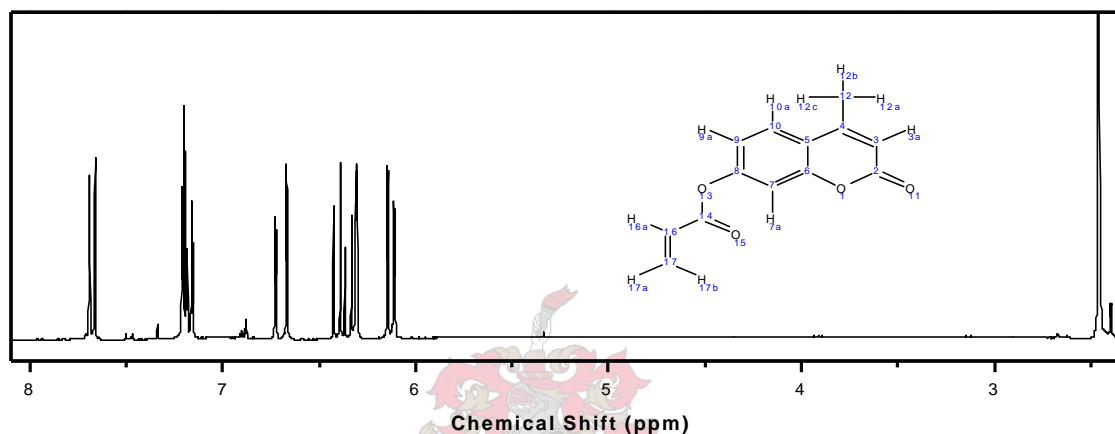


Figure 4.4: ¹H-NMR spectrum (DMSO-*d*₆, 600 MHz) of 4-methyl-2-oxo-2H-chromen-7-yl acrylate (B₂).

In the ¹³C-NMR and APT-NMR spectra (Fig. 4.5), the appearance of C-14, 16 and 17 with chemical shifts (δ) of 160.65, 125.54 and 133.72 is indicative of ester formation. C-2 appears at $\delta = 163.95$. Signals due to C-3, 7, 9 and 10 appear at $\delta = 114.49$, 127.41, 118.15 and 110.41, respectively. C-8, which attaches the ester functional group to the aromatic ring, appears at $\delta = 153.08$. C-4 and the methyl carbon (C-12) appears at $\delta = 152.13$ and 18.36, respectively.

In Fig. 4.5b, the positive peaks represent all -CH₂ and -C atoms whilst the negative peaks represent all -CH₃ and -CH atoms.

The use of APT-NMR spectroscopy as a classification tool (separating -CH₂ and -C atoms from -CH₃ and -CH atoms) in conjunction with ¹³C-NMR spectroscopy was successfully used to determinate carbon-atoms present in compounds A₂ and B₂, as indicated in Figs. 4.3 and 4.5.

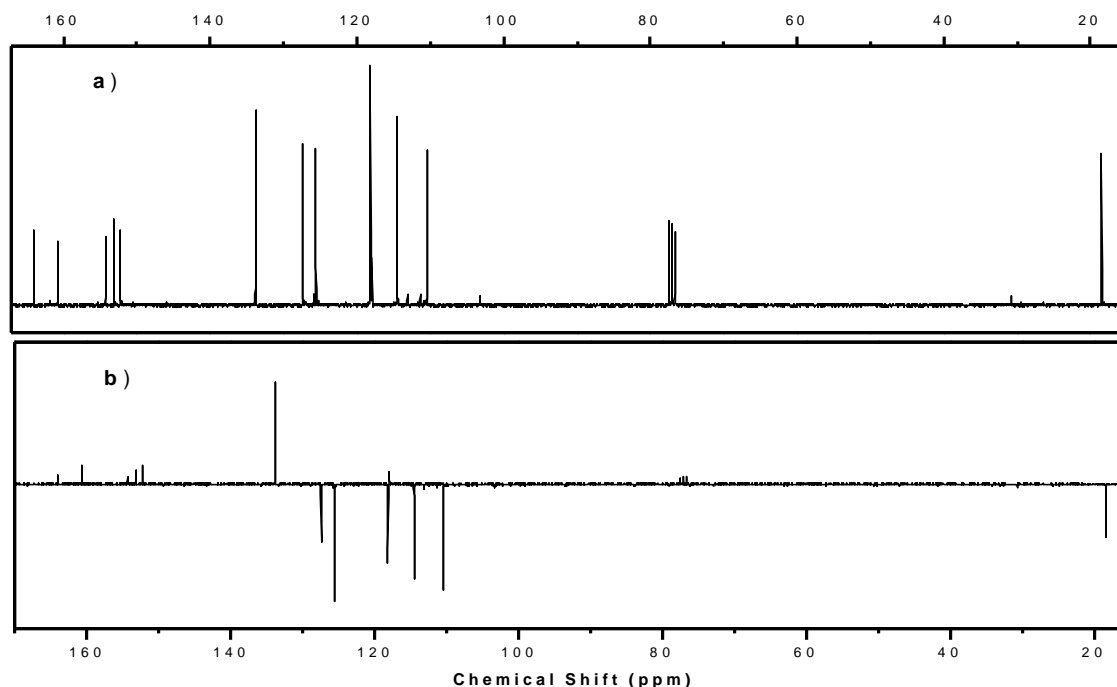


Figure 4.5: (a) ¹³C-NMR spectrum (DMSO-*d*₆, 150 MHz) and (b) APT NMR spectrum of 4-methyl-2-oxo-2H-chromen-7-yl acrylate (**B**₂).

4.3.3 Infrared spectroscopy analysis

Esters show two characteristic absorption regions arising from C=O and C-O stretching vibrations. (Figs. 4.6 and 4.7) The carbonyl (C=O) stretching frequency in saturated acyclic esters appears at a slightly higher frequency (20 to 30 cm⁻¹) than those in ester groups contained within cyclic esters (lactones). This is a consequence of the inductive effect of the electronegative alkoxy-oxygen exerting an electron withdrawal effect on the carbonyl carbon. This inductive effect results in a shorter and stronger carbonyl bond.⁷ Structural assignment can become tenuous when frequency ranges overlap. In cases like these, ester carbonyl frequency is lowered by conjugation or lactone carbonyl absorption shifted to higher frequency by purposely attaching an oxygen to an adjacent carbon, thereby modifying the molecule.

The effect of changes in electronic environment on the position of absorption of the carbonyl group in esters, e.g. the effect of conjugation, etc., follows the same pattern as in cyclic esters.⁸ Six, five, and four membered ring lactones absorb near 1750, 1780 and 1820 cm⁻¹ respectively. Phenyl and vinyl esters, which have (-O-CO-C=C) bonding systems, absorb at higher frequencies than saturated esters.

The C-O stretching vibration in esters results in very strong bands in the 1300 to 1100 cm^{-1} region. The band is of complex origin, but is generally regarded to arise mainly from the acyl-oxygen bond. The use of this absorption band is limited since other strong bands, e.g. ether (C-O-C) stretching, also appear in this region.

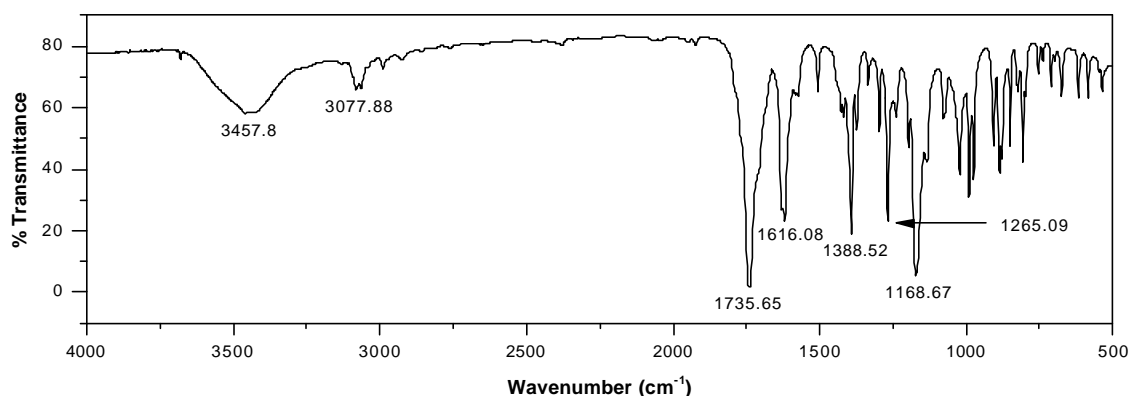


Figure 4.6: Fourier transform infrared analysis of 2-oxo-2H-chromen-7-yl acrylate (A_2).

Aromatic ortho-disubstituted CH (4 adjacent out of plane deformations) is observed within the spectral range 960 to 735 cm^{-1} . Within the spectral range of 1170 to 1020 cm^{-1} , aromatic ortho-disubstituted CH (in plane hydrogen bending) is observed. Variable peak intensity for the aromatic ortho-disubstituted ring between 1525 to 1470 cm^{-1} , and strong peak intensity between 1625 and 1590 cm^{-1} is observed.

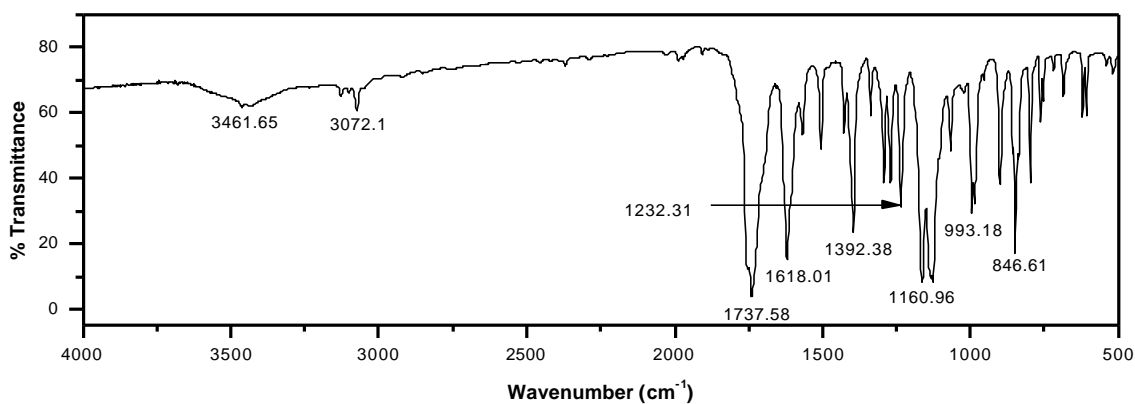


Figure 4.7: Fourier transform infrared analysis of 4-methyl-2-oxo-2H-chromen-7-yl acrylate (B_2).

4.3.4 Fluorescence studies

A plot of fluorescence intensity versus concentration should be linear at low concentrations and reach a plateau at higher concentrations. At even higher concentrations quenching becomes so great that the fluorescence intensity decreases (inner – cell effect).⁹⁻¹² Fig. 4.8a illustrates this point. This is advantageous because the lower the amount of tagging agent required, the more commercially viable the tagging process becomes. However, at very low concentrations, one may run the risk of being unable to detect the UV tag in the bulk sample. Thus, the concentration of all samples was kept constant at 1×10^{-6} M ($\pm 1 \times 10^{-8}$ M). Fluorescence analysis was performed at room temperature ($26 \pm 0.1^\circ\text{C}$) as an increase in temperature decreases fluorescence intensity¹³⁻¹⁶ (Fig. 4.8b). The temperature of analysis depended on the temperature to which the tagging agent would be exposed to in its final application. Furthermore, due to the fluorescence quenching nature of oxygen, samples were nitrogen purged for 30 minutes prior to analysis.

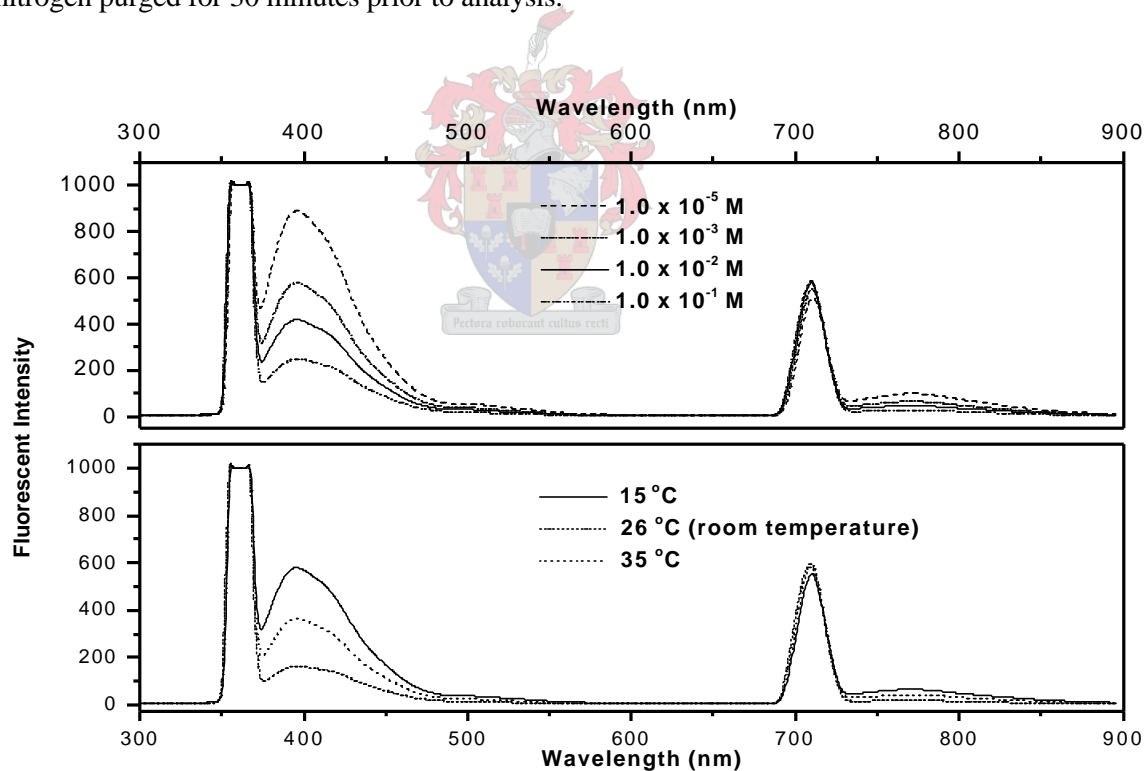


Figure 4.8: (a) The effect of concentration and (b) the effect of temperature on the fluorescence intensity of 2-oxo-2H-chromen-7-yl acrylate (A_2).

Ideally, the solvent used in fluorescence analysis should not exhibit any fluorescence in the region of interest to avoid any interference with the sample being analysed. Chloroform (freshly distilled) was chosen for two reasons: No fluorescence occurs and chloroform has a

relatively low dielectric constant (4.8 to 5.0). The low dielectric constant shifts both the absorption and fluorescence peaks to higher frequencies, thus resulting in higher intensities for both the absorption and fluorescence peaks.^{17,18} (Fig. 4.9)

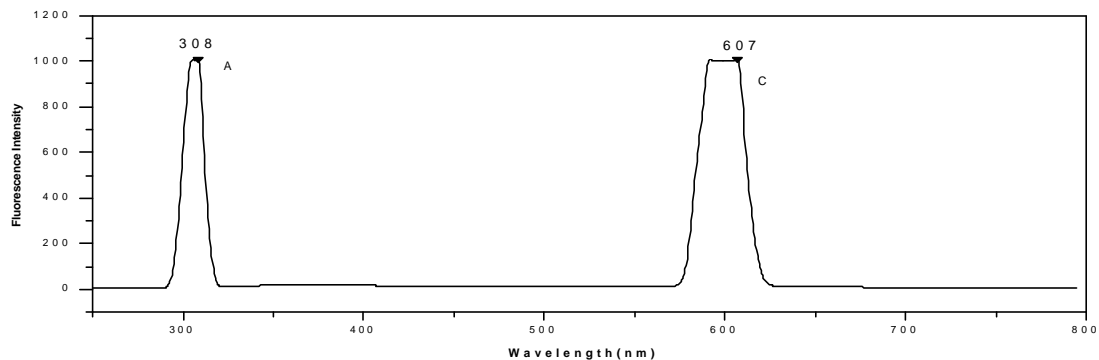


Figure 4.9: Illustration of the absence of fluorescence in chloroform.

Peak A (Fig. 4.9) is the result of Rayleigh scattering in which the emitted light and exciting light have the same wavelength. Peak C is due to Raman scattering and these are satellites of Rayleigh scattering appearing at higher wavelengths. The frequency difference from the exciting radiation will always remain constant in Raman scattering.

Fig. 4.10 and Fig. 4.11 show the fluorescence behaviour of 7-hydroxy-2H-chromen-2-one (A_1), 2-oxo-2H-chromen-7-yl acrylate (A_2), 7-hydroxy-4-methyl-2H-chromen-2-one (B_1) and 4-methyl-2-oxo-2H-chromen-7-yl acrylate (B_2). A number of observations can be made from these figures. Firstly, the emitted wavelength of the starting materials (7-hydroxy-2H-chromen-2-one (A_1) and 7-hydroxy-4-methyl-2H-chromen-2-one (B_1)) and the end products (2-oxo-2H-chromen-7-yl acrylate (A_2) and 4-methyl-2-oxo-2H-chromen-7-yl acrylate (B_2)) are similar (peak B). This indicates that fluorescence behaviour was maintained after esterification was performed. Esterification did not modify the aromatic hydrocarbon but only the side-groups; hence the moiety responsible for fluorescence was preserved.

Secondly, peak B is broader than peaks A and C, indicating the complexity and reduced symmetry in structure of samples A_1 , A_2 and B_1 and B_2 . Finally, the presence of a second order Rayleigh-scattering peak (peak D) is due to further light scattering of the exciting beam at longer wavelengths, brought on by the presence of the samples A_1 , A_2 , B_1 and B_2 .

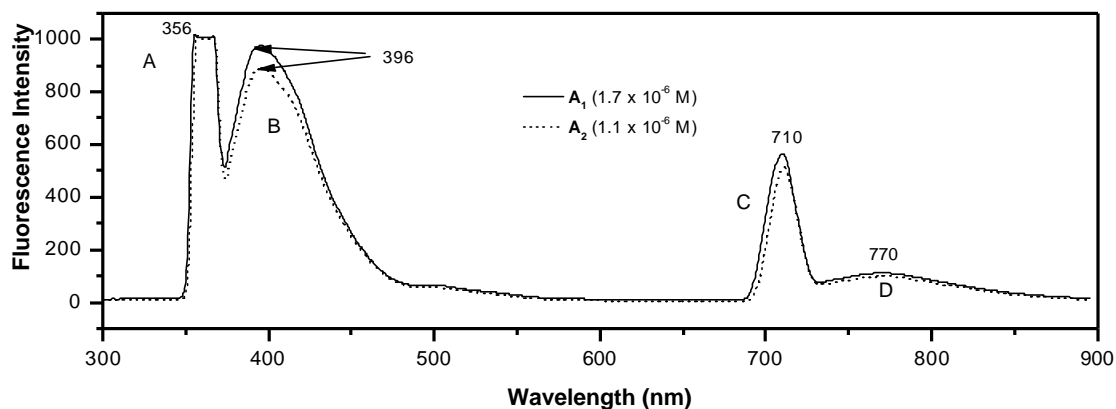


Figure 4.10: Similarity in the wavelength at which 7-hydroxy-2H-chromen-2-one (A₁) and 2-oxo-2H-chromen-7-yl acrylate (A₂) fluoresce at 26 ± 0.1 °C.

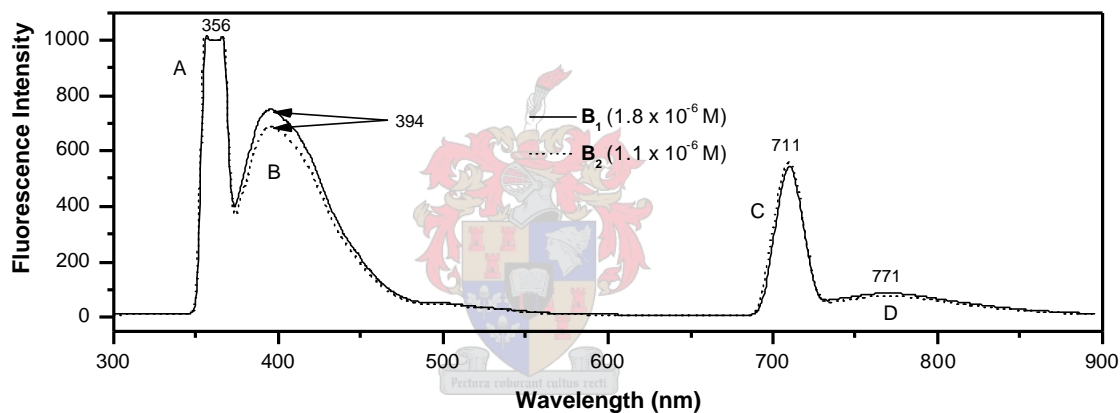


Figure 4.11: Similarity in the wavelength at which 7-hydroxy-4-methyl-2H-chromen-2-one (B₁) and 4-methyl-2-oxo-2H-chromen-7-yl acrylate (B₂) fluoresce at 26 ± 0.1 °C.

4.4. Conclusions

NMR and infrared analysis showed that esterification of the hydroxy groups in the fluorescent tags, A₁ and B₁, chosen for this study was successful. The synthesis of 2-oxo-2H-chromen-7-yl acrylate (A₂) and 4-methyl-2-oxo-2H-chromen-7-yl acrylate (B₂) by esterification of A₁ and B₁ was successful. Fluorescence analysis, conducted at 26 ± 0.1 °C and at a concentration of ± 1 × 10⁻⁶ M in chloroform, showed that fluorescence could be maintained after esterification of the hydroxy groups contained within the molecular structure of the selected commercially available fluorescent compounds.

References

- (1) Mann, F. G.; Saunders, B. C. *Practical organic chemistry*, 4 Ed.; Longman Singapore Publishers Pty Ltd: Singapore, 1994.
- (2) Bentley, T. W.; Llewellyn, G. J. *Org. Chem.* **1996**, *61*, 7927.
- (3) Fleming, I. *Tetrahedron Lett.* **1993**, *34*, 7287.
- (4) Smith, M. B.; March, J. *March's advanced org. chem: reactions, mechanism and structures*; John Wiley and Sons, Inc.: New York, 2001.
- (5) Reddy, B. S. R.; Balasubramanian, S. *Eur. Polym. J.* **2002**, *38*, 803-813.
- (6) D'Agosto, F.; Charreyre, M. T.; Veron, L.; Llauro, M. F.; Pichot, C. *Chem. Phys.* **2001**, *202*, 1689 - 1699.
- (7) Furniss, B. S.; Hannaford, A. J.; Rogers, V.; Smith, P. W. G.; Tatchell, A. R. *Vogel's Textbook of practical organic chemistry*, 4 Ed.; Longman Inc.: New York, 1978.
- (8) Brugel, W. *An introduction to infrared spectroscopy*; Methuen and Co. Ltd: New York, 1962.
- (9) Miller, J. N. *Standards in fluorescence spectroscopy: ultraviolet spectrometry group*; Chapman and Hall: London, 1981; Vol. 2.
- (10) Miller, J. N. *Standards in fluorescence spectroscopy: techniques in visible and ultraviolet spectroscopy*; Chapman and Hall: London, 1981; Vol. 2.
- (11) Baden, N.; Kajimoto, O.; Hara, K. *J. Phys. Chem. B.* **2002**, *106*, 8621-8624.
- (12) Guilbault, G. G. *Practical fluorescence: theory, methods, and techniques*; Marcel Dekker, Inc.: New York, 1973.
- (13) Parker, C. A. *Photoluminescence of solutions*; Elsevier: Amsterdam, 1986.
- (14) Olmsted, J. *Chem. Phys. Letters* **1976**, *38*, 287.
- (15) Bowen, E. J.; Sahu, J. *J. Phys. Chem.* **1959**, *63*, 4.
- (16) Suzuki, S.; Fujii, T.; Imai, A.; Akahori, H. *J. Phys. Chem.* **1977**, *81*, 1592.
- (17) Sambursky, S.; Wofsohn, G. *Phys. Rev.* **1942**, *62*, 357.
- (18) Sambursky, S.; Wofsohn, G. *Faraday Soc. Trans.* **1940**, *36*, 427.

Chapter 5

Solubility parameters of solvents and monomers

5.1 Introduction

Optimal solubility of reagents is crucial for any chemical reaction to be efficient. Therefore, solubilities of the selected compounds, 7-hydroxy-2H-chromen-2-one (A_1), 7-hydroxy-4-methyl-2H-chromen-2-one (B_1), 2-oxo-2H-chromen-7-yl acrylate (A_2) and 4-methyl-2-oxo-2H-chromen-7-yl acrylate (B_2) in common solvents such as ethanol, methanol, tetrahydrofuran, and chloroform, were investigated. The compounds displayed poor solubility (< 0.2%) in all the above-mentioned solvents. Hence the need arose for determining solubility parameters, as this would reduce time consumed of selecting suitable solvents on a ‘trial and error’ basis. See also Sec. 3.3.

5.2 Determination of solubility parameters

The solubility parameter d was calculated by using group molar attraction constants of 7 hydroxy-2H-chromen-2-one (A_1), 7 hydroxy-4-methyl-2H-chromen-2-one (B_1), 2-oxo-2H-chromen-7-yl acrylate (A_2) and 4-methyl-2-oxo-2H-chromen-7-yl acrylate (B_2) (Fig. 5.1 and 5.2), as proposed by Small, van Krevelen, Hoy and Fedors.^{1,2}



Figure 5.1: Chemical structures of (a) 7-hydroxy-2H-chromen-2-one (A_1) and (b) 7-hydroxy-4-methyl-2H-chromen-2-one (B_1).

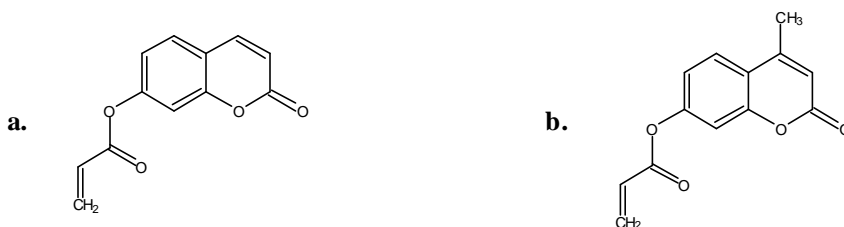


Figure 5.2: Chemical structures of (a) 2-oxo-2H-chromen-7-yl acrylate (A_2) and (b) 4-methyl-2-oxo-2H-chromen-7-yl acrylate (B_2).

Table 5.1 shows the values of the group molar attraction constants for various functional groups as well as values for the group molar volumes.

Table 5.1: Group molar attraction constants and group molar volumes according to van Krevelen, Small, Hoy and Fedors.^{1,2}

Structural Group	F ($J^{1/2} \cdot mol^{-1} \cdot cm^{-3/2}$)			E_{coh} (J/mol)	V ($cm^3 \cdot mol^{-1}$)	V ($cm^3 \cdot mol^{-1}$)
	Small (1953)	Krevelen (1965)	Hoy (1970)	Fedors (1974)	Hoy (1970)	Fedors & van Krevelen (1990)
-CH ₃	438	420	303.5	4710	21.55	33.5
-CH ₂ -	272	280	269	4940	15.55	16.1
R ₂ CH-	57	140	176	3430	9.56	-1.0
R ₃ C-	-190	0	65.5	1470	3.56	-19.2
H ₂ C=	495	560	249	4310	19.17	28.5
-CH=	454	444	173	4310	13.18	13.5
R ₂ C=	266	304	173	4310	7.18	-5.5
Phenyl	1504	1517	1398	31940	13.42	71.4
Phenyl (trisubstituted)	1346	1377	1442.3	31940	13.42	33.4
-OH	-	754	485	29800	10.65	10.0
-O-	143	256	235	3350	6.45	3.8
-CHO	-	-	600	21350	23.3	22.3
-CO-	563	685	538	17370	17.27	10.8
Cyclopentyl	-	1384	1295.1	24240	-	-
Cyclohexyl	-	1664	1473.3	29180	-	-
-F	250	164	84.5	4190	18	11.2
-Cl	552	471	419.6	11550	24	19.504

For the structural groups of A_1 and A_2 (Fig. 5.1), values for E_{coh} and V were assigned according to Table 5.1. The results shown in Table 5.2 were used in evaluating the solubility parameters.

Table 5.2: Group molar attraction constants for A_1 and A_2 .

Structural Group	A_1		A_2	
	E_{coh} (J/mol)	V ($cm^3 \cdot mol^{-1}$)	E_{coh} (J/mol)	V ($cm^3 \cdot mol^{-1}$)
-OH	29800	10.0	-	-
Phenyl (trisubstituted)	31940	33.4	31940	33.4
-O-	3350	3.8	3350	3.8
-O-	-	-	3350	3.8
-CO-	17370	10.8	17370	10.8
-CO-	-	-	17370	10.8
-CH=	4310	13.5	4310	13.5
-CH=	4310	13.5	4310	13.5
-CH=	-	-	4310	13.5
H ₂ C=	-	-	4310	28.5
Total	<i>91080</i>	85	<i>90620</i>	<i>131.6</i>

By substituting the values of Table 5.2 into the following equation, the solubility parameter of A_1 was calculated:

$$d = \left(\frac{E_{coh}}{V} \right)^{\frac{1}{2}} = \left(\frac{91080 \text{ J} \cdot \text{mol}^{-1}}{85 \text{ cm}^3 \cdot \text{mol}^{-1}} \right)^{\frac{1}{2}} = 32.73 \text{ J}^{1/2} \cdot \text{cm}^{-3/2}$$

and the solubility parameter of A_2 was calculated to be $26.24 \text{ J}^{1/2} \cdot \text{cm}^{-3/2}$.

The solubility of a given compound in various solvents is governed by its chemical structure whereby, as the molecular mass of the compound increases, the solubility will

decrease. However, this statement holds for compounds that are similar in chemical structure (oligomers, tetramers and higher). Hence, the solubility parameters of compounds A_1 and A_2 cannot be compared to each other, as they are different chemical compounds and have molecular weights of 162.1 and 216.1 $g.mol^{-1}$, respectively.

Via a similar calculation, the results, appearing in Table 5.3, were used in evaluating the solubility parameters of B_1 and B_2 .

Table 5.3: Group molar attraction constants for B_1 and B_2 .

Structural Group	B_1		B_2	
	E_{coh} (J/mol)	V ($cm^3.mol^{-1}$)	E_{coh} (J/mol)	V ($cm^3.mol^{-1}$)
-OH	29800	10.0	-	-
Phenyl (trisubstituted)	31940	33.4	31940	33.4
-O-	3350	3.8	3350	3.8
-O-	-	-	3350	3.8
-CO-	17370	10.8	17370	10.8
-CO-	-	-	17370	10.8
-CH=	4310	13.5	4310	13.5
-CH=	-	-	4310	13.5
-CH ₃	4710	33.5	4710	33.5
R ₂ C=	4310	-5.5	4310	-5.5
H ₂ C=	-	-	4310	28.5
Total	<i>95790</i>	<i>99.5</i>	<i>95330</i>	<i>146.1</i>

In this case, the solubility parameters of B_1 and B_2 were calculated as 31.03 and 25.54 $J^{1/2}.cm^{-3/2}$, respectively. Similar scenarios, when compared to A_1 and A_2 , were witnessed for B_1 and B_2 with molecular masses of 176.2 and 230.2 $g.mol^{-1}$, respectively.

5.3 Modification of solubility parameters

The values of the solubility parameters of A_1 , B_1 , A_2 and B_2 were refined by calculating the values for d_d , d_p and d_h from the group molar contributions tabulated in Table 5.4, as proposed by Hoftyzer and van Krevelen.¹ (Sec. 3.3.1)

Table 5.4: Group molar attraction constants for the 3-value solubility parameter concept according to van Krevelen.¹

Structural Group	F_{d_i} ($J^{1/2} \cdot mol^{-1} \cdot cm^{-3/2}$)	F_{p_i} ($J^{1/2} \cdot mol^{-1} \cdot cm^{-3/2}$)	E_{h_i} (J / mol)
-CH ₃	420	0	0
-CH ₂ -	270	0	0
R ₂ CH-	80	0	0
R ₃ C-	-70	0	0
H ₂ C=	400	0	0
-CH=	200	0	0
R ₂ C=	70	0	0
Phenyl	1620	0	0
-NH-	160	210	3100
-CN	430	1100	2500
-OH	210	500	20000
-COO-	390	490	7000
-O-	100	400	3000
-CHO	470	800	4500
-CO-	290	770	2000
-COOH	530	420	10000
-F	(220)	-	-
-Cl	450	550	400
-Br	(550)	-	-

These results, tabulated in Table 5.5, were used in evaluating the solubility parameters of A_1 and A_2 according to the 3-value solubility parameter concept.

Table 5.5: Group molar attraction constants for A_1 and A_2 according to the 3-value solubility parameter concept.

Structural Group	A_1			A_2		
	F_{d_i}	$F_{p_i}^2$	E_{h_i}	F_{d_i}	$F_{p_i}^2$	E_{h_i}
-OH	210	250000	20000	-	-	-
Phenyl	1270	12100	0	1270	12100	0
-O-	100	160000	3000	100	160000	3000
-O-	-	-	-	100	160000	3000
-CO-	290	592900	2000	290	592900	2000
-CO-	-	-	-	290	592900	2000
-CH=	200	0	0	200	0	0
-CH=	200	0	0	200	0	0
-CH=	-	-	-	200	0	0
H ₂ C=	-	-	-	400	0	0
Total	<i>2270</i>	<i>1015000</i>	<i>25000</i>	<i>3050</i>	<i>1517900</i>	<i>10000</i>

These results, appearing in Table 5.6 were used in evaluating the solubility parameters of B_1 and B_2 according to the 3-value solubility parameter concept.

Table 5.6: Group molar attraction constants for B_1 and B_2 according to the 3-value solubility parameter concept.

Structural Group	B_1			B_2		
	F_{d_i}	$F_{p_i}^2$	E_{h_i}	F_{d_i}	$F_{p_i}^2$	E_{h_i}
-OH	210	250000	20000	-	-	-
Phenyl	1270	12100	0	1270	12100	0
-O-	100	160000	3000	100	160000	3000
-O-	-	-	-	100	160000	3000
-CO-	290	592900	2000	290	592900	2000
-CO-	-	-	-	290	592900	2000
-CH=	200	0	0	200	0	0
-CH=	-	-	-	200	0	0
-CH ₃	420	0	0	420	0	0
R ₂ C=	70	0	0	70	0	0
H ₂ C=	-	-	-	400	0	0
Total	<i>2560</i>	<i>1015000</i>	<i>25000</i>	<i>3340</i>	<i>1517900</i>	<i>10000</i>

The contributions of dispersion forces d_d , polar forces d_p and hydrogen bonding d_h are shown in Table 5.7.

Table 5.7 Values for d_d , d_p and d_h in $J^{1/2}.cm^{-3/2}$ of A_1 , B_1 , A_2 and B_2 , calculated from group molar contributions according to Hoftyzer and van Krevelen.¹

Compd.	d_d	d_d^2	d_p	d_p^2	d_h	d_h^2
A₁	26.71	713.20	11.85	140.48	17.15	294.12
A₂	23.18	537.14	9.36	87.65	8.72	75.99
B₁	25.73	661.96	10.13	102.52	15.85	251.26
B₂	22.86	522.63	8.43	71.11	8.27	68.45

A comparison between the 3-value solubility concept and calculations using cohesive energy (Table 5.8) is necessary to reiterate the refinement the former method has over the latter.

Table 5.8: A tabulated comparison of the solubility parameters calculated by Fedors³ using the cohesive energy concept and the 3-value solubility concept, in $J^{1/2}.cm^{-3/2}$ proposed by Hoftyzer and van Krevelen.¹

Compd.	V ($cm^3.mol^{-1}$)	$d = \left(\frac{E_{coh}}{V} \right)^{\frac{1}{2}}$ Cohesive energy concept proposed by Fedors	$d_t = (d_d^2 + d_p^2 + d_h^2)^{\frac{1}{2}}$ 3-value solubility concept proposed by Hoftyzer and van Krevelen
A₁	85	32.73	33.88
A₂	131.6	26.24	26.47
B₁	99.5	31.03	31.87
B₂	146.1	25.54	25.73

Tables 5.9 and 5.10 lists the values of d_h and d_v (contribution of dispersion and polar forces to the solubility parameter) for the compounds A_1 , B_1 , A_2 , B_2 and selected common solvents, which were used in conjunction with each other to plot a graph illustrating the solvents that could be used in dissolving the compounds.

Table 5.9: Solubility parameters for A₁, B₁, A₂ and B₂ evaluated by the 3-value solubility concept in $J^{1/2}.cm^{-3/2}$.

Compd.	d_d	d_p	d_h	d_v	d_t
A ₁	26.71	11.85	17.15	29.22	33.88
A ₂	23.18	9.36	8.72	25.00	26.48
B ₁	25.73	10.13	15.85	27.65	31.87
B ₂	22.86	8.43	8.27	24.36	25.73

Table 5.10: Hansen solubility parameters for selected common solvents evaluated by the 3-value solubility concept in $J^{1/2}.cm^{-3/2}$.³

Solvents	d_d	d_p	d_h	d_v	d_t
Acetone	15.5	10.4	7.0	18.67	19.94
Acetonitrile	15.3	18.0	6.1	23.62	24.40
Benzene	18.4	0.0	2.0	18.40	18.51
Butane	14.1	0.0	0.0	14.10	14.10
Carbon tetrachloride	17.8	0.0	0.6	17.80	17.81
Chloroform	17.8	3.1	5.7	18.07	18.95
Cyclohexane	16.8	0.0	0.2	16.80	16.80
Cyclopentane	16.4	0.0	1.8	16.40	16.50
Decane	15.7	0.0	0.0	15.70	15.70
Dibenzyl ether	17.3	3.7	7.3	17.69	19.14
Diethylene glycol	16.6	12.0	20.7	20.48	29.12
Dimethyl sulfoxide	18.4	16.4	10.2	24.65	26.68
1,4 - Dioxane	19.0	1.8	7.4	19.09	20.47
Ethyl acetate	15.8	5.3	7.2	16.67	18.15
Ethylene glycol	17.0	11.0	26.0	20.25	32.95
1 - Heptene	15.0	1.1	2.6	15.04	15.26
1 - Hexene	14.7	1.1	0.0	14.74	14.74
Octane	15.5	0.0	0.0	15.50	15.50
Toluene	18.0	1.4	2.0	18.05	18.16
Triethylamine	17.8	0.4	1.0	17.80	17.83
Tetrahydrofuran	16.8	5.7	8.0	17.74	19.46
Methanol	15.1	12.3	22.3	19.48	29.61
Ethanol	15.8	8.8	19.4	18.09	26.52
Water	15.6	16.0	42.4	22.3	47.9
Methyl methacrylate	15.8	6.5	5.4	17.08	17.92
Butyl acrylate	15.6	6.2	4.9	16.79	17.49

The preferred solvents will lie in an area around the substance (this area can be denoted by a circle of which the radius of the circle⁴ is determined by the compound itself), as can be seen in Fig. 5.3. In Table 5.11, results show that after 8 hours, only 40 to 60% of A_2 and B_2 dissolved in diethylene glycol and 1,4-dioxane (solvents 3 and 5 respectively), whilst 90% of A_2 and B_2 dissolved in acetonitrile and dimethyl sulfoxide. Therefore, the diameter of the circle includes all solvents that displayed a 90% and above solubility parameter.

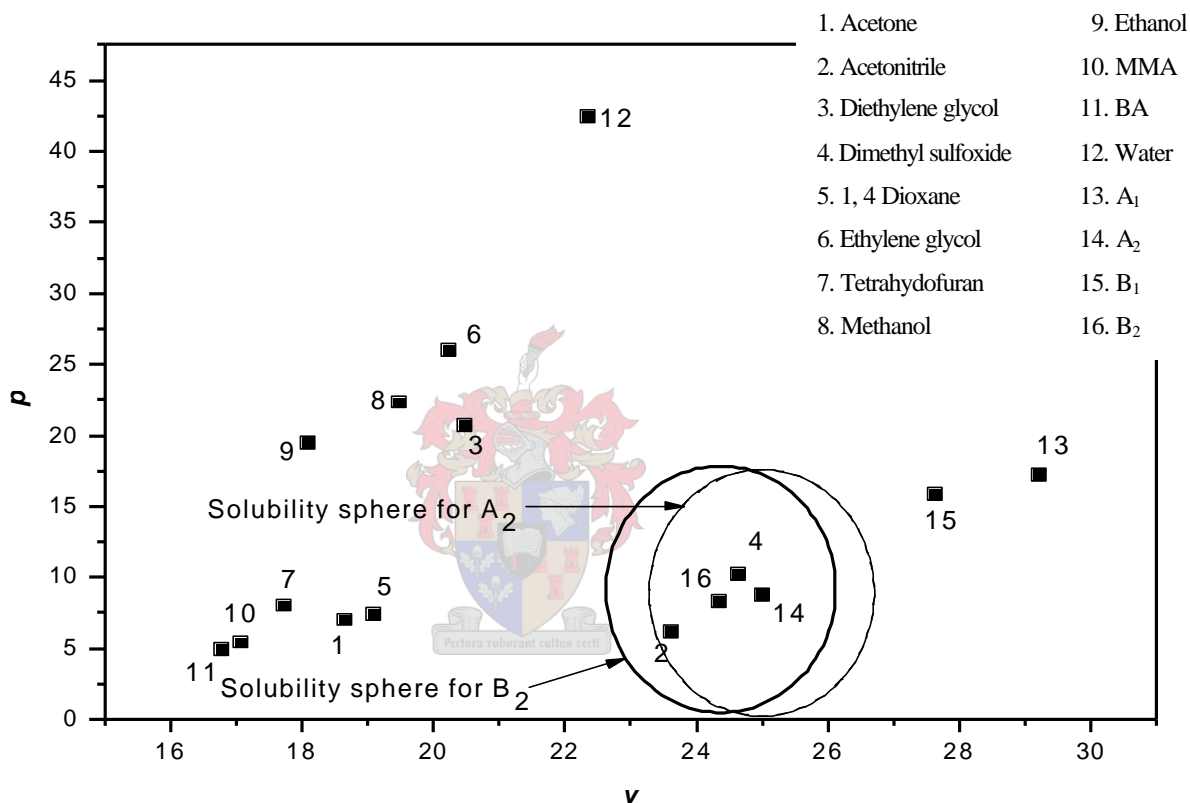


Figure 5.3: Hansen solubility parameters for A_1 , B_1 , A_2 and B_2 in selected solvents.

The solvents situated inside the solubility sphere (Fig. 5.3) represent good solvents: solvents 8, 9, 10, 11 and 12 are poor solvents and solvents 3, 5 and 6 are intermediate solvents.

5.4 Experimental verification

0.1 grams (0.00043 moles) of A_2 and B_2 were weighed and placed in five separate conical flasks containing 5 mL of acetonitrile, dimethyl sulfoxide, diethylene glycol, 1,4-dioxane and methanol, respectively. The conical flasks were sealed with stoppers and

vigorously stirred with a magnetic stirrer bar on a magnetic stirrer plate for four two-hour intervals. Data were obtained by filtering the undissolved particles from the solution, and weighing the dried powder after it was air-dried, through the use of vacuum filtration.

The solvents were selected on the assumption that acetonitrile and dimethyl sulfoxide (found inside the solubility sphere, Fig. 5.3) were good solvents, diethylene glycol and 1,4-dioxane were intermediate solvents, and methanol was a poor solvent. Table 5.11 shows the results (percentage soluble) of this experiment at two-hour intervals.

Table 5.11: Tabulation of the percentages of A₂ and B₂ that were soluble in selected solvents at two-hour time intervals, determined experimentally.

Time Interval (Hours)	Acetonitrile		Dimethyl sulfoxide		Diethylene glycol		1,4 - Dioxane		Methanol	
	A ₂	B ₂	A ₂	B ₂	A ₂	B ₂	A ₂	B ₂	A ₂	B ₂
2	100	98.3	89.8	82.4	48.1	31.5	35.7	23.2	5.6	3.2
4	100	100	96.6	91.5	59.4	48.3	45.3	36.1	7.2	4.8
6	100	100	100	99.7	62.1	55.9	58.5	39.9	7.5	5.2
8	100	100	100	100	63.5	58.0	60.3	42.3	7.9	5.4

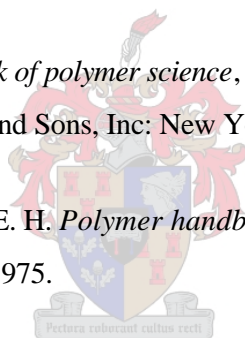
Evidently, acetonitrile and dimethyl sulfoxide were good solvents, displaying maximum solubility within a minimum time frame. Diethylene glycol, 1,4 - dioxane (being intermediate solvents) and methanol (poor solvent) did not show the same degree of effectiveness.

5.5 Conclusions

It was established that the use of solubility parameters eliminated the tediousness of physically ascertaining the correct solvents for the particular chemical reactions. Theoretical analysis revealed acetonitrile to be the most favourable solvent for dissolving the compounds used in this study and this was verified by experimental data. This information was used to proceed with the next step of this project, i.e. polymerisation.

References

- (1) van Krevelen, D. W. *Properties of polymers: their correlation with chemical structure; their numerical estimation and prediction from additive group contributions*, 3 Ed.; Elsevier Science Publishers: Amsterdam, 1997.
- (2) Barton, A. F. M. *CRC Handbook of solubility parameters and other cohesion parameters*, 2 Ed.; CRC Press: Boca Raton, Fla., 1991.
- (3) Hansen, C. M. *Hansen solubility parameters: a user's handbook*; C.R.C. Press: Boca Raton, Fla., 2000.
- (4) Van Zyl, A. J. P. M.Sc. thesis; University of Stellenbosch: Stellenbosch, 2001; 221.
- (5) Billmeyer, F. W. *Textbook of polymer science*, 2 Ed.; Wiley-Interscience, a Division of John Wiley and Sons, Inc: New York, 1962.
- (6) Brandrup, J.; Immergut, E. H. *Polymer handbook*, 2 Ed.; Wiley-Interscience Publication: New York, 1975.



Chapter 6

Solution polymerisation studies

6.1 Introduction

The aim of this part of the study was to produce fluorescent-tagged polymers. This was to be done by incorporating fluorescent monomers (A_2 and/or B_2) into a selected polymer chain. Further studies were then undertaken to determine the fluorescence of the polymers as well as the reactivity ratios for the copolymerization systems.

A prerequisite of this study was that the tagged polymer must be highly compatible with existing paint polymer resins (Sec. 1.4) to prevent any rheological and/or integrity changes of the product. For this reason, butyl acrylate (BA) and methyl methacrylate (MMA) were chosen as the most suitable monomers for this study. These two monomers are frequently used as comonomers in the production of acrylate-methacrylate copolymers for binders and paint resins.¹

6.2 Experimental

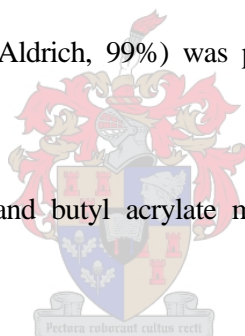
6.2.1 Chemicals and their purification

Acetonitrile (ACN, Merck, 99%) was purified by distillation. 250 mL of commercially available acetonitrile was placed in a 500 mL round bottom flask, along with bumping granules, and heated to $\pm 1^\circ\text{C}$ above the boiling point of acetonitrile (81.6°C). The resulting vapour was condensed with the use of a distillation condenser, collected in a flask and stored at 2°C . MgSO_4 was also added to ensure a completely water-free product.

Methyl methacrylate (MMA, Aldrich, 99%) was purified by removing any inhibitors and other impurities by distillation. The monomer was first washed with 0.3 M potassium hydroxide (KOH) solution to remove the hydroquinone inhibitor. 400 mL of methyl methacrylate monomer and 100 mL of KOH solution was brought into a 500 mL separation funnel and carefully shaken to ensure that most of the inhibitor was washed out into the aqueous KOH phase. This was repeated three times, after which the bottom layer (KOH solution) was carefully removed. The monomer was transferred to a 1-liter round bottom flask and boiling stones added. The flask was subsequently connected to a distillation set-up. Distillation was done under vacuum and with low heat applied to the flask. Care had to be taken in controlling this purification step by restricting the temperature of the vapour to below 55°C. The first 40 mL fraction collected was discarded to ensure that the distilled monomer was free from any impurities and water. The second fraction was collected and stored at 2°C to inhibit polymerization.

The butyl acrylate monomer (BA, Aldrich, 99%) was purified in the same manner as MMA was.

The distilled methyl methacrylate and butyl acrylate monomers used in all further reactions were never more than 5 days old.



The free radical initiator that was used for all the experiments was 2,2'-azobisisobutyronitrile (AIBN, Delta Scientific, 98%). An inert internal reference 1,3,5-trioxane (Fluka AG, 97%), used for reactivity ratio determinations, was used as received. The water was distilled and deionised (DDI).

6.2.2 Instrumentation

NMR spectra were recorded on a 300 MHz Varian VXR spectrometer equipped with a Varian magnet (7.0 T), and a 600 MHz Varian Unity Inova spectrometer equipped with an Oxford magnet (14.09 T). Standard pulse sequences were used for obtaining ^1H spectra. Polymers were dissolved in deuterated chloroform.

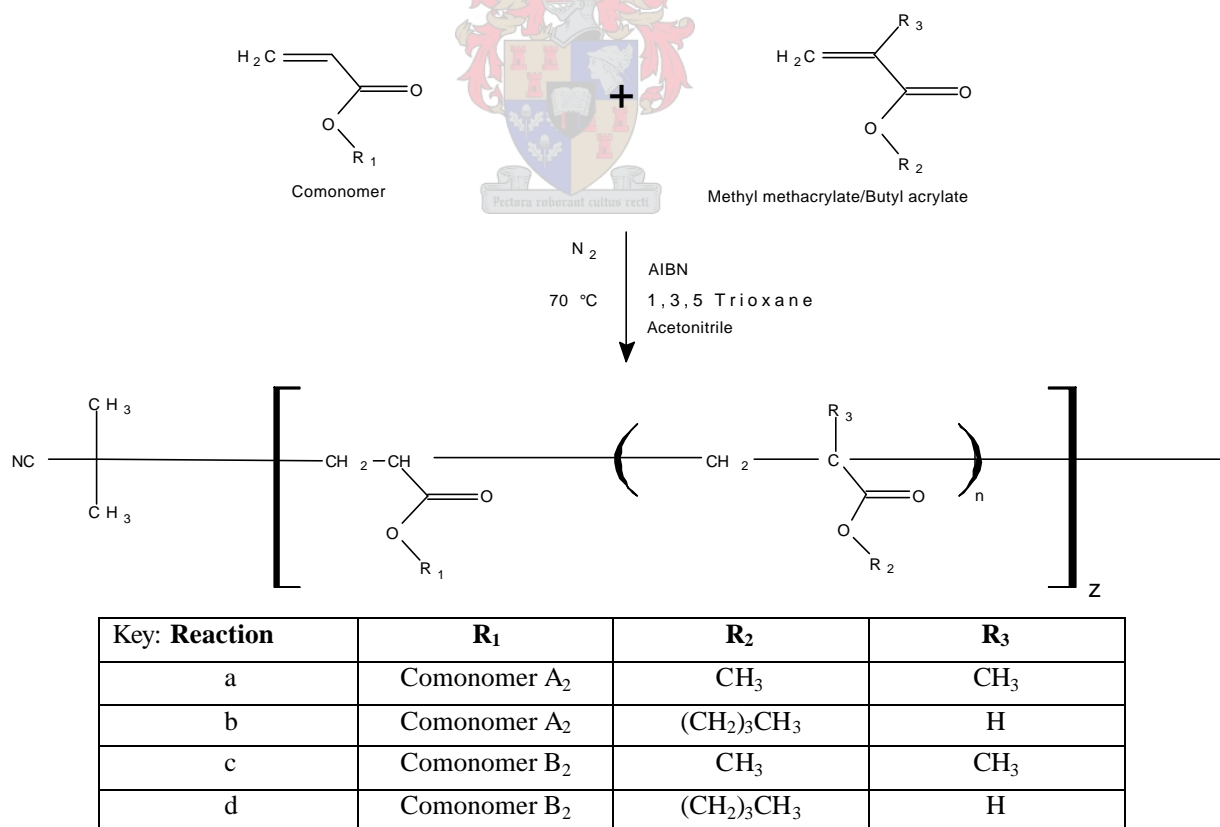
Fluorescence analysis was conducted on a Perkin Elmer Luminescence Spectrometer LS 50B and 10 mm Quartz cuvettes (PECSA Analytical) were used for all analyses.

6.2.3 Determination of reactivity ratios

The reaction schemes for the copolymerisation of

- 2-oxo-2H-chromen-7-yl acrylate (A_2) and methyl methacrylate
- 2-oxo-2H-chromen-7-yl acrylate (A_2) and butyl acrylate
- 4-methyl-2-oxo-2H-chromen-7-yl acrylate (B_2) and methyl methacrylate
- 4-methyl-2-oxo-2H-chromen-7-yl acrylate (B_2) and butyl acrylate

in acetonitrile, using AIBN as the free radical initiator at 70°C ($\pm 1^\circ\text{C}$), are shown in Scheme 6.1. Individual monomer concentrations were followed using $^1\text{H-NMR}$ spectroscopy. This type of analytical technique is frequently used to determine the amounts of each monomer in a copolymer, it is widely accepted and used both in industry and academia for the study of polymerisation kinetics.^{2,4} 1,3,5-Trioxane was added as an inert internal reference to determine monomer concentrations, by comparing the signals of the vinylic protons corresponding to the different monomers.⁵



Scheme 6.1: Reaction scheme for the copolymerisation utilising AIBN as an initiator.

The research conducted in this thesis was limited to batch reactions, where all the reactants were charged at the beginning of the reaction.⁶ The purified monomers and all but 2 mL of solvent were added into a clean three necked round bottom flask that was heated to 70°C ($\pm 1^\circ\text{C}$) while being purged with nitrogen for 25 minutes. The flask was fitted with a condenser, nitrogen purge and magnetic stirrer bar. (Fig. 6.1) A thermocouple (temperature regulator) was used to control the temperature of the oil bath.

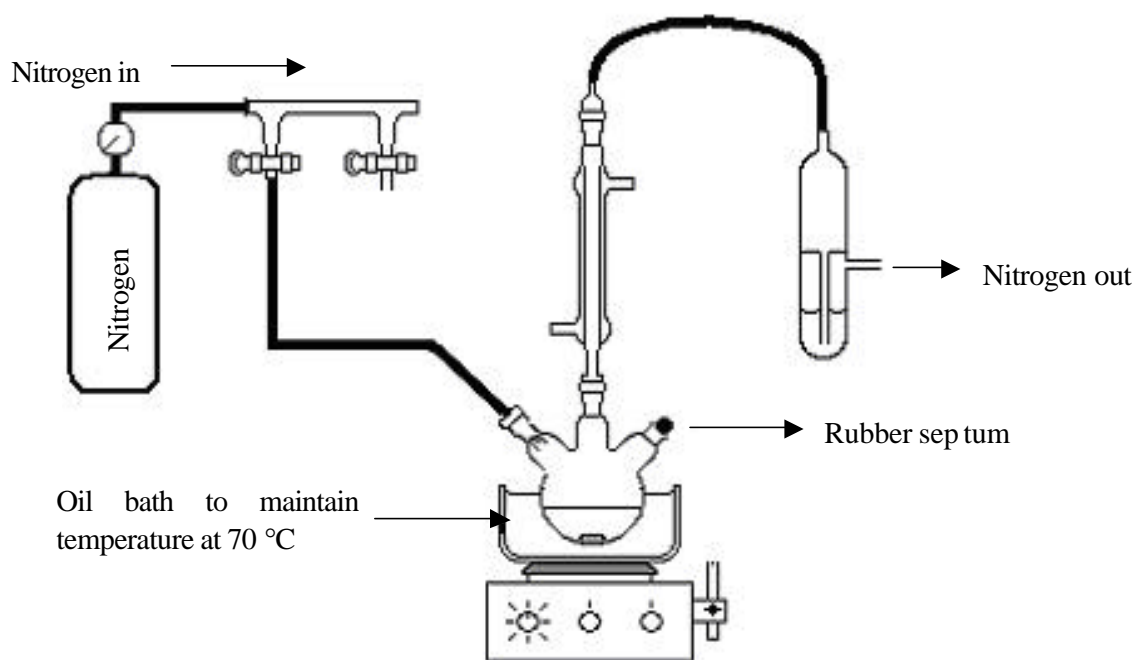


Figure 6.1: Apparatus set-up for the copolymerisation reactions.

After initial purging, the initiator was added to the reaction solution to start the polymerisation reaction. The additional 2 mL solvent was used to rinse traces of initiator and added to the reaction flask. Various amounts of monomers were used to change the charging ratios in a systematic manner. In all cases the total monomer concentration was kept constant. The amount of AIBN that was added to the reactions was held constant at a half mole percent relative to the total monomer concentration.

The amount of 1,3,5-trioxane added was the equivalent of half the total molar amount of monomer to compensate for the 3 extra protons found on the 1,3,5-trioxane molecule, compared to the vinylic protons of the monomers. Tables 6.1 through 6.4 indicate the amounts of each monomer, solvent and initiator that were used to produce a methodical study of the copolymer composition.

Table 6.1: Amounts of comonomers, initiator, internal reference and solvent used in the copolymerisation study of *Reaction a.*

A ₂ :MMA Ratio	A ₂ [Conc] *	MMA [Conc] *	AIBN mass (g)	Trioxane mass (g)	Total [Monomer]*	ACN (mL)
1:1	0.3303	0.3565	0.0396	0.1044	0.6868	7.015
1:3	0.1716	0.5151	0.0399	0.0547	0.6867	7.081
1:6	0.0984	0.5901	0.0398	0.0312	0.6885	7.034
1:9	0.0687	0.6181	0.0395	0.0217	0.6868	7.005
2:1	0.4578	0.2288	0.0395	0.1446	0.6866	7.012

Table 6.2: Amounts of comonomers, initiator, internal reference and solvent used in the copolymerisation study of *Reaction b.*

A ₂ :BA Ratio	A ₂ [Conc] *	BA [Conc] *	AIBN mass (g)	Trioxane mass (g)	Total [Monomer]*	ACN (mL)
1:1	0.3299	0.3277	0.0379	0.1044	0.6576	7.024
1:3	0.1643	0.4931	0.0378	0.0519	0.6574	7.012
1:6	0.0938	0.5633	0.0378	0.0296	0.6571	7.003
1:9	0.0657	0.5917	0.0379	0.0208	0.6574	7.014
2:1	0.4383	0.2191	0.0378	0.1382	0.6574	7.002

Table 6.3: Amounts of comonomers, initiator, internal reference and solvent used in the copolymerisation study of *Reaction c.*

B ₂ :MMA Ratio	B ₂ [Conc] *	MMA [Conc] *	AIBN mass (g)	Trioxane mass (g)	Total [Monomer]*	ACN (mL)
1:1	0.3153	0.3055	0.0357	0.0995	0.6208	7.006
1:3	0.1601	0.4798	0.0369	0.0506	0.6399	7.014
1:6	0.0922	0.5474	0.0368	0.0291	0.6396	7.008
1:9	0.0643	0.5759	0.0369	0.0203	0.6402	7.015
2:1	0.4263	0.2128	0.0370	0.1353	0.6391	7.044

Table 6.4: Amounts of comonomers, initiator, internal reference and solvent used in the copolymerisation study of *Reaction d.*

B ₂ :BA Ratio	B ₂ [Conc] *	BA [Conc] *	AIBN mass (g)	Trioxane mass (g)	Total [Monomer]*	ACN (mL)
1:1	0.3138	0.3138	0.0361	0.0990	0.6275	7.002
1:3	0.1568	0.4774	0.0365	0.0495	0.6342	7.007
1:6	0.0897	0.5379	0.0361	0.0283	0.6276	7.003
1:9	0.0629	0.5650	0.0362	0.0198	0.6279	7.016
2:1	0.4185	0.2093	0.0362	0.1324	0.6278	7.025

* [Concentration] in moles/litre.

For each different MMA/A₂, MMA/B₂, BA/A₂ and BA/B₂ starting compositions, ¹H-NMR spectra were recorded of each reaction mixture before the start of the reaction and after running the reaction for 30 minutes. A sample of about 700 μL of the reaction mixture was transferred to an NMR tube containing 4 drops of CDCl₃. The ratio of the integrated signals of the internal reference, before and after the reactions, was used to calculate individual monomer incorporation.

The copolymer compositions arising from twenty different feed compositions (expressed in terms of molar fractions) were used in a non-linear least-squares fitting to Eqn. 6.1, to determine the reactivity ratios.^{7,8}

$$F_1 = \frac{r_1 f_1^2 + f_1 f_2}{r_1 f_1^2 + 2f_1 f_2 + r_2 f_2^2} \quad 6.1$$

F_1 is the fraction of monomer M_1 in the copolymer, f_1 and $f_2 = 1 - f_1$ the fractions of monomer M_1 and monomer M_2 in the feed respectively, and r_1 and r_2 the reactivity ratios.

The feed ratio of 1:1 (A₂/B₂:MMA/BA) was allowed to polymerise to 80% monomer conversion and the data obtained analysed as above. Since the reactivity ratios were indicative of the nature of the copolymer sequence, this step was essential to indicate the pattern of incorporation of both monomers, in each reaction system, as a function of time. The original feed composition, tabulated in Tables 6.1 through 6.4, was scaled-up to accommodate for the higher number of sample retrievals needed. (Table 6.5)

Table 6.5: Amounts of monomers, initiator, internal reference and solvent used in the copolymerisation study.

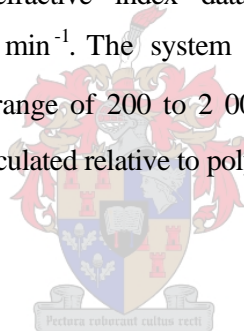
Polym No.	A ₂ (mol)	MMA (mol)	B ₂ (mol)	BA (mol)	AIBN (mol)	Trioxane (mol)	Total [Monomer]	ACN (mL)
1	0.023168	0.023488	-	-	0.002333	0.0116	4.9680	70.153
2	0.023227	-	-	0.023424	0.002333	0.0116	4.9610	70.245
3	-	0.023428	0.023119	-	0.002327	0.0116	4.9630	70.060
4	-	-	0.023146	0.023409	0.002328	0.0116	4.9660	70.029

Placing the reaction flasks in ice baths subsequently quenched the reactions. The contents of all polymerisation reactions were precipitated by pouring into an excess of methanol and filtered by vacuum filtration using a Buchner funnel and vacuum. Further drying of the copolymer was performed in a vacuum oven at an elevated temperature (up to 70°C) to allow for the methanol to evaporate. The copolymers were allowed to dry at 70°C for a minimum of 10 hours. Once dried, the copolymers were weighed and analysed further.

6.2.4 Molecular weight analyses

Samples were prepared for size exclusion chromatography (SEC) analysis by drying the polymer *in vacuo* and redissolving *ca.* 5 mg of the polymer in 1 mL of THF (HPLC-grade). Analyses were carried out with a SEC system comprising of a Waters 410 Differential Refractometer, Waters 717_{plus} Autosampler and Waters 600E System Controller. The molecular weights were determined from refractive index data analysed with Millennium³² V3.05 software. The flow rate was 1 mL min⁻¹. The system was calibrated using six narrow molar mass polystyrene standards in the range of 200 to 2 000 000 g.mol⁻¹, supplied by Polymer Labs. All molecular weights were calculated relative to polystyrene.

6.3 Results and discussion



6.3.1 Copolymerization kinetics

¹H-NMR spectrometry was used in this study to determine individual monomer conversions for a number of different starting compositions, which facilitated the determination of F_{MMA} , f_{MMA} and F_{BA} , f_{BA} values. F_{A_2} , f_{A_2} , F_{B_2} and f_{B_2} values were obtained in the same manner.

Figs. 6.2 and 6.3 show the signals corresponding to the vinylic protons of the two respective monomers relative to 1,3,5-trioxane.

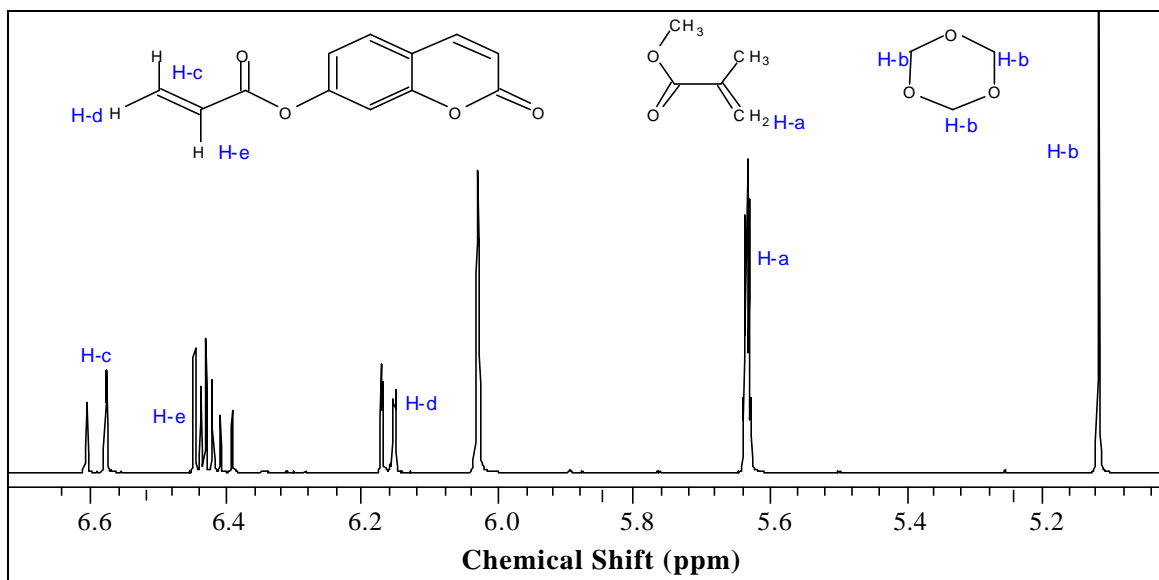


Figure 6.2: A typical ¹H-NMR spectrum of a MMA/A₂ (6:1) copolymerisation reaction mixture in (CDCl₃) showing the region of interest. (Reaction a)

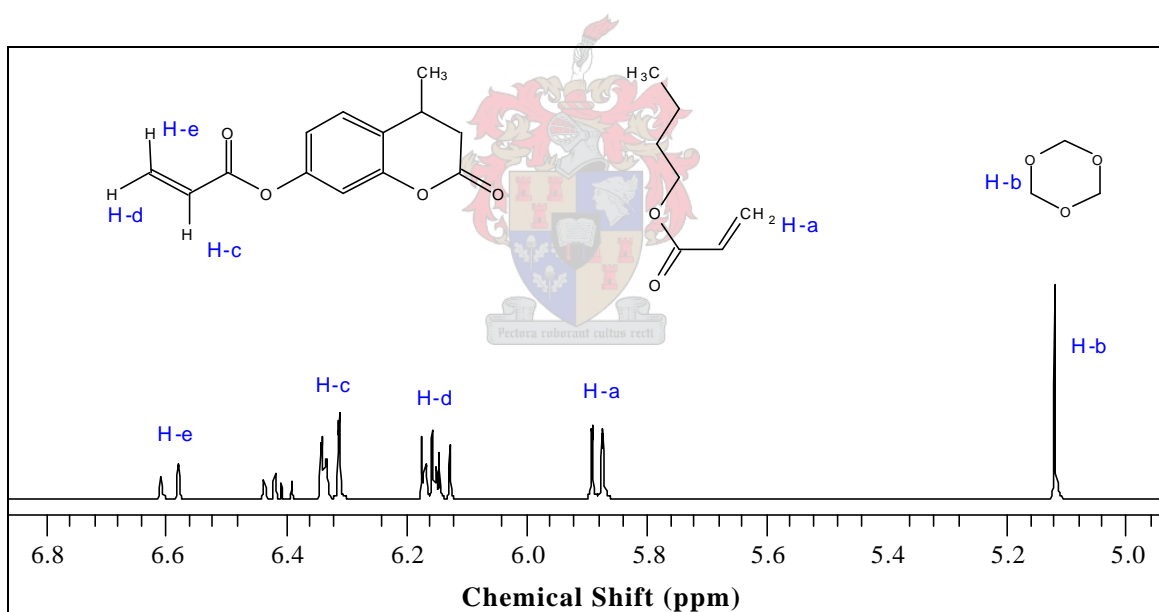


Figure 6.3: A typical ¹H-NMR spectrum of a BA/B₂ (6:1) copolymerisation reaction mixture in (CDCl₃) showing the region of interest. (Reaction d)

By use of the following equation:

$$\left(\frac{R_t}{R_o}\right) \times [M]_0 = [M]_t \quad 6.2$$

$$\text{and} \quad [M]_r = [M]_0 - [M]_i \quad 6.3$$

where R_i is the ratio of the integrated signals of monomer to reference after the reaction and R_0 is the same ratio before the start of the reaction. $[M]_0$ and $[M]_i$ are the initial and final concentrations of each monomer respectively. $[M]_r$ is the concentration of each monomer that is incorporated into the copolymer. Subtracting $[M]_i$ from the initial concentration $[M]_0$ of each comonomer, the amount of incorporation could be calculated. All copolymers with conversions higher than 20% were not used in the current study on reactivity ratios due to the possibility of compositional drift that could arise at higher conversions.

Tables 6.6 through 6.9 (see pages 83 through 84) show the percentage incorporation of A_2/B_2 when copolymerised with MMA and BA respectively. F_c is the mole fraction of c in the formed copolymer. As the molar fraction of MMA or BA increases in the feed, a higher incorporation of A_2/B_2 results. Even when the molar fraction of A_2/B_2 in the feed is higher than that of MMA or BA, only a certain percentage was incorporated. It could therefore be concluded that incorporation of A_2/B_2 was dependent on the availability of MMA/BA in the sample.

The calculated reactivity ratios, obtained by least-squares fitting to Eqn. 6.1, are shown in Table 6.10. They were used to compute and graphically illustrate theoretical values of the fraction of monomer M_1 in the copolymer at various feed fractions.

Table 6.10: Reactivity ratios for the copolymer systems.

System	r_1 (MMA/BA)	r_2 (A_2/B_2)
MMA/ A_2	1.96	0.52
BA/ A_2	1.93	0.48
MMA/ B_2	1.97	0.53
BA/ B_2	1.98	0.43

Table 6.6: ¹H-NMR spectroscopy results for MMA/A₂ copolymerisation reactions.

Polymer no.	Intensity of A ₂ at t = 0min	Intensity of A ₂ at t = 30min	[A ₂] ₀ mol/L at t = 0min	[A ₂] _t mol/L at t = 30min	Intensity (MMA) at t = 0min	Intensity (MMA) at t = 30min	[MMA] ₀ mol/L at t = 0min	[MMA] _t mol/L at t = 30min	<i>F</i> _{A₂}	<i>F</i> _{MMA}	% Incorp. of A ₂ in copolymer	% Incorp. of MMA in copolymer
1	2.8	2.7	0.2467	0.2379	2.5	2.3	0.2663	0.2450	0.2926	0.7074	3.57	8.00
2	2.3	2.2	0.1282	0.1227	6.4	5.7	0.3847	0.3426	0.1170	0.8830	4.35	10.94
3	1.9	1.8	0.0735	0.0696	15.1	13.0	0.4408	0.3795	0.0593	0.9407	5.26	13.91
4	1.2	1.1	0.0513	0.0470	14.6	11.9	0.4617	0.3764	0.0477	0.9523	8.33	18.49
5	3.0	2.9	0.3420	0.3306	1.7	1.6	0.1709	0.1608	0.5314	0.4686	3.33	5.88



Table 6.7: ¹H-NMR spectroscopy results for BA/A₂ copolymerisation reactions.

Polymer no.	Intensity of A ₂ at t = 0min	Intensity of A ₂ at t = 30min	[A ₂] ₀ mol/L at t = 0min	[A ₂] _t mol/L at t = 30min	Intensity (BA) at t = 0min	Intensity (BA) at t = 30min	[BA] ₀ mol/L at t = 0min	[BA] _t mol/L at t = 30min	<i>F</i> _{A₂}	<i>F</i> _{BA}	% Incorp. of A ₂ in copolymer	% Incorp. of BA in copolymer
6	2.0	1.9	0.2464	0.2354	2.00	1.8	0.2448	0.2204	0.3117	0.6883	4.50	10.00
7	1.5	1.4	0.1227	0.1146	5.50	4.8	0.3683	0.3214	0.1486	0.8514	6.67	12.73
8	1.2	1.1	0.0701	0.0643	12.50	10.5	0.4208	0.3535	0.0799	0.9201	8.33	16.00
9	1.0	0.9	0.0491	0.0442	17.70	14.1	0.4419	0.3520	0.0518	0.9482	10.00	20.34
10	2.6	2.5	0.3274	0.3148	1.30	1.2	0.1636	0.1510	0.5001	0.4999	3.85	7.69

Table 6.8: ¹H-NMR spectroscopy results for MMA/B₂ copolymerisation reactions.

Polymer no.	Intensity of B ₂ at t = 0min	Intensity of B ₂ at t = 30min	[B ₂] ₀ mol/L at t = 0min	[B ₂] _t mol/L at t = 30min	Intensity (MMA) at t = 0min	Intensity (MMA) at t = 30min	[MMA] ₀ mol/L at t = 0min	[MMA] _t mol/L at t = 30min	<i>F</i> _{B₂}	<i>F</i> _{MMA}	% Incorp. of B ₂ in copolymer	% Incorp. of MMA in copolymer
11	2.6	2.5	0.2355	0.2265	2.6	2.4	0.2282	0.2107	0.3404	0.6596	3.85	7.69
12	1.8	1.7	0.1196	0.1130	2.8	2.5	0.3585	0.3201	0.1475	0.8525	5.56	10.71
13	1.3	1.2	0.0688	0.0635	12.8	10.9	0.4091	0.3484	0.0801	0.9199	7.69	14.84
14	1.9	1.7	0.0480	0.0429	22.9	18.9	0.4302	0.3475	0.0576	0.9424	10.53	19.21
15	2.1	2.0	0.3185	0.3034	1.1	1.0	0.1599	0.1454	0.5106	0.4894	4.76	9.09

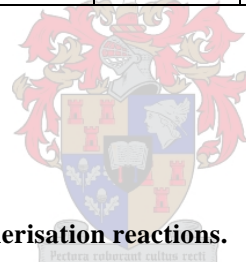


Table 6.9: ¹H-NMR spectroscopy results for BA/B₂ copolymerisation reactions.

Polymer no.	Intensity of B ₂ at t = 0min	Intensity of B ₂ at t = 30min	[B ₂] ₀ mol/L at t = 0min	[B ₂] _t mol/L at t = 30min	Intensity (BA) at t = 0min	Intensity (BA) at t = 30min	[BA] ₀ mol/L at t = 0min	[BA] _t mol/L at t = 30min	<i>F</i> _{B₂}	<i>F</i> _{BA}	% Incorp. of B ₂ in copolymer	% Incorp. of BA in copolymer
16	1.9	1.8	0.2344	0.2221	2.6	2.3	0.2344	0.2073	0.3133	0.6867	5.26	11.54
17	1.3	1.2	0.1172	0.1082	6.8	5.8	0.3566	0.3042	0.1467	0.8533	7.69	14.71
18	1.2	1.1	0.0670	0.0614	12.9	10.8	0.4018	0.3364	0.0786	0.9214	8.33	16.28
19	2.1	1.9	0.0469	0.0424	24.9	20.2	0.4220	0.3423	0.0531	0.9469	9.52	18.88
20	1.9	1.8	0.3126	0.2962	0.9	0.8	0.1563	0.1389	0.4865	0.5135	5.26	11.11

A plot of instantaneous copolymer composition versus feed composition could be constructed comparing theoretical and experimental data points. These compositional diagrams (Fig. 6.4) show that no azeotrope existed for the systems under investigation. There also appears to be a preference toward MMA and BA in cases where one of these monomers was copolymerised with A_2/B_2 .

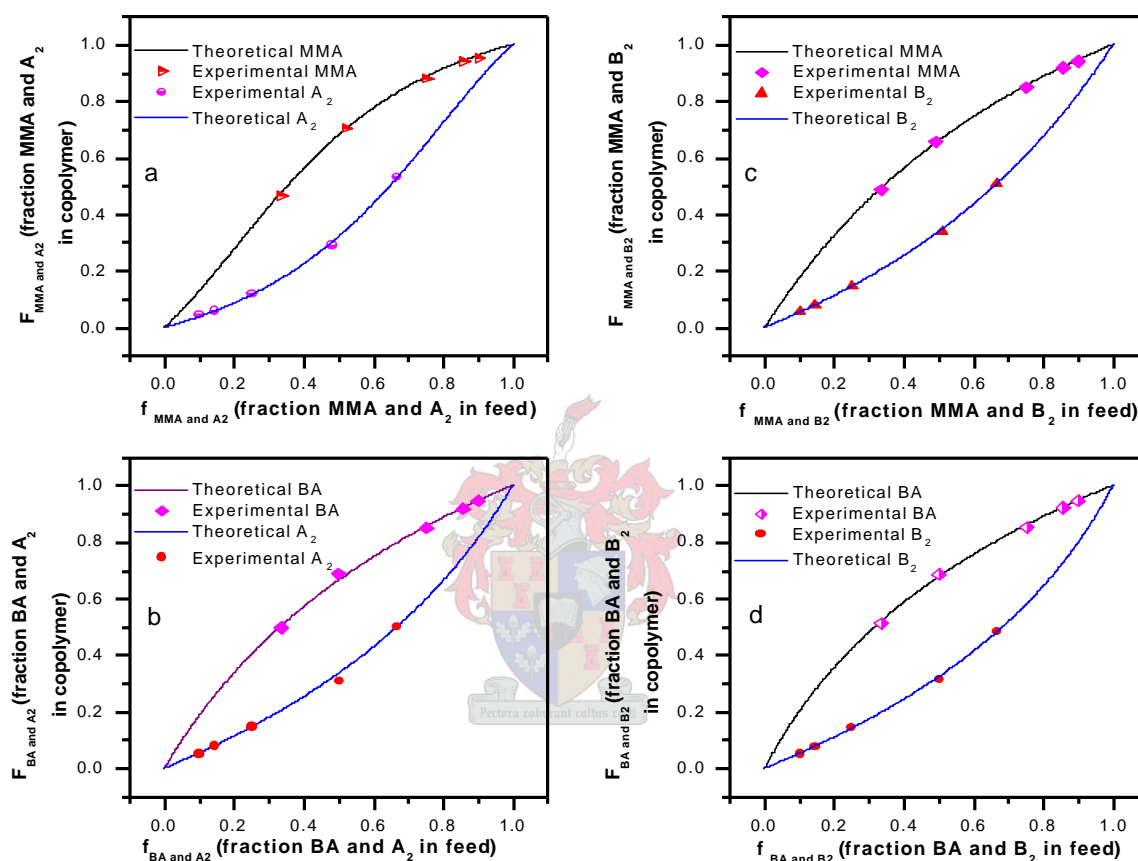


Figure 6.4: Instantaneous copolymer composition versus feed composition for reactions (a), (b), (c) and (d) after a 30-minute reaction period.

The reaction mixture consisting of a molar feed ratio of 1:1 (A_2/B_2 :MMA/BA) was allowed to polymerise for 15 hours ($\pm 80\%$ conversion). The original feed compositions, tabulated in Tables 6.1 through 6.4, were scaled up to accommodate for the higher number of sample retrievals needed.

Fig. 6.5 shows that A_2/B_2 was incorporated at a steady rate for ± 8 hours, thereafter a plateau was reached. Due to the inability of A_2/B_2 homopolymerisation to occur, this plateau was probably due to the decreased availability of MMA/BA monomers in the reaction mixture.

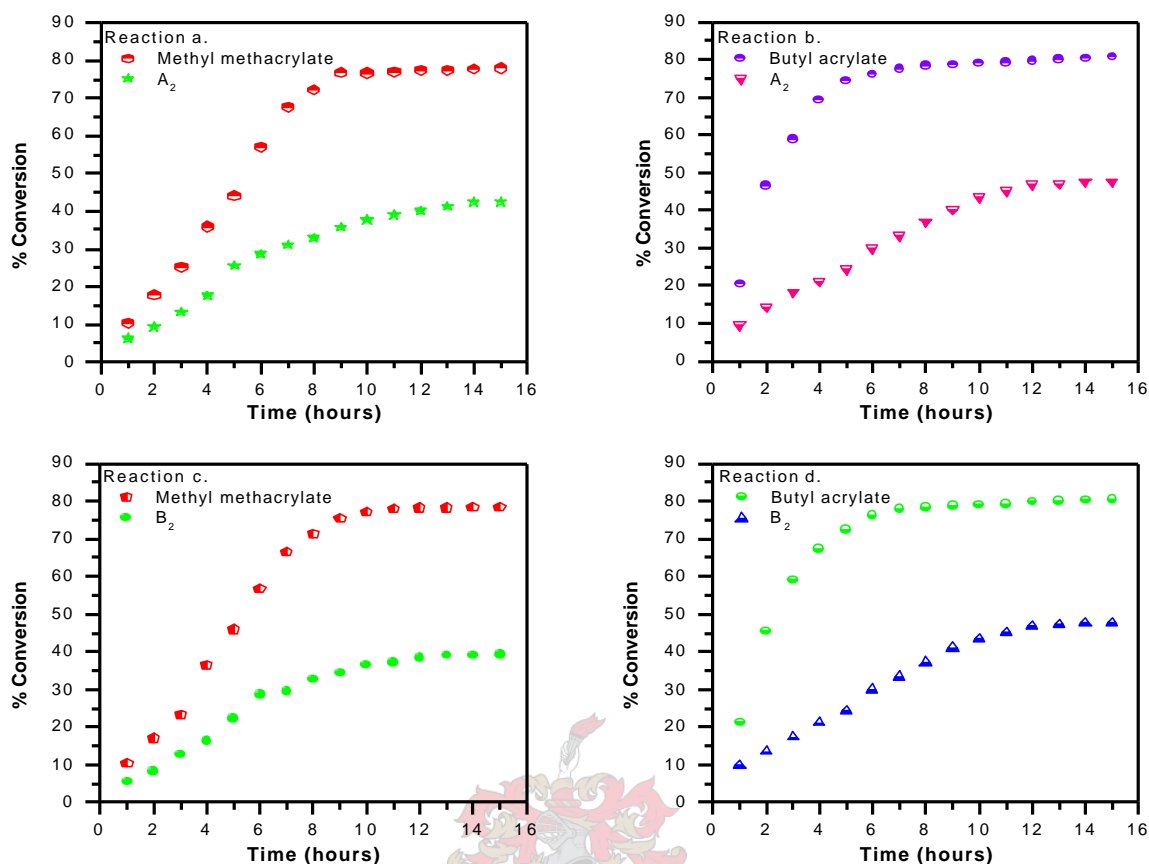


Figure 6.5: ¹H NMR spectroscopy results for the incorporation of respective monomers in reactions (a), (b), (c) and (d) as a function of time.

6.3.2 Molecular weight determinations

Results of analyses done on the final copolymers are shown in Table 6.11. As a result of the conventional free radical polymerization mechanism that was followed, the molecular weight distributions of the final copolymers were broad.

Table 6.11: Molecular weight data of polymers.

Polymers	M_w	M_n	M_w / M_n
Poly(MMA-co-A ₂)	14254	2341	6.089
Poly(BA-co-A ₂)	17900	2467	7.254
Poly(MMA-co-B ₂)	12524	1789	7.000
Poly(BA-co-B ₂)	107542	9675	11.115

6.3.3 Fluorescence studies

Accurate fluorescence analysis on the final polymer was complicated by the possibility of unreacted probe being present in the isolated sample. TLC was used to first confirm that the final polymer was pure.

Apart from merely detecting fluorescence in the dried polymer samples, the fluorescence intensity of the entire dry polymer sample (0.714 g) needed to be determined. Fluorescence analysis was carried out on a fraction of the sample (representative of the entire sample), which was diluted to $\pm 1 \times 10^{-2} \text{ g.L}^{-1}$ in chloroform overnight. Calibration curves were set-up, using various concentrations of A_2 and B_2 (Fig. 6.6). By detecting the fluorescence intensity of the representative sample, a direct calibration to the fluorescence intensity of the entire polymer sample was achieved. In this case, the fluorescence intensity of the entire polymer sample was greater than 1000 units, thus the total concentration of the substance responsible for emitting fluorescence could not be accurately determined. Analysis was performed at room temperature ($26 \pm 0.1^\circ\text{C}$). Due to the fluorescence quenching nature of oxygen, samples were nitrogen purged for 30 minutes prior to analysis.

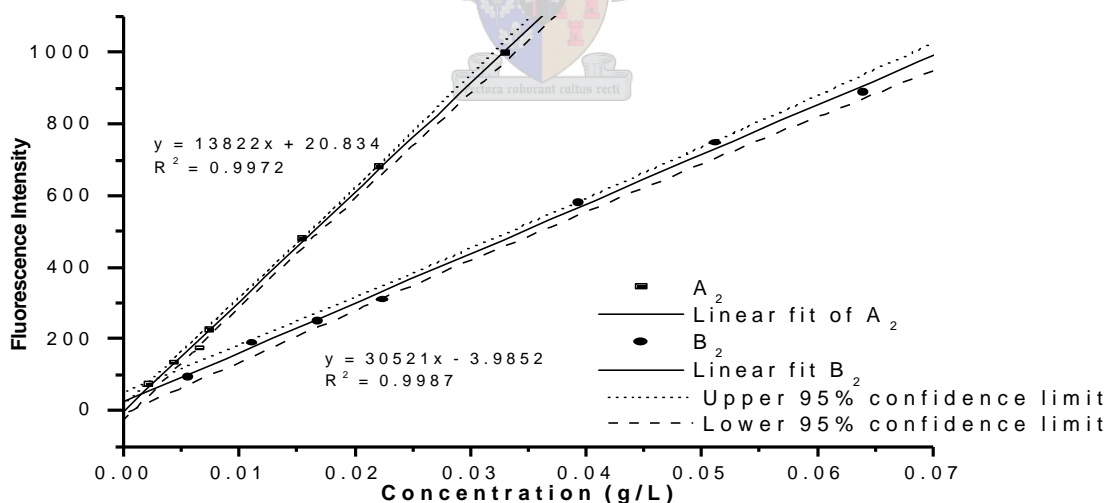


Figure 6.6: Calibration curves for the fluorescence analysis of A_2 and B_2 in chloroform.

Chloroform was chosen as the ideal solvent because of its low dielectric constant,^{9,10} (See Sec. 4.3.4) also as methyl methacrylate and butyl acrylate do not display any fluorescent properties as shown in Fig. 6.7. This allows fluorescence analysis to be accurately conducted without any interference by the sample in question.

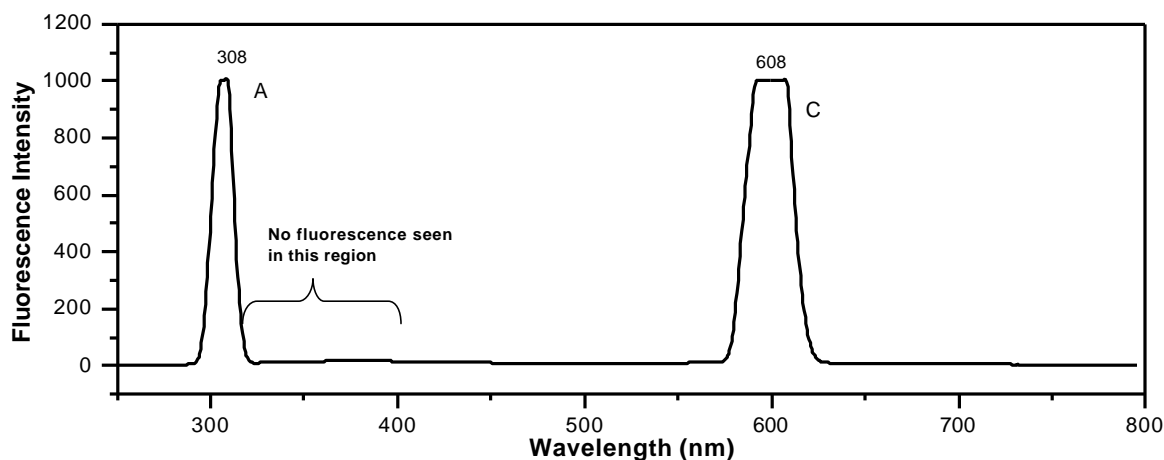


Figure 6.7: Illustration of the absence of fluorescence in a mixture of methyl methacrylate (1×10^{-6} M) and butyl acrylate (1.0×10^{-6} M) in chloroform.

Peak A denotes Rayleigh scattering; and Peak C is due to the effect of Raman scattering. Both of which have been discussed in Sec. 4.3.4.

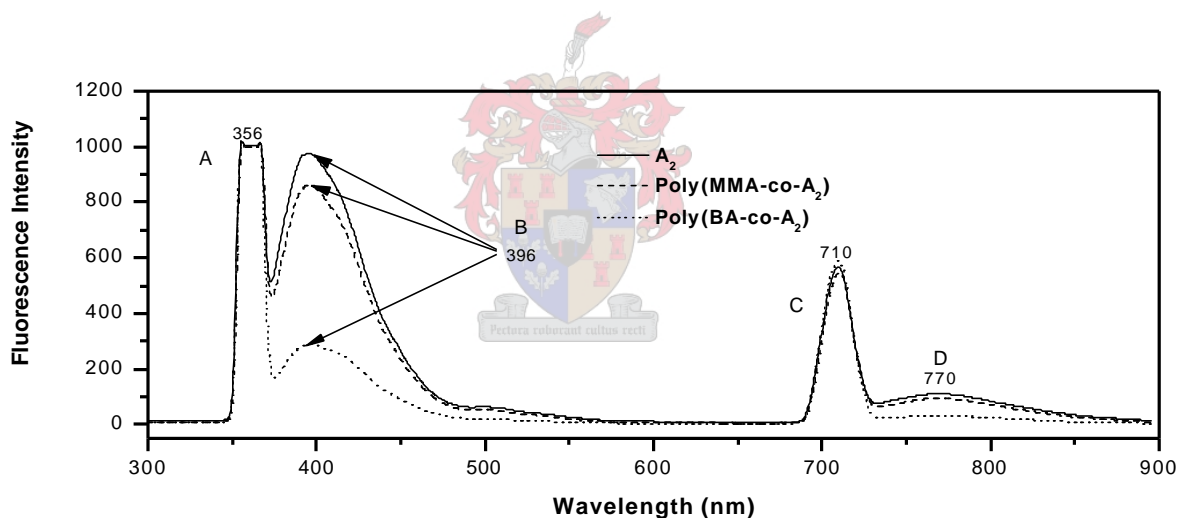


Figure 6.8: Fluorescence analysis of (a) 2-oxo-2H-chromen-7-yl acrylate (A_2), (b) poly(MMA-co- A_2) and (c) poly(BA-co- A_2) copolymers.

As shown in Figs. 6.8 and 6.9, the components used in the copolymerisation reactions did not interfere with the fluorescent nature of 2-oxo-2H-chromen-7-yl acrylate (A_2) and 4-methyl-2-oxo-2H-chromen-7-yl acrylate (B_2), with regard to the wavelength at which these compounds appear (peak B). This indicates that fluorescence was maintained throughout the copolymerisation process. The presence of a second order Rayleigh scatter (peak D) is evident, as seen in Sec. 4.3.4.

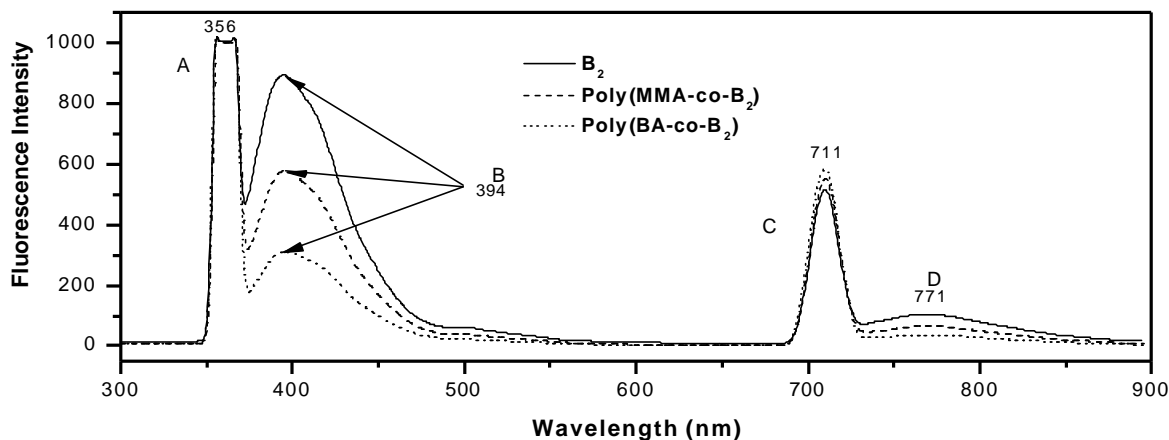


Figure 6.9: Fluorescence analysis of (a) 4-methyl-2-oxo-2H-chromen-7-yl acrylate (B_2), (b) poly(MMA-co- B_2) and (c) poly(BA-co- B_2) copolymers.

6.4 Conclusions

By assuming a terminal model (Sec. 3.2.2, pg 32), reactivity ratios in the conventional free radical copolymerisation of MMA/BA and A_2/B_2 were determined by monitoring the percentage of incorporation of individual free monomer using $^1\text{H-NMR}$ spectroscopy. Simple least-squares non-linear fitting procedures to the copolymer equation (Eqn. 6.1) were used to determine the values of the reactivity ratios, which was used to construct plots of instantaneous copolymer compositions versus feed compositions. These compositional diagrams showed that no azeotrope existed for the systems under investigation and there appears to be a preference for MMA and BA when one of these monomers is copolymerised with A_2/B_2 .

Fluorescence studies showed that fluorescence was maintained in the following copolymers: poly(MMA-co- A_2), poly(MMA-co- B_2), poly(BA-co- A_2) and poly(BA-co- B_2).

References

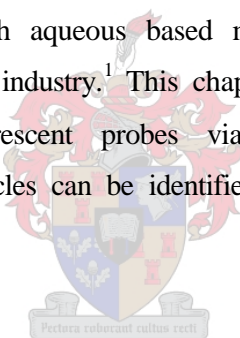
- (1) Wilks, E. S. *Industrial polymers handbook: products, processes and application*; Wiley-VCH Verlag: Weinheim, 2001; Vol. 2.
- (2) Brandolini, A. J. *NMR spectroscopy of polymer and polymer additives*; Marcel Dekker: New York, 2000.
- (3) Tonelli, A. E. *NMR spectroscopy and polymer microstructures: the conformational connection*; Wiley-VCH: New York, 1989.
- (4) Macomber, R. S. *NMR spectroscopy: essential theory and practice*; Brace Jovanovich Publishers: New York, 1988.
- (5) D'Agosto, F. C. M. T., Veron, L., Llauro, M.F., Pichot, C. *Macromol. Chem. Phys.* **2001**, *202*, 1689-1699.
- (6) Biesenberger, J. A.; Sebastian, D. H. *Principles of polymerisation engineering*; Wiley: New York, 1983.
- (7) Brar, A. S.; Kumar, R. *J. Mol. Struct.* **2002**, *616*, 37-47.
- (8) Ito, H.; Dalby, C.; Pomerantz, A.; Sherwood, M.; Sato, R.; Sooriyakumaran, R.; Guy, K.; Breyta, G. *Macromolecules* **2000**, *33*, 5080-5089.
- (9) Sambursky, S.; Wofsohn, G. *Faraday Soc. Trans.* **1940**, *36*, 427.
- (10) Sambursky, S.; Wofsohn, G. *Phys. Rev.* **1942**, *62*, 357.

Chapter 7

Fluorescent - tagged paints

7.1 Introduction

The rapid increase in environmental concerns and government regulations to substitute volatile solvents with aqueous based mediums has encouraged the use of miniemulsion polymerisation in industry.¹ This chapter describes the preparation of latex particles containing the fluorescent probes via miniemulsion polymerisation, and determining whether these particles can be identified and quantified when dispersed in a paint polymer resin.



7.2 Experimental

7.2.1 Materials

Methyl methacrylate (MMA, Aldrich, 99%) and butyl acrylate (BA, Aldrich, 99%) were distilled as described in chapter 5. n-Hexadecane (ACROS, 99%), 2,2'-azobisisobutyronitrile (AIBN, Delta Scientific, 98%) and sodium dodecyl sulphate (SDS, BDH, 90%) were used as received. The water was distilled and deionised (DDI) with a Millipore Milli-Q purification system.

7.2.2 Synthesis of latexes by miniemulsification-ultrasonication

Methyl methacrylate/butyl acrylate, hexadecane, AIBN and A₂/B₂ were premixed with a SDS/water solution for 1 hour.² A miniemulsion was obtained by sonicating the mixture with a Sonics & Materials Inc. Vibracell VCX 750 ultrasonicator for 10 minutes at

an amplitude of 80% (the energy input varied, as shown in Table 7.1, for each reaction system). The relatively low quantities of A₂ and B₂ used in reactions were due to their poor solubility in methyl methacrylate and butyl acrylate. (Chapter 5, Sec. 5.3). In order to avoid polymerisation occurring due to heating, the solution was continuously stirred (400 rpm) in a jacketed vessel. After miniemulsification the mixture was transferred to a 100 mL glass reactor, which was suspended in a thermostatted oil bath, and equipped with a condenser and nitrogen purge inlet. (Chapter 6, Fig. 6.1) Nitrogen was bubbled through the reaction mixture and samples were retrieved at 5-minute intervals. The samples were quenched by placing the entire reaction flasks in an ice bath, which cooled the reaction mixtures to temperatures that essentially stopped the decomposition of the AIBN initiator. Conversion data were calculated via a gravimetric method. The formulations for the above reactions can be seen in Table 7.1.

Table 7.1: Miniemulsion recipes (quantities given in grams) for the synthesis of the respective latexes.

	Reaction components	Poly(MMA-co-A ₂)	Poly(MMA-co-B ₂)	Poly(BA-co-A ₂)	Poly(BA-co-B ₂)	Poly (MMA)	Poly (BA)
Oil phase	AIBN	0.0501	0.0500	0.0501	0.0502	0.0501	0.0502
	MMA	10.0055	10.0031	-	-	10.0037	10.0042
	BA	-	-	10.0010	10.0012	-	-
	A ₂	0.7002	-	0.7010	-	-	-
	B ₂	-	0.6989	-	0.6956	-	-
	Hexadecane	0.4301	0.4309	0.4302	0.4305	0.4305	0.4308
Water phase	SDS	1.0019	1.0005	1.0002	1.0010	1.0013	1.0004
	Water	40.0021	40.0073	40.0011	40.0032	40.0080	40.0025
	Sonication (kJ)	108396	118563	103569	114695	110702	118952

7.2.3 Analytical techniques

7.2.3.1 Size-exclusion chromatographic analysis

Molar mass distributions were measured via size-exclusion chromatography (SEC). Dried latex samples were dissolved in THF (HPLC-grade) (5 mg/mL) and filtered through a 0.45 µm nylon filter. Analyses were carried out with a SEC system comprising a Waters 410 Differential Refractometer, Waters 717_{plus} Autosampler and Waters 600E

System Controller. The molar mass was determined from refractive index data analysed with Millennium³² V3.05 software. The eluent was THF (sparged with IR-grade helium) and the flow rate was 1 mL min⁻¹. The volume of the injected samples was 100 µL. The system was calibrated using six narrow molar mass polystyrene standards in the range of 200 to 2 000 000 g.mol⁻¹, supplied by Polymer Laboratories. All molecular masses were calculated relative to polystyrene. A Waters 2487 Dual Wavelength Absorbance detector was used in series with the refractive index detector to detect the copolymers as they eluted from the size-exclusion column. Analyses were carried out at a wavelength of 320 nm since UV analysis, carried out with a Perkin Elmer UV-vis Spectrometer (Lambda 20) equipped with UVWinlab-version⁴⁰ software, showed that A₂/B₂ absorbed light at 320 nm.

7.2.3.2 Transmission electron microscopy analysis

For TEM analysis, 20 µL aliquots of dispersed sample (in water) were applied to a carbon coated copper grid. Excess sample was removed by blotting with filter paper. The samples were contrasted with a 2% uranyl acetate solution, which acts as a negative stain. The grids were air dried and viewed on a LEO 912 electron microscope with a CCD camera, operated at 120 kV.

7.2.3.3 Particle size analysis

Photon correlation spectroscopy (PCS) was used to carry out particle size analyses, which may be used to study particle sizes at a sub micron level. PCS measures Brownian motion and relates this to the size of the particles (the rate of movement of the particles is inversely proportional to the size of the particles).^{3,4}

The velocity of the particles is defined by the diffusion coefficient D , as given in Eqn. 7.1, and is referred to as the Stokes-Einstein equation:

$$d(H) = \frac{kT}{3\eta pD} \quad 7.1$$

The particle sizes of the latex particles were determined by a Malvern Zetasizer 1000HS. The instrument compares the amount of light scattered by the latex particles to that scattered by the solvent, using a correlator. Since larger particles move slower than smaller

particles, a relationship between the amount of scattered light and the velocity at which the particles are moving is obtained, which can be transformed by Eqn. 7.1 to obtain the volume of the latex particles.

The coefficient of variation (*COV*) of the distribution of the particles is provided by the Malvern Zetasizer 1000HS. The (*COV*) and the polydispersity index (*PDI*), the latter given in terms of the width of the peak obtained, is related by Eqn. 7.2,⁵

$$PDI = \left(1 + \frac{s^2}{m^2} \right)^{\frac{1}{2}} = \left[1 + \frac{(COV)^2}{100^2} \right]^{\frac{1}{2}} \quad 7.2$$

with *m* being the number average diameter and *s* is the variance of the particle size distribution.

7.2.3.4 UV studies

To determine whether the fluorescent latex particles can be identified when dispersed in a paint polymer resin, two commercially available paint samples were homogenised with varying concentrations of fluorescent latex particles. One paint sample contained 10% titanium dioxide and the other was titanium dioxide free. Due to the broadness of the fluorescence peak (Chapter 4, Figs. 4.9 and 4.10) over a wide range of wavelengths, a common bench-top UV-lamp (at 365 nm) was used to detect fluorescence in the dried paint polymer resins. It offers simple identification of the tagged paint on a wall.

UV-reflectance, determined with a GBC UV/visible 920 Spectrometer, was used as an analytical method to quantify the minimum amount of fluorescent polymer needed to tag a certain quantity of paint. Various compositions were formulated for each system and analyses carried out on the dried materials.

7.3 Results and discussion

Polymers containing a butyl acrylate composition tended to show a greater percentage of conversion within 5 minutes compared to polymers containing a methyl methacrylate composition. (Fig. 7.1) However, each reaction system plateaus at 70 percent conversion after 35 minutes.

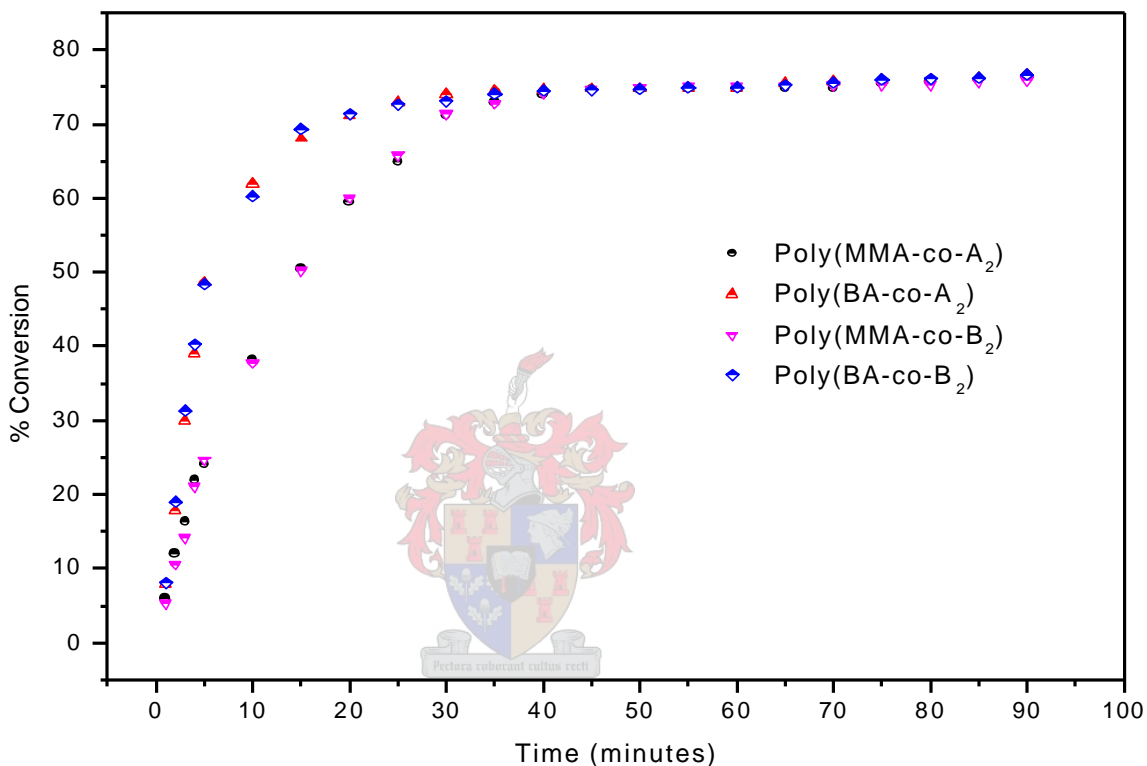


Figure 7.1: Percentage conversion of methyl methacrylate and butyl acrylate during copolymerisation of A₂ and B₂ as a function of time.

7.3.1 Size-exclusion chromatographic analysis

The combination of a differential refractometer with an absorbance detector confirmed the distribution of A₂/B₂ along the copolymer sequence. Fig. 7.2 illustrates that A₂ and B₂ were homogeneously distributed throughout the copolymer sequences, in that the UV and refractive index detectors give essentially the same response for all molecular masses short as well as long chains.

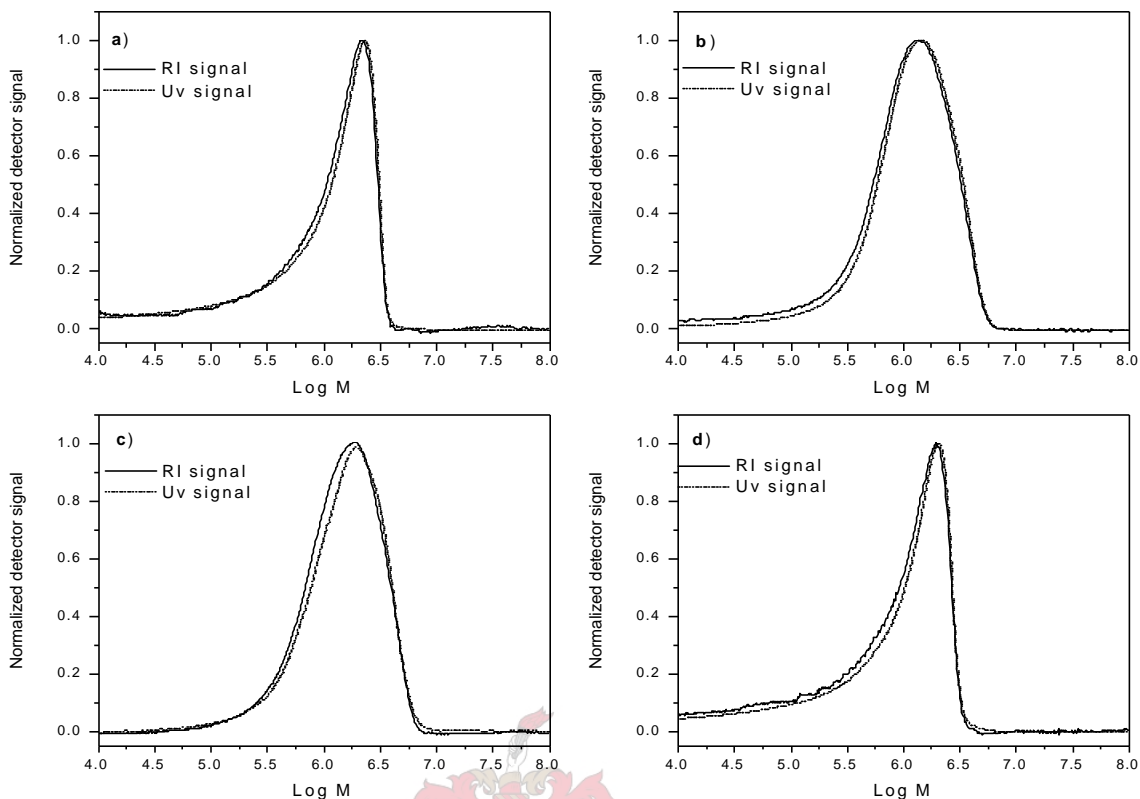


Figure 7.2: Molecular weight distributions of (a) poly(MMA-co-A₂), (b) poly(MMA-co-B₂), (c) poly(BA-co-A₂) and (d) poly(BA-co-B₂).

Analyses were done on the final copolymers as shown in Table 7.2. As a result of the conventional free radical miniemulsion polymerisation mechanism that was followed, the molecular weight distributions of the final copolymers were broad.

Table 7.2: Molecular weight data of the synthesised polymers.

Copolymers	M_w	M_n	M_w/M_n
Poly(MMA-co-A ₂)	1238695	208916	5.929
Poly(BA-co-A ₂)	2230462	507603	4.394
Poly(MMA-co-B ₂)	1229453	264203	4.653
Poly(BA-co-B ₂)	1309680	631387	2.074

7.3.2 TEM analysis

From TEM analyses, several observations were made. Firstly, no significant morphological variation was evident when the homopolymers were physically compared to the copolymers. This was expected since MMA/BA will exhibit a higher degree of incorporation into the polymers because it is known to be more reactive than A_2 and B_2 .

Secondly, all samples showed a significant degree of monodispersity, which correlated well with particle size analyses.

Thirdly, the coalescing nature via deformation of butyl acrylate was evident through the appearance of ‘softer’ particles, which were hexagonal¹ or ‘bee-hive’ in morphology and had a characteristic film forming property at low temperatures. Methyl methacrylate polymers on the other hand, displayed more ‘harder’ spherical morphologies whilst still retaining a film forming ability at higher temperatures.

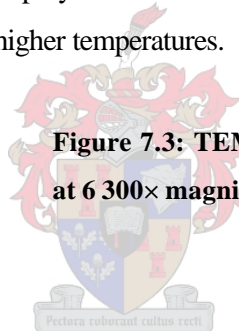
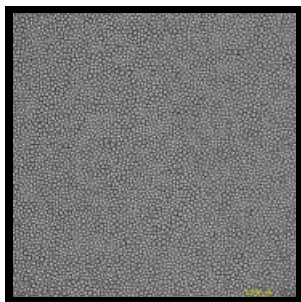


Figure 7.3: TEM image of a poly(MMA-co- A_2) sample at 6 300 \times magnification.

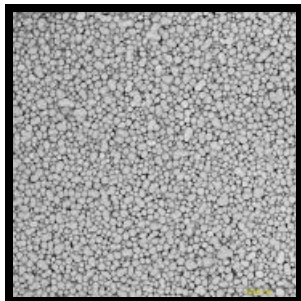


Figure 7.4: TEM image of a poly(BA-co- A_2) sample at 6 300 \times magnification.

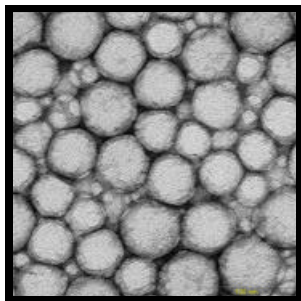


Figure 7.5: TEM image of a poly(MMA-co- A_2) sample at 80 000 \times magnification, showing the contrasting effect of 2% uranyl acetate.

7.3.3 Particle size analysis

Analyses were done on the final copolymers and results tabulated in Table 7.3. For all systems the amount of surfactant, monomer and, water, and conditions for agitation (time, temperature and amplitude) were kept constant. The MMA homo/copolymers had a smaller particle size than those of the BA homo/copolymers, primarily due to its higher solubility in the aqueous phase.¹ Since the particle size after polymerisation is proportional to the initial droplet size,¹ MMA is expected to have a smaller particle size when compared to BA.

Table 7.3: Particle sizes of polymers.

Test	Poly(MMA-co-A ₂)	Poly(BA-co-A ₂)	Poly(MMA-co-B ₂)	Poly(BA-co-B ₂)	Poly(MMA)	Poly(BA)
Ave. mean (nm)	55.8	72.6	55.5	76.2	56.8	67.1
Polydispersity	0.05	0.02	0.08	0.01	0.04	0.05
Intensity mean (nm)	58.5	73.2	58.0	76.5	57.9	68.6
Volume mean (nm)	52.4	69.8	40.3	74.7	51.9	60.2

7.3.4 Paint studies

Fig. 7.6 and Fig. 7.7 show that paint samples that are not homogenised with fluorescent latex particles do not show any fluorescent behaviour. It is also noted that the intensity of fluorescence increases with an increase in concentration of the fluorescent latex particles.

Titanium dioxide absorbs light over a wide range of wavelengths (Fig. 7.7a) thus resulting in masking of UV absorption of the fluorescent latex particles.⁶ It was for this reason that a high concentration of fluorescent latex particles was used to tag a paint containing 10% titanium dioxide, to ensure that the tag had a greater chance of absorbing light compared to the titanium dioxide.

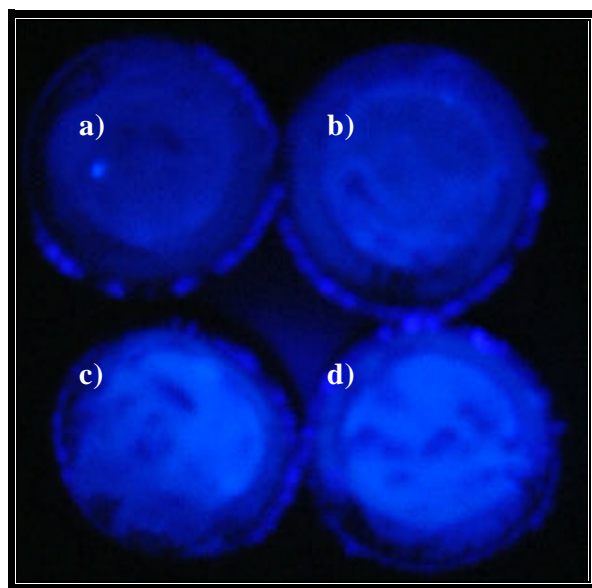


Figure 7.6: Paint without titanium dioxide: UV lamp illumination at 365 nm of (a) paint without fluorescent latex particles, (b), (c) and (d) paint containing 0.25%, 0.5% and 1.0% fluorescent latex particles respectively.

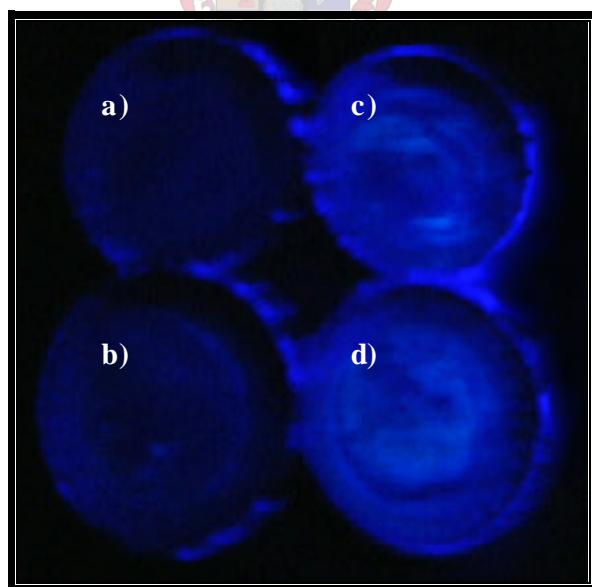


Figure 7.7: Paint containing 10.0% titanium dioxide: UV lamp illumination at 365 nm of (a) paint without fluorescent latex particles, (b), (c) and (d) paint containing 5.0%, 10.0% and 15.0% fluorescent latex particles respectively.

Fig.7.8 illustrates the region of interest analysed in a typical UV-reflectance spectrum. There is no interference by the paint sample in the region of 321 nm, which allows for an accurate and reliable determination.

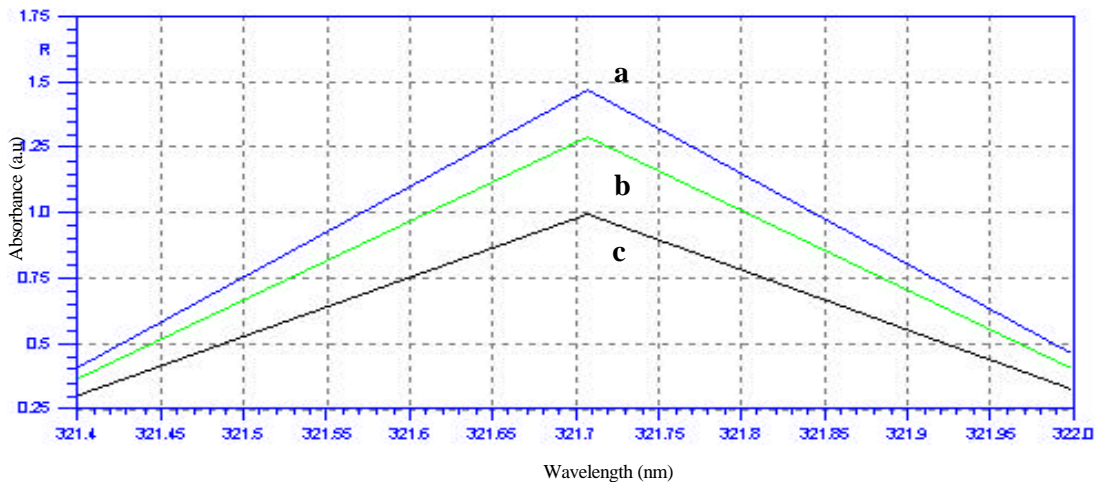


Figure 7.8: A typical UV-reflectance spectrum showing the regions of interest of (a) paint without titanium dioxide but containing 1.0% poly(MMA-co-A₂), (b) paint without titanium dioxide but containing 0.75% poly(BA-co-A₂) and (c) paint containing titanium dioxide homogenised with 20.0% poly(MMA-co-A₂).

Table 7.4 shows that a minimum of 0.25 to 0.50% of fluorescent latex particles is needed to tag a certain quantity of paint that contains no titanium dioxide.

Table 7.4: UV-reflectance data at 321 nm when 1.0, 0.75, 0.5 and 0.25% of each reaction system are homogenised with a paint that is free of titanium dioxide.

Reaction system added to paint mix	UV-reflectance in (a.u)			
	1%	0.75%	0.5%	0.25%
Poly(MMA-co-A ₂)	1.472	1.296	0.724	0.367
Poly(BA-co-A ₂)	1.412	1.199	0.694	0.324
Poly(MMA-co-B ₂)	1.456	1.235	0.714	0.341
Poly(BA-co-B ₂)	1.401	1.278	0.687	0.319

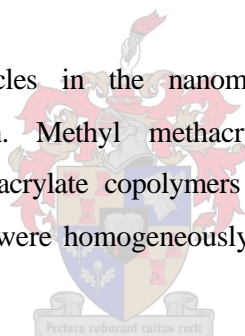
Table 7.5 shows that a minimum of 5 to 10% of fluorescent latex particles is needed to tag a paint that contains 10% titanium dioxide.

Table 7.5: UV-reflectance data at 321 nm when 5.0, 10.0, 15.0 and 20.0% of each reaction system are homogenised with a paint that contains 10% titanium dioxide.

Reaction system added to paint mix	UV-reflectance in (a.u)			
	5%	10%	15%	20%
Poly(MMA-co-A ₂)	0.225	0.501	0.732	1.001
Poly(BA-co-A ₂)	0.215	0.591	0.702	0.987
Poly(MMA-co-B ₂)	0.232	0.511	0.725	1.014
Poly(BA-co-A ₂)	0.219	0.594	0.712	1.005

7.4 Conclusions

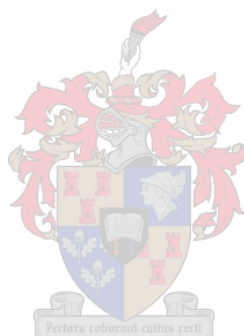
Fluorescent latex particles in the nanometer range have been prepared by miniemulsification-ultrasonication. Methyl methacrylate copolymers (70% conversion within 35 minutes) and butyl acrylate copolymers (70% conversion within 15 minutes) contained fluorescent tags that were homogeneously distributed throughout the copolymer sequences.



A bench-top UV lamp and UV-reflectance studies confirmed the fact that the fluorescent latex particles could adequately be identified and quantified when dispersed in a paint polymer resin.

References

- (1) Antonietti, M.; Landfester, K. *Prog. Polym. Sci.* **2002**, *27*, 689-757.
- (2) Van Zyl, A. J. P. M.Sc. thesis; University of Stellenbosch: Stellenbosch, 2001; 221.
- (3) In *Malvern instruments, PCS Training course, Version 1.26 software*, 1996.
- (4) Schnablegger, H.; Glatter, O. *Jnl. of Colloid and Interface* **1993**, *158*, 228.
- (5) Reimers, J. L.; Schork, F. J. *Jnl. Appl. Polym. Sci.* **1996**, *60*, 251.
- (6) www.kemira.com



Chapter 8

Conclusions and recommendations

8.1 Conclusions

Acrylic monomers 2-oxo-2H-chromen-7-yl acrylate (A_2) and 4-methyl-2-oxo-2H-chromen-7-yl acrylate (B_2) were successfully synthesized, using an esterification reaction, from the starting materials 7-hydroxy-2H-chromen-2-one (A_1) and 7-hydroxy-4-methyl-2H-chromen-2-one (B_1). The title compounds could be identified and characterized using NMR and infrared spectroscopy. Fluorescence analysis, used to determine the emitted wavelengths, of both the starting materials (A_1 and B_1) and the end products (A_2 and B_2) were found to be similar, indicating that the fluorescent character and integrity were maintained after esterification.



Calculation of the solubility parameters of monomers and solvents used in this study indicated that acetonitrile was the most suitable solvent for dissolving the monomers. This was verified by experimental analysis.

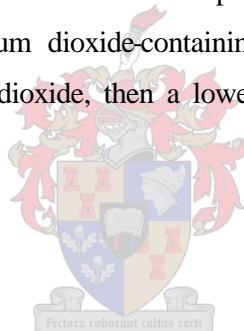
Copolymers of MMA/BA and A_2/B_2 were synthesised by conventional free radical solution copolymerisation. $^1\text{H-NMR}$ spectroscopy was used to monitor the percentage incorporation of individual free monomers. By assuming the terminal model, the reactivity ratios of each system were determined by using a least-squares non-linear fitting procedure to the copolymer equation (Eqn. 6.1). This allowed for the construction of composition diagrams (instantaneous copolymer composition versus feed composition), which showed that no azeotrope existed for the systems under investigation. There furthermore appeared to be a preference for MMA and BA when one of these monomers was copolymerised with A_2/B_2 .

In addition, fluorescence studies conducted on precipitated polymer samples showed that fluorescence was maintained during the copolymerisation process.

A miniemulsion polymerisation process was used to produce fluorescent latex particles. A size-exclusion chromatograph linked to a UV detector confirmed the synthesis of fluorescent copolymers. Methyl methacrylate copolymers (70% conversion after 35 minutes) and butyl acrylate copolymers (70% conversion after 15 minutes) contained fluorescent monomers that were homogeneously distributed throughout the copolymer sequence.

UV analysis showed that a minimum of 0.25 to 0.50% and 10.0 to 15.0% of fluorescent latex particles is required for the fluorescence to be observed in a titanium dioxide-free and titanium dioxide-containing paint, respectively. UV-reflectance studies indicated that a minimum of 0.25 and 5.0% of fluorescent latex particles respectively, are required to tag titanium dioxide-free and titanium dioxide-containing paint. If a sample of paint can be extracted to free it of titanium dioxide, then a lower amount of fluorescent latex particles would be suitable for detection.

8.2 Recommendations



Although the objectives of this study were attained, it has set the stage for the possibility of a number of recommendations. These recommendations could lead to an increase in the commercial value of the project as well as to contribute to future research efforts based on this or similar work.

To increase commercial viability, several pathways are foreseen. Firstly, it has been proven that fluorescent tags fulfil most of the commercial aspects of an excellent tagging agent, especially with regards to simple detection procedures. However, the fluorescent-tagging agents synthesised in this study still need to undergo time consuming technical testing, as discussed in Chapter 1.

Secondly, the procedures for the synthesis of fluorescent latex particles will have to be adapted. Particle size and morphology were established by ultrasonication of the latex sample. However, this process does have some disadvantages, e.g. excessive heat

generated, broad polydispersities and limited sample quantities. A microfluidizer, where larger sample quantities can be easily handled, can be used to overcome these problems. There is also no heat build-up and a tremendous reduction in the broadness of the particle size distribution.

The synthesis of fluorescent tags that absorb light at a wavelength that is not masked by the presence of titanium dioxide is another possible way of increasing commercial viability. This procedure will allow for the reduction in the amount of fluorescent latex particles required to tag a paint containing titanium dioxide, without the need for extraction. Thus, even lower amounts of tag would be used.

Another possibility is to introduce the tag to a paint additive, e.g. a rheology modifier or surface tension reducer.

